

ABSTRACT

Title of Dissertation: LONG-TERM IMPACTS OF AMAZON FOREST DEGRADATION ON CARBON STOCKS AND ANIMAL COMMUNITIES: COMBINING SOUND, STRUCTURE, AND SATELLITE DATA

Danielle Ivonne Rappaport, Doctor of Philosophy, 2020

Dissertation directed by: Professors Douglas Morton and Ralph Dubayah, Department of Geographical Sciences

The Amazon forest plays a vital role in the Earth system, yet forest degradation from logging and fire jeopardizes carbon storage and biodiversity conservation along the deforestation frontier. Policies to reduce forest carbon emissions (REDD+) will fall short of their intended goals unless carbon and biodiversity losses from forest degradation can be monitored over time. Emerging remote sensing tools, lidar and ecoacoustics, provide a means to monitor carbon and biodiversity across spatial, temporal, and taxonomic scales to address data gaps on species distributions and time-scales for recovery. This dissertation uses a novel multi-sensor perspective to characterize the long-term ecological legacy of Amazon forest degradation across a 20,000 km² landscape in Mato Grosso, Brazil. It combines high-density airborne lidar, 1100 hours of acoustic surveys, and annual time series of Landsat data to pursue three complementary studies. Chapter 2 establishes the bedrock of the investigation

by sampling fine-scale measurements of structure across a large diversity of burned and logged forests to model the initial loss and time-dependent recovery of carbon stocks and habitat structure. Chapter 3 models the interactions between sound and structure to predict acoustic community variation, and to account for attenuation in dense tropical forests. Lastly, Chapter 4 uses sound to go beyond structure to identify degradation thresholds and likely taxonomic drivers of variation in the ‘acoustic guild’ over time. Soundscapes reveal strong and sustained shifts in insect assemblages following fire, and a decoupling of biotic and biomass recovery following logging that defy theoretical predictions (*Acoustic Niche Hypothesis*). The synergies between lidar and acoustic data confirm the long-term legacy of forest degradation on both forest structure and animal communities in frontier Amazon forests. After multiple fires, forests become carbon-poor, habitats become simplified, and animal communication networks became quieter, less connected, and more homogenous. The combined results quantify large potential benefits to protecting already-burned Amazon forests from recurrent fires. This dissertation paves the way for greater integration of remote sensing and analysis tools to enhance capabilities for bringing biomass and biodiversity monitoring to scale. Additional measurements will reduce uncertainty around the breakpoints that drive carbon and biodiversity loss following degradation.

LONG-TERM IMPACTS OF AMAZON FOREST DEGRADATION ON
CARBON STOCKS AND ANIMAL COMMUNITIES:
COMBINING SOUND, STRUCTURE, AND SATELLITE DATA

by

Danielle Ivonne Rappaport

Dissertation submitted to the Faculty of the Graduate School of the
University of Maryland, College Park, in partial fulfillment
of the requirements for the degree of
Doctor of Philosophy
2020

Advisory Committee:
Dr. Ralph Dubayah, Co-Chair
Dr. Douglas Morton, Co-Chair
Dr. Andy Royle
Dr. Matthew Hansen
Dr. Bill Fagan

© Copyright by
Danielle Ivonne Rappaport
2020

Dedication

I dedicate this dissertation to my abuelita, Dr. Ivonne Lastra, for illuminating my path.

Acknowledgements

First of all, I'd like to share my enormous gratitude to my committee for their consistently great advice. Thanks so much to each of you, Doug, Ralph, Andy, Bill, and Matt, for helping me grow the confidence to do science, and for your openness and willingness to engage with my ideas. I owe distinct recognition to Doug, who provided immeasurable guidance and support during every leg of this journey. Thanks for all your painstaking hours coaching me through the world of scientific discovery. I am truly grateful for all that I learned from you. To Ralph: thanks so much for welcoming me in your lab, encouraging me to chase after my own ideas, and emphasizing the importance of balance and humor.

My most heartfelt appreciation to Jesse and my mom for being such an amazing source of love and light and for making sure that I got back from the frontier in one piece! Lots of love to David and my dad and David for teaching me independent thinking from a very young age. Besitos, my lovely tias for shining your light on me. Thank you Carla for all your support.

So grateful for my chosen sisters, Nouf, Niloo, Ash, Kristina, Aida, Nora, Amy, Sarah, Alaine, and Gabi. Our friendships sustained me through this journey!

Shout-out to all the good people in the GEL lab (Hao, Shannon, Suzanne, Jamis, Donal, Laura, Wenlu, John, Rachel) and in the broader GEOG community (Viviana, Cortney, Kelly, Meredith, Diana, Amanda, Amy)! And, many thanks to the GEOG admin (Rachel, Vivre, Liz) for getting me through UMD's red tape.

Uma profunda gratidão pelas ajudas: Eveline, Michael, Maiza, Marcos, Gisele Turquinho, Veronika, Marconi, e Baixinho.

Table of Contents

Dedication.....	ii
Acknowledgements	iii
List of Tables	vi
List of Figures.....	viii
1 Introduction	1
<u>1.1 Background and motivation</u>	1
1.1.1 The growing importance of Amazon forest degradation	1
1.1.2 Traditional observations from field and satellite data.....	2
1.1.3 Emerging synergies between lidar and ecoacoustic data	4
1.1.4 Deriving biodiversity patterns from sound	5
1.2 Research objectives and dissertation structure.....	8
2 Quantifying long-term changes in carbon stocks and forest structure from Amazon forest degradation	15
2.1 Introduction.....	16
2.2 Methods	20
2.2.1 Study area	20
2.2.2 Data and analysis	21
2.3 Results.....	25
2.4 Discussion.....	33
2.5 Conclusion	38
2.6 Supplemental Materials	45
2.6.1 Degradation and deforestation classification methods.....	45
2.6.1 Supplemental figures and tables	47
3 Acoustic space occupancy: Combining ecoacoustics and lidar to model biodiversity variation and detection bias across heterogeneous landscapes	58
3.1 Introduction.....	59
3.2 Materials and Methods.....	65
3.2.1 Case study region.....	65
3.2.2 Lidar surveys and analysis.....	66
3.2.3 Acoustic surveys and analysis	66
3.2.4 Acoustic space occupancy model	67
3.3 Results.....	74
3.4 Discussion.....	81
3.5 Conclusion	86
4 Animal soundscapes reveal key markers of Amazon forest degradation from fire and logging	92
4.1 Introduction.....	93
4.2 Methods	96
4.2.1 Study site	96
4.2.2 Acoustic processing and acoustic space use	98
4.2.3 Network analyses.....	99
4.3 Results.....	101

4.4 Discussion.....	111
5 Research Synthesis and Future Directions.....	128
5.1 Research synthesis, significance, and next steps.....	128
5.1.1 The ecosystem legacy of forest degradation.....	129
5.1.2 Making the most of acoustic data for biodiversity monitoring.....	133
5.2 Scaling up my understanding of forest degradation in future work.....	144
5.2.1 To inform management.....	144
5.2.2 To inform policy.....	146
5.3 Conclusion.....	147

List of Tables

Table 2-1. Lidar-based estimates of the fraction of original canopy cover, number of canopy tree clusters, and the distribution of ACD in degraded forests..	31
Table 2-2. Estimates based on the multiple linear regression models of aboveground carbon density predicted at four standard reporting periods following the most common logging and fire pathways. For each degradation class, modeled ACD and 95% confidence interval (in parentheses) are shown as the percentage of the intact forest reference (113.5 Mg C ha ⁻¹).	31
Table S 2-1. The lidar data were collected by Sustainable Landscapes Brazil, and can be freely accessed from: https://www.paisagenslidar.cnptia.embrapa.br/webgis/ . Acquisition dates, names and corresponding stand IDs are listed below. Additional stand-level information can be derived from Table S2.	53
Table S 2-2. Attributes of 58 forest stands derived from the combination of Landsat and lidar data, including aboveground carbon density (ACD, Mg C ha ⁻¹), frequency, and age since last degradation event	54
Table S 2-3. Best-fit regression equations to predict time-dependent recovery of aboveground carbon density (Mg-C ha ⁻¹) of logged stands and stands burned once, twice, and three or more times. <i>Model 1</i> considers once-burned stands as a single class, while <i>Model 2</i> further partitions once-burned stands into low- or high-severity areas based on post-fire changes in canopy reflectance	56
Table S 2-4. Best-fit regression equations to predict time-dependent recovery of residual canopy (<i>Model 3</i>) and density of canopy trees (<i>Model 4</i>) of logged stands and stands burned once, twice, and three or more times.	57

Table 3-1. Lidar and ecoacoustic covariates evaluated for models of detection and occupancy. The only candidate covariates not fit to both model components were n and $(C_n + S_n)$, which were exclusively used as detection and observation covariates, respectively.....68

Table 3-2. The model with the most substantial level of empirical support is shown with coefficients (SE) presented separately for the detection and occupancy components. Covariate descriptions are provided in Table 1.....69

List of Figures

Figure 1-1. Dissertation framework.	9
Figure 2-1. Degraded and intact forest stands were distributed across 20,000 km ² in the Brazilian state of Mato Grosso (top inset).....	21
Figure 2-2. Forests affected by multiple fires had the largest differences in aboveground carbon density (ACD) compared to median ACD in intact forests (red line). Additionally, ACD distributions between burned and logged-and-burned forests were similar for once-burned forests. The violin plots summarize ACD distributions as a function of fire frequency and degradation class	27
Figure 2-3. Ring patterns in burned forests indicate diurnal differences in fire line intensity, and increasing fire frequency results in a progressive loss of forest biomass and structural diversity. Lidar-based estimates of aboveground carbon density (ACD, Mg C ha ⁻¹) at 0.25-hectare resolution for 5000 x 200 m transects are overlaid on post-fire Landsat NDVI for once-burned (a) twice-burned (b) and thrice-burned (c) forest stands.....	27
Figure 2-4. Patterns of aboveground biomass recovery following forest degradation highlight the magnitude and duration of ACD accumulation following fire. a) Relationship between ACD and stand age for logged, once-burned, twice-burned, and thrice-burned stands. b) Initial fire severity in once-burned forests further explains the heterogeneity in residual carbon stocks.....	32
Figure 3-1. The locations of the ecoacoustic and lidar surveys (red polygons; n = 34) shown in relation to the case study landscape (2014 Landsat composite, bands 543) and broader regional context (map inset).	65
Figure 3-2. Naive observations per hour for the 33 sites used for model calibration. Colors correspond to the degree of canopy openness of the corresponding sites (higher values of shrub standard deviation indicate greater canopy loss from degradation). The greyscale indicates the percentage of sites with ≥ 5 detections.	75
Figure 3-3. Naive observations per frequency band. Colors correspond to the degree of canopy openness and the greyscale corresponds to the percentage of sites with ≥ 5 detections.	75
Figure 3-4. The combined effects of signal frequency and forest structure, indicated by the standard deviation of shrub-classified lidar returns, on top-ranked model predictions of detection probability (p), assuming 12 samples/hour and mean values for other detection covariates (not shown).	78

Figure 3-5. The influence of sample density on frequency-dependent detection probability (p) predicted from the top-ranked model.....	78
Figure 3-6. Predicted occupancy (blue scale) overlaid with naive detected occupancy aggregated over five days (orange outline) for four study sites with differing fractional canopy cover (CC).	80
Figure 3-7. Predicted occupancy probability (Ψ) over the 24-hour cycle and frequency spectrum for two divergent habitats, a heavily degraded forest (44% canopy cover), and an intact forest (93% canopy cover).	81
Figure 4-1. Triplicate recording sites were installed in 39 locations distributed across 9,400 km ² in northern Mato Grosso to characterize acoustic communities following forest degradation. The three close-up panels show the characteristic variability in degraded vegetation as seen from satellite imagery (2014 Landsat, 543-RGB), and the distribution of sampling effort designed to capture this heterogeneity.	97
Figure 4-2. Patterns of acoustic space infilling do not conform to expectations from the Acoustic Niche Hypothesis when evaluated in terms of structural intactness (biomass) and degradation history (fire frequency, logging age). The contradictory responses to fire (green) and logging (orange) by acoustic communities indicate no predictable variability in acoustic space occupancy (ASO) with time since logging, despite the important role of degradation history in governing the recovery of ecosystem structure. The cumulative proportion of ASO aggregated hourly is presented for the full daily cycle and for specific time windows of biological relevance for birds and insects to pinpoint the likely taxonomic contributions to daily trends.	104
Figure 4-4. Mean partner diversity shows the frequency dependence of soundscape differences among individual site replicates (left) and degradation strata (right) after logging (top) and fire (bottom). After recurrent burns, there is an overall reduction in partner diversity, but the sharpest declines in specific pseudo-taxa do not coincide with the strongest source of deviation in an otherwise comparable pattern among logged forests.....	105
Figure 4-5. Soundscape transitions show coordinated losses and gains of pseudo-taxa after fire and logging as a function of degradation frequency, timing, and severity. 2D soundscape matrices show distinct trajectories of biotic assembly after fire versus logging, and capture localized heterogeneity from burn damages even within a single fire, most obvious as coordinated silences during the early morning period.	107
Figure 4-6. The increased evenness of the spread of links from 1 to 5 fires indicates that recurrent fire results in a soundscape that is more homogenous and composed of fewer dominant and rare links. The non-linear patterns of evenness with increasing regeneration after logging are not clearly differentiated by logging history.....	108

Figure 4-7. The clustering of adjacent nodes, as indicated by the cluster coefficient at the level of sound frequencies (top) and sound hours (bottom), shows that fire recurrence directly affects the connectedness of the soundscape and the likelihood that adjacent pseudo-taxa coordinate activity as part of a larger clique. 110

Figure 5-1. Modeled peaks of acoustic activity from mixture model analysis (mean +/- sd) of burned (top) and logged (bottom) sites (distinct color per site) show the appearance and disappearance of pseudo-taxa, conforming to our understanding of degradation history. 139

Figure 5-2. These two examples of soundscape predictions from the mixture model for two spatially proximate replicates within the same logging class (15 yr) indicate that the modes of the predicted soundscape surface do not consistently conform with our visual inspection, which suggests further testing needs to be done to standardize optimal selection of component mixtures, which curiously varied between 4 and 7 in the examples shown above. 140

Figure S 2-1. Climatology of mean monthly precipitation for the study region based on 0.25° data for 2007-2017 from the Tropical Rainfall Measuring Mission (TRMM, 3B43v7).. 47

Figure S 2-2. The spatial, spectral, and temporal patterns of forest damage and recovery were used to separate deforestation, selective logging, and understory forest fire damages in Amazon forests. Patch size, shape, and the magnitude of forest damages were the first set of criteria for classification, followed by tests for the multi-year NDVI trajectory (third row) to separate deforestation from selective logging and understory forest fires. Small patches typical of logging infrastructure (1-3 Landsat pixels) were evaluated based on tests for spatial clustering. 48

Figure S 2-3. The recovery of aboveground carbon density over time for logged and burned forests. Although biomass accumulates with increasing time since last disturbance, the carbon consequences of both logging and fire were persistent. The median and interquartile range of each group are indicated with the black circle and line. The tails of the violins are trimmed to the range of data, and all violins have the same area prior to trimming the tails. Distinct letters indicate significant differences among distributions from a pairwise Wilcoxon test with a Holm correction procedure to adjust α for multiple testing. 49

Figure S 2-4. Fire frequency and time since last fire were more important than logging history for ACD variability in degraded forests. In these two figures, burned forest ACD is separated by fire frequency for three age classes of years since last degradation event. The top panel (a) separates logged and burned forests from burned forests, whereas the bottom panel (b) presents data for all burned forests, regardless of logging history. The historical presence of logging does not influence the long-

term (>3 years) cumulative effect of multiple fire events, once fire frequency and age are considered50

Figure S 2-5. The recovery trajectories for canopy structure following logging, single, and recurrent fires complement ACD information regarding the restoration of ecosystem function following forest degradation. The trajectory of two complementary indices derived from lidar, % residual canopy (a) and density of canopy trees per hectare (b) indicate that fire results in the largest and most persistent alterations to canopy structure.51

Figure S 2-6. Within-fire differences in ACD from initial fire severity were evident more than a decade following fire damages. Violin plots show ACD distributions following single burns for recent fires (≤ 2 years) and older fires (11-14 years).52

Figure S 2-7. Patterns of canopy mortality following a single fire event are not uniform. Post-fire variability in canopy structure following high- and low-severity damages can help explain the observed variability in post-fire ACD. The density plots compare distributions of the residual canopy structure aggregated at 0.25 ha for the once-burned forests burned in the 2010 drought year, where intra-stand differences from initial fire severity were most preserved. The two distributions are significantly different (Wilcoxon test with $p < 0.05$).52

Figure S 4-1. Companion figure to Fig. 4-2, which shows consistent results with ASO-based analyses. Partner diversity of hours is shown for key time intervals, along with the system-level network analog, generality, which shows the mean number of sounds per hour calculated at the daily time step.122

Figure S 4-2. The mean number of links per frequency (generality) and per hour (vulnerability).123

Figure S 4-3. ASO-degradation relationships aggregated hourly for the 24-hour cycle.124

Figure S 4-4. Comparison of correlations show comparable ASO-degradation relationships irrespective of scale of aggregation (hourly vs. minute).125

1 Introduction

1.1 Background and motivation

1.1.1 The growing importance of Amazon forest degradation

The Amazon forest plays a vital role in the Earth system, which is under increasing threat from human activity (Brando et al. 2019). Amazonia supports more species diversity than any other terrestrial ecosystem (Mittermeier et al. 2005), and accounts for over a quarter of the global forest carbon stocks (Saatchi et al. 2011).

Degraded Amazon forests are growing in extent and make up an increasing proportion of the cumulative impact of human activity (Asner et al. 2005; Morton et al. 2013; Aragão et al. 2018). A quarter of existing tropical forests are designated for selective logging (Edwards et al. 2019), which is expanding across the leading frontier of agricultural expansion in the Brazilian Amazon (Pereira et al 2010). Furthermore, a combination of economic and climate pressures have increased fire risk in the Amazon relative to baseline periods, according to the satellite record. During the 2010 Amazon drought event, approximately 8 times more forest area was burned than deforested for agricultural expansion (Morton et al. 2013, INPE). The more recent 2015/2016 El Niño exposed the central stem of the Amazon to fire risk and broke record in terms of forest area affected by active fires relative to deforestation (Aragão et al. 2018). This past year highlighted the alarming vulnerability of frontier forests to rapid increases in fire risk from changing economic behavior associated with deforestation. Although 2019 did not have anomalous drought, it was the most active fire year since 2010. Models project increased

degradation risk with future Amazon drought (Duffy et al. 2015, Le Page et al. 2017). Combined, economic uncertainty in a hotter, drier Amazon will continue to make fire an important agent of change in the future.

Policies to reduce emissions from deforestation and forest degradation (REDD+) risk falling short of intended goals unless carbon and biodiversity losses from degradation can be monitored over time. Land-use and land-cover change is a major contributor to greenhouse gas emissions, but carbon fluxes from tropical deforestation and degradation continue to represent one of the largest uncertainties in the terrestrial carbon budget (Houghton 2012). The paucity of large-scale studies on the long-term impacts of forest degradation has undermined efforts to quantify emissions for global carbon accounting and climate mitigation (Le Quere et al. 2016, Andrade et al. 2017).

1.1.2 Traditional observations from field and satellite data

Unlike deforestation, forest degradation is not binary, and the heterogeneity and time-dependence of degradation impacts are difficult to constrain with small field plots or moderate resolution (30-250 m) satellite measurements alone. Amazon frontier landscapes are expansive mosaics of agricultural land uses and fragmented, degraded, and regenerating forests with heterogeneous structural and floristic properties based on diverse legacies from decades of land use. Mapping the extent of human modification of Amazon forests from logging and fire means being able to measure fine-scale variability in ecosystem structure across broad spatial and temporal scales. This poses an enormous monitoring challenge, as conventional field

techniques seldom translate to landscape scales. Once logged and burned forests have been identified, quantifying the time-dependent change in carbon stocks from forest degradation is an additional challenge. In the largest field-based assessment of degraded forest carbon stocks in Amazonia, Berenguer et al. (2014) reported carbon losses that ranged between 18% and 57%, reflecting large uncertainties in the relationships between carbon retention and degradation type, timing, severity, and frequency.

Forest degradation alters more than just carbon stocks. Barlow et al. (2016) suggest that Amazon forest degradation may double the biodiversity loss from deforestation alone. Logging and fire alter the structure and composition of vegetation through selective removal or mortality of tree species, and repeated logging or fire exposure may suppress forest regeneration (sometimes referred to as ‘arrested succession’), modify soils, and deplete seed banks (Cochrane and Schulze 1999; Slik, Verburg, and Kessler 2002). These changes in forest ecosystem composition and structure alter resource availability for Amazonian fauna, and suitable conditions for nesting, foraging and predator protection (Barlow and Peres 2004; Barlow et al. 2006; Burivalova et al. 2015).

Addressing the tropical biodiversity crisis from deforestation and forest degradation requires an efficient, distributed monitoring system to assess species abundance and diversity. Traditional, ground-based biodiversity inventories are logistically prohibitive to conduct at scale, and limited taxonomic expertise perpetuates large data discrepancies for lesser-known taxa, such as insects, which constitute the bulk of tropical biodiversity (Meyer et al. 2013). Remote sensing

technologies are an essential part of any pantropical monitoring system. Operational satellites like Landsat and MODIS have been critical for monitoring the extent of degradation from fire and logging in the Amazon (e.g., Asner et al. 2005; Morton et al. 2013; Hansen et al. 2013). However, subtle yet sustained changes in ecosystem structure and biodiversity from forest degradation are not as readily apparent from space, notwithstanding the recent launches of the ICESat-2 and GEDI lidar systems, and integration with other datasets is necessary for routine carbon and biodiversity monitoring.

1.1.3 Emerging synergies between lidar and ecoacoustic data

Aligning carbon-focused policies with conservation goals requires improved monitoring of biodiversity across spatial, temporal, and taxonomic scales to address data gaps on species distributions and the recovery time-scales for forest and animal communities. Advances in remote sensing technologies may be able to bridge the scale gaps between field and satellite observations to measure subtle ecosystem variability through time and at policy-relevant extents. Lidar and acoustic remote sensing are two emerging technologies that complement field and satellite data for studies of carbon, ecosystem structure, and biodiversity (Bergen et al. 2009; Aide et al. 2013; Vierling et al. 2013; Farina and Pieretti 2014); yet the synergies between these two approaches have hardly been explored (Pekin et al. 2012, Bustamante et al. 2015).

Lidar is a precise remote sensing method for collecting detailed information about three-dimensional (3D) forest structure. Lidar sensors can be flown in low-

altitude aircraft to collect fine-scale information over large spatial domains (e.g., Longo et al. 2016). Lidar-derived structural parameters, such as canopy height, leaf area, and aboveground carbon density, have been successfully used for habitat and species modeling (Goetz et al. 2007; Bergen et al. 2009; Dubayah et al. 2010).

Ecoacoustics is an emergent remote sensing approach for assessing biodiversity across diurnal and seasonal time scales and broad geographic extents (Blumstein et al. 2011; Aide et al. 2013; Fuller et al. 2015). One of the key advantages over traditional in-situ surveys is that passive recording devices can be simultaneously deployed in multiple sites to dramatically reduce the effort and cost associated with large-scale monitoring due. The current generation of automated recording devices are low cost (<\$500) and highly reliable (REF). Furthermore, rapid advances in battery technology support long-term monitoring (>20 days) in a non-invasive manner. Acoustic recordings provide a permanent digital record that can be repeatedly analyzed and independently validated following data collection to support future investigations well beyond the original scope of the acquisition.

1.1.4 Deriving biodiversity patterns from sound

Remote acoustic surveys hold great promise for supporting routine monitoring of wildlife. However, the nascent field of ecoacoustics is still grappling with methodological and analytical challenges associated with sound recordings. For example, ecoacoustics, as with other methods for quantifying species presence or absence, must account detection biases from sampling and sound attenuation. Standardizing biodiversity indicators from sound data also depends on improved

techniques for capturing information about multiple taxa in complex tropical forest environments with complex signaling assemblages and multi-species choruses.

Clearly, acoustic surveys are only able to capture sound-generating organisms, sometimes referred to as “the acoustic guild.” However, even the subset of animal species that create sounds within the range of typical recording units (2-20 kHz) represents a broad sample of forest biodiversity from avian, amphibian, and insect species, along with sensitivity to some frequencies associated with bats. The advantages of automated recording devices are dense or concurrent sampling, full daily coverage, and long sampling intervals (5-20 days). Together, these benefits provide a robust, repeatable survey methodology for the acoustic guild, especially compared to traditional ground surveys, which are typically conducted during narrow time periods to target specific taxa (La and Nudds 2016).

Passive acoustic monitoring devices also generate large volumes of data, necessitating automated approaches to filter and analyze thousands of hours of sound recordings. There are several distinct analytical pathways for deriving information about biodiversity from acoustic surveys, each with clear trade-offs in terms of efficiency and ecological utility. Most previous efforts to utilize acoustic data for biodiversity monitoring have focused on detecting known vocalizations associated with individual species (Aide et al. 2013), but there is broad interest in evaluating whether the collection of all vocalizations and stridulations, or soundscapes, may serve as a surrogate of community composition. Since taxonomic groups emit acoustic signals (vocalizations, stridulations) at routine periods of the day and at standard frequency ranges, soundscapes are “community fingerprints” relevant to

multiple taxa, which can be analyzed to circumvent species ID.

This dissertation directly addresses two critical shortfalls of soundscape-based indicators that have heretofore limited the ability to bring acoustic-based monitoring to scale (Eldridge et al., 2018; Wood et al., 2019): First, more advanced statistical methods need to be developed to detect compositional change from remote audio surveys in the complex acoustic environments characteristic of tropical forests (multi-species choruses assemblages). Recent research interest in soundscapes has generated numerous acoustic diversity indices that consider variation in energy as a function of either time or frequency, not both (e.g., Sueur et al. 2014). However, current soundscape indices are not well equipped to support standardized assessments of biodiversity change across space or time (' β -diversity soundscape indices') (Sueur et al., 2014), and are readily confounded by environmental variation and noise (Buxton et al., 2018). Recent pan-tropical research suggests that measuring acoustic space occupancy across both time *and* frequency may be a more effective proxy for tropical species diversity (e.g. Aide et al., 2016; Eldridge et al. 2016, Eldridge et al. 2018). This dissertation aims to go one step further by advancing methods to probe the component elements and interactions that drive differences in overall occupancy.

Second, operationalizing sound-derived biodiversity indicators also depends on improved handling of observation bias from sound attenuation and other sampling artifacts (e.g. data sparsity). The likelihood of detecting a soniferous species occupying a site depends not only on whether it is acoustically active during a given survey, but also on a myriad of factors that influence its detectability, such as interference with vegetation, which may selectively scatter and mask the propagation

of specific frequencies in complex forested environments (Wiley & Richards, 1982). Most existing soundscape indices ignore detection error and regard the soundscape as an unbiased representation of the underlying animal community. Unless properly addressed, frequency attenuation may skew biodiversity inferences from acoustic data in dense forest habitats (Royle, 2018).

1.2 Research objectives and dissertation structure

This dissertation (Fig. 1-1) draws from a novel multi-sensor perspective to characterize the ecological legacy of degradation across a 20,000 km² landscape in northern Mato Grosso, Brazil, which is one of the most fire-prone frontier regions in the Amazon ‘arc of deforestation.’ It combines high-density airborne lidar, 1100 hours of acoustic surveys, and annual time series of Landsat data to quantify changes in forest structure, carbon stocks, and biodiversity following logging and fire. Chapters 2-4 pursue three complementary lines of evidence to advance our understanding of frontier tropical forest ecosystems in the context of global change. Chapter 2 establishes the bedrock of the investigation by using high-density measurements of structure sampled over 3000 ha from a diversity of degraded forests (N = 58) to model the initial loss and time-dependent recovery of carbon stocks and habitat structure following fire and logging. Chapter 3 models the interactions between sound and structure to predict acoustic community variation, and to account for attenuation in dense tropical forests. Chapter 4 uses sound data to extend our understanding of the degradation process beyond carbon alone, and identifies the specific degradation sequences and pseudo-taxa that give rise to variation in the

‘acoustic guild’ over time. Lastly, Chapter 5 discusses methodological, scientific, management, and policy implications of the results outlined in Chapters 2-4, and concludes with future steps for advancing our understanding of the forest degradation process.

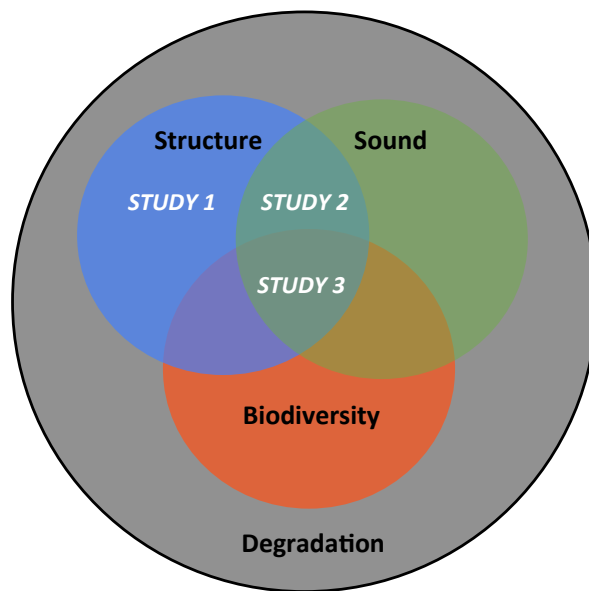


Figure 1-1. Dissertation framework.

References

- Andrade, Rafael B., Jennifer K. Balch, Amoreena L. Parsons, Dolores Armenteras, Rosa Maria Roman-Cuesta, and Janette Bulkan. 2017. "Scenarios in Tropical Forest Degradation: Carbon Stock Trajectories for REDD+." *Carbon Balance and Management* 12 (1): 6.
- Aragão, Luiz E. O. C., Liana O. Anderson, Marisa G. Fonseca, Thais M. Rosan, Laura B. Vedovato, Fabien H. Wagner, Camila V. J. Silva, et al. 2018. "21st Century Drought-Related Fires Counteract the Decline of Amazon Deforestation Carbon Emissions." *Nature Communications* 9 (1): 1–12.
- Asner, Gregory P., David E. Knapp, Eben N. Broadbent, Paulo JC Oliveira, Michael Keller, and Jose N. Silva. 2005. "Selective Logging in the Brazilian Amazon." *Science* 310 (5747): 480–482.
- Barlow, Jos, Gareth D. Lennox, Joice Ferreira, Erika Berenguer, Alexander C. Lees, Ralph Mac Nally, James R. Thomson, Silvio Frosini de Barros Ferraz, Julio Louzada, and Victor Hugo Fonseca Oliveira. 2016. "Anthropogenic Disturbance in Tropical Forests Can Double Biodiversity Loss from Deforestation." *Nature* 535 (7610): 144.
- Barlow, Jos, and Carlos A Peres. 2004. "Ecological Responses to El Niño-Induced Surface Fires in Central Brazilian Amazonia: Management Implications for Flammable Tropical Forests." *Philosophical Transactions of the Royal Society B: Biological Sciences* 359 (1443): 367–80.
- Barlow, Jos, Carlos A. Peres, L. M. P. Henriques, P. C. Stouffer, and J. M. Wunderle. 2006. "The Responses of Understorey Birds to Forest Fragmentation, Logging and Wildfires: An Amazonian Synthesis." *Biological Conservation* 128 (2): 182–192.
- Berenguer, Erika, Joice Ferreira, Toby Alan Gardner, Luiz Eduardo Oliveira Cruz Aragão, Plínio Barbosa De Camargo, Carlos Eduardo Cerri, Mariana Durigan, Raimundo Cosme De Oliveira, Ima Célia Guimarães Vieira, and Jos Barlow. 2014. "A Large-Scale Field Assessment of Carbon Stocks in Human-Modified Tropical Forests." *Global Change Biology*.
- Bergen, K. M., S. J. Goetz, R. O. Dubayah, G. M. Henebry, C. T. Hunsaker, M. L. Imhoff, R. F. Nelson, G. G. Parker, and V. C. Radeloff. 2009. "Remote Sensing of Vegetation 3-D Structure for Biodiversity and Habitat: Review and Implications for Lidar and Radar Spaceborne Missions." *Journal of Geophysical Research: Biogeosciences* 114 (G2).

- Blumstein, Daniel T., Daniel J. Mennill, Patrick Clemins, Lewis Girod, Kung Yao, Gail Patricelli, Jill L. Deppe, et al. 2011. “Acoustic Monitoring in Terrestrial Environments Using Microphone Arrays: Applications, Technological Considerations and Prospectus.” *Journal of Applied Ecology* 48 (3): 758–67.
- Brando, Paulo M., Lucas Paolucci, Caroline C. Ummenhofer, Elsa M. Ordway, Henrik Hartmann, Megan E. Cattau, Ludmila Rattis, Vincent Medjibe, Michael T. Coe, and Jennifer Balch. 2019. “Droughts, Wildfires, and Forest Carbon Cycling: A Pantropical Synthesis.” *Annual Review of Earth and Planetary Sciences* 47 (1): 555–81.
- Burivalova, Zuzana, Tien Ming Lee, Xingli Giam, Çağan Hakkı Şekercioğlu, David S. Wilcove, and Lian Pin Koh. 2015. “Avian Responses to Selective Logging Shaped by Species Traits and Logging Practices.” *Proceedings of the Royal Society of London B: Biological Sciences* 282 (1808): 20150164.
- Bustamante, Mercedes, Iris Roitman, Thomas M. Aide, Ane Alencar, Liana Anderson, Luiz Aragão, Gregory P. Asner, et al. 2015. “Towards an Integrated Monitoring Framework to Assess the Effects of Tropical Forest Degradation and Recovery on Carbon Stocks and Biodiversity.” *Global Change Biology*.
- Buxton, Rachel T., Megan F. McKenna, Mary Clapp, Erik Meyer, Erik Stabenau, Lisa M. Angeloni, Kevin Crooks, and George Wittemyer. 2018. “Efficacy of Extracting Indices from Large-Scale Acoustic Recordings to Monitor Biodiversity.” *Conservation Biology* 32 (5): 1174–84.
- Cochrane, Mark A., and Mark D. Schulze. 1999. “Fire as a Recurrent Event in Tropical Forests of the Eastern Amazon: Effects on Forest Structure, Biomass, and Species Composition1.” *Biotropica* 31 (1): 2–16.
- Dubayah, R. O., S. L. Sheldon, D. B. Clark, M. A. Hofton, J. B. Blair, G. C. Hurtt, and R. L. Chazdon. 2010. “Estimation of Tropical Forest Height and Biomass Dynamics Using Lidar Remote Sensing at La Selva, Costa Rica.” *Journal of Geophysical Research: Biogeosciences* 115 (G2): n/a–n/a.
- Duffy, Philip B., Paulo Brando, Gregory P. Asner, and Christopher B. Field. 2015. “Projections of Future Meteorological Drought and Wet Periods in the Amazon.” *Proceedings of the National Academy of Sciences* 112 (43): 13172–13177.
- Edwards, David P., Jacob B. Socolar, Simon C. Mills, Zuzana Burivalova, Lian Pin Koh, and David S. Wilcove. 2019. “Conservation of Tropical Forests in the Anthropocene.” *Current Biology* 29 (19): R1008–20.

- Eldridge, Alice, Michael Casey, Paola Moscoso, and Mika Peck. 2016. "A New Method for Ecoacoustics? Toward the Extraction and Evaluation of Ecologically-Meaningful Soundscape Components Using Sparse Coding Methods." *PeerJ* 4: e2108.
- Eldridge, Alice, Patrice Guyot, Paola Moscoso, Alison Johnston, Ying Eyre-walker, and Mika Peck. 2018. "Sounding out Ecoacoustic Metrics: Avian Species Richness Is Predicted by Acoustic Indices in Temperate but Not Tropical Habitats." *Ecological Indicators*.
- Farina, Almo, and Nadia Pieretti. 2014. "Sonic Environment and Vegetation Structure: A Methodological Approach for a Soundscape Analysis of a Mediterranean Maqui." *Ecological Informatics* 21: 120–132.
- Fuller, Susan, Anne C. Axel, David Tucker, and Stuart H. Gage. 2015. "Connecting Soundscape to Landscape: Which Acoustic Index Best Describes Landscape Configuration?" *Ecological Indicators* 58: 207–215.
- Goetz, Scott, Daniel Steinberg, Ralph Dubayah, and Bryan Blair. 2007. "Laser Remote Sensing of Canopy Habitat Heterogeneity as a Predictor of Bird Species Richness in an Eastern Temperate Forest, USA." *Remote Sensing of Environment* 108 (3): 254–63.
- Hansen, M. C., P. V. Potapov, R. Moore, M. Hancher, S. A. Turubanova, A. Tyukavina, D. Thau, et al. 2013. "High-Resolution Global Maps of 21st-Century Forest Cover Change." *Science* 342 (6160): 850–53.
- Houghton, R. A. 2012. "Carbon Emissions and the Drivers of Deforestation and Forest Degradation in the Tropics." *Current Opinion in Environmental Sustainability* 4 (6): 597–603.
- La, Van T., and Thomas D. Nudds. 2016. "Estimation of Avian Species Richness: Biases in Morning Surveys and Efficient Sampling from Acoustic Recordings." *Ecosphere* 7 (4).
- Le Page, Yannick, Douglas Morton, Corinne Hartin, Ben Bond-Lamberty, José Miguel Cardoso Pereira, George Hurtt, and Ghassem Asrar. 2017. "Synergy between Land Use and Climate Change Increases Future Fire Risk in Amazon Forests." *Earth System Dynamics (Online)* 8 (PNNL-SA-119758).
- Le Quéré, Corinne, Robbie M. Andrew, Josep G. Canadell, Stephen Sitch, Jan Ivar Korsbakken, Glen P. Peters, Andrew C. Manning, et al. 2016. "Global Carbon Budget 2016." *Earth System Science Data* 8 (2): 605–49.
- Longo, Marcos, Michael M. Keller, Maiza N. dos-Santos, Veronika Leitold, Ekena R. Pinagé, Alessandro Baccini, Sassan Saatchi, Euler M. Nogueira, Mateus Batistella, and Douglas C. Morton. 2016. "Aboveground Biomass Variability across Intact and Degraded

- Forests in the Brazilian Amazon.” *Global Biogeochemical Cycles*, January, 2016GB005465.
- Meyer, V., S. S. Saatchi, J. Chave, J. Dalling, S. Bohlman, G. A. Fricker, C. Robinson, and M. Neumann. 2013. “Detecting Tropical Forest Biomass Dynamics from Repeated Airborne Lidar Measurements.” *Biogeosciences Discuss.* 10 (2): 1957–92.
- Mittermeier, Russell A., Gustavo A.b. Da Fonseca, Anthony B. Rylands, and Katrina Brandon. 2005. “A Brief History of Biodiversity Conservation in Brazil.” *Conservation Biology* 19 (3): 601–7.
- Morton, D. C., Y. Le Page, R. DeFries, G. J. Collatz, and G. C. Hurtt. 2013. “Understorey Fire Frequency and the Fate of Burned Forests in Southern Amazonia.” *Philosophical Transactions of the Royal Society B: Biological Sciences* 368 (1619): 20120163.
- Pekin, Burak K., Jinha Jung, Luis J. Villanueva-Rivera, Bryan C. Pijanowski, and Jorge A. Ahumada. 2012. “Modeling Acoustic Diversity Using Soundscape Recordings and LIDAR-Derived Metrics of Vertical Forest Structure in a Neotropical Rainforest.” *Landscape Ecology* 27 (10): 1513–1522.
- Pereira, Henrique M., Paul W. Leadley, Vânia Proença, Rob Alkemade, Jörn P. W. Scharlemann, Juan F. Fernandez-Manjarrés, Miguel B. Araújo, et al. 2010. “Scenarios for Global Biodiversity in the 21st Century.” *Science* 330 (6010): 1496–1501.
- Royle, J. Andrew. 2018. “Modelling Sound Attenuation in Heterogeneous Environments for Improved Bioacoustic Sampling of Wildlife Populations.” Edited by Robert Freckleton. *Methods in Ecology and Evolution* 9 (9): 1939–47.
- Saatchi, Sassan S., Nancy L. Harris, Sandra Brown, Michael Lefsky, Edward T. A. Mitchard, William Salas, Brian R. Zutta, et al. 2011. “Benchmark Map of Forest Carbon Stocks in Tropical Regions across Three Continents.” *Proceedings of the National Academy of Sciences* 108 (24): 9899–9904.
- Slik, JW Ferry, Rene W. Verburg, and Paul JA Kessler. 2002. “Effects of Fire and Selective Logging on the Tree Species Composition of Lowland Dipterocarp Forest in East Kalimantan, Indonesia.” *Biodiversity & Conservation* 11 (1): 85–98.
- Sueur, Jérôme, Almo Farina, Amandine Gasc, Nadia Pieretti, and Sandrine Pavoine. 2014. “Acoustic Indices for Biodiversity Assessment and Landscape Investigation.” *Acta Acustica United with Acustica* 100 (4): 772–781.
- Vierling, Lee A., Kerri T. Vierling, Patrick Adam, and Andrew T. Hudak. 2013. “Using Satellite and Airborne LiDAR to Model Woodpecker Habitat Occupancy at the Landscape Scale.” *PLoS ONE* 8 (12).

Wiley, R. H., and D. G. Richards. 1982. *Acoustic Communication in Birds*. Vol. 1. Academic Press New York, NY.

Wood, Connor M., Viorel D. Popescu, Holger Klinck, John J. Keane, R. J. Gutiérrez, Sarah C. Sawyer, and M. Zachariah Peery. 2019. “Detecting Small Changes in Populations at Landscape Scales: A Bioacoustic Site-Occupancy Framework.” *Ecological Indicators* 98 (March): 492–507.

2 Quantifying long-term changes in carbon stocks and forest structure from Amazon forest degradation¹

Abstract

Despite sustained declines in Amazon deforestation, forest degradation from logging and fire continues to threaten carbon stocks, habitat, and biodiversity in frontier forests along the Amazon arc of deforestation. Limited data on the magnitude of carbon losses and rates of carbon recovery following forest degradation have hindered carbon accounting efforts and contributed to incomplete national reporting to reduce emissions from deforestation and forest degradation (REDD+). We combined annual time series of Landsat imagery and high-density airborne lidar data to characterize the variability, magnitude, and persistence of Amazon forest degradation impacts on aboveground carbon density (ACD) and canopy structure. On average, degraded forests contained 45.1% of the carbon stocks in intact forests, and differences persisted even after 15 years of regrowth. In comparison to logging, understory fires resulted in the largest and longest-lasting differences in ACD. Heterogeneity in burned forest structure varied by fire severity and frequency. Forests with a history of one, two, and three or more fires retained only 54.4%, 25.2%, and

¹ The material in this chapter was co-authored and previously published: Rappaport, Danielle I., Douglas C. Morton, Marcos Longo, Michael Keller, Ralph Dubayah, and Maiza Nara dos-Santos. 2018. "Quantifying Long-Term Changes in Carbon Stocks and Forest Structure from Amazon Forest Degradation." *Environmental Research Letters* 13 (6): 065013.

7.6% of intact ACD, respectively, when measured after a year of regrowth. Unlike the additive impact of successive fires, selective logging before burning did not explain additional variability in modeled ACD loss and recovery of burned forests. Airborne lidar also provides quantitative measures of habitat structure that can aid the estimation of co-benefits of avoided degradation. Notably, forest carbon stocks recovered faster than attributes of canopy structure that are critical for biodiversity in tropical forests, including the abundance of tall trees. We provide the first comprehensive look-up table of emissions factors for specific degradation pathways at standard reporting intervals in the Amazon. Estimated carbon loss and recovery trajectories provide an important foundation for assessing the long-term contributions from forest degradation to regional carbon cycling and advance our understanding of the current state of frontier forests.

2.1 Introduction

Changes in Amazon forest carbon stocks are a significant source of greenhouse gas emissions from human activity (van der Werf *et al* 2009, Pan *et al* 2011, Aguiar *et al* 2016). Understanding the long-term response of Amazon forests to land use and climate is essential for balancing the global carbon budget and improving climate projections (e.g. Gatti *et al* 2014, Friedlingstein *et al* 2014). Although annual deforestation rates in the Brazilian Amazon have declined by 80% since 2004 (Hansen *et al* 2014, INPE 2015), forest degradation from fire and logging remains a threat to forest carbon stocks across the *Amazon arc of deforestation* (Morton *et al* 2013). The magnitude of carbon losses from forest degradation is large

(Longo *et al* 2016), but the long-term consequences of fire and logging on forest structure and composition remain uncertain (Andrade *et al* 2017).

Decades of Amazon frontier expansion have left a mosaic of degraded forests along the Amazon arc of deforestation (Asner *et al* 2005, Morton *et al* 2013). Nearly 3% of southern Amazonia burned between 1999–2010, and the persistence of burned frontier forests (Morton *et al* 2013) underscores the importance of considering fire separately from deforestation for complete forest carbon accounting. Selective logging is also widespread across the leading edge of frontier expansion. In 2009 alone, 14.2 million m³ of round wood was extracted from the largest logging centers in the Brazilian Legal Amazon (Pereira *et al* 2010). Canopy damage in logged forests can increase vulnerability to additional disturbances, including fire (Uhl and Vieira 1989, Holdsworth and Uhl 1997), but the feedbacks and synergies among disturbance agents, as well as the long-term impacts of degradation, are still largely unresolved.

The scarcity of large-scale, long-term studies on fire and logging impacts has undermined efforts to quantify emissions from Amazon forest degradation for global carbon accounting (Le Quere *et al* 2016) and climate mitigation efforts (Andrade *et al* 2017). Reducing land-use emissions is one cost-effective climate mitigation pathway (e.g. Canadell and Raupach 2008, Griscom *et al* 2017), including efforts to reduce emissions from deforestation and forest degradation (REDD+) under the United Nations Framework Convention on Climate Change. To be eligible for REDD+ performance-based payments, countries must be able to monitor, report, and verify (MRV) reductions in carbon emissions from degradation or deforestation. However, because of large uncertainties regarding net carbon emissions from fire and logging,

degradation has remained poorly integrated within the REDD+ accounting framework (Mertz *et al* 2012, Goetz *et al* 2015) and excluded from national reporting (e.g. Brazil 2014).

The challenge to quantify degradation emissions stems from the heterogeneity and time-dependence of degradation impacts (Longo *et al* 2016, Andrade *et al* 2017). The variability in degradation impacts may result from regional differences in underlying biomass distributions (Avitabile *et al* 2016, Longo *et al* 2016), forest resilience to fire (Brando *et al* 2012, Flores *et al* 2017), and land use (Aragão and Shimabukuro 2010). Discrepancies in emissions estimates also stem from methodological differences among studies. Field-based studies provide valuable context for understanding the long-term impacts of degradation (e.g. Berenguer *et al* 2014), but forest inventory measurements typically have limited spatial and temporal coverage due to cost constraints. By contrast, experimental studies control for much of the variability in degradation history but may be limited in their capacity to simulate the diversity of degradation impacts (e.g. Brando *et al* 2014).

Consequently, existing estimates for committed carbon emissions from Amazon understory fires vary by an order of magnitude, ranging from $\sim 20 \text{ Mg C ha}^{-1}$ (Brando *et al* 2014) to 263 Mg C ha^{-1} (Alencar *et al* 2006). Airborne lidar provides the spatially extensive and structurally detailed information on forest structure and aboveground carbon stocks needed to reconcile previous estimates of degradation emissions and quantify co-benefits of avoided degradation (Goetz *et al* 2015, Longo *et al* 2016, Sato *et al* 2016).

Here, we used a purposeful sample of high-density airborne lidar to capture a

broad range of degraded and intact forest conditions in the southern Brazilian Amazon. For each forest stand, we combined degradation history information from annual time series of Landsat data with airborne lidar data to characterize canopy structure and estimate aboveground carbon density (ACD) using a lidar-biomass model specifically developed for frontier forests in the Brazilian Amazon (Longo *et al* 2016). Our large-area lidar coverage and sampling chronosequence addressed two questions: (1) What are the trajectories of loss and recovery of forest carbon stocks and habitat structure following fire and logging in frontier Amazon forests? (2) How do degradation type, frequency, and severity contribute to variability in degraded forest carbon stocks and habitat structure over time? Our study directly targets a lingering data gap for REDD+ (Andrade *et al* 2017) by quantifying the rates of ACD recovery over 1 to 15-year time horizons following a broad range of degradation pathways, including sequential impacts of logging and burning. These time-varying emissions estimates, or emissions factors, can be combined with activity data on the extent of forest degradation to establish REDD+ baselines; confirm the relative contributions from fire, logging, and regeneration to regional net forest carbon emissions; and estimate the consequences to mitigation targets if degradation remains omitted from greenhouse gas accounting. Airborne lidar also provides detailed, quantitative information on habitat structure that may support an improved understanding of the biodiversity co-benefits of reducing forest degradation—an integral, but poorly formalized component of REDD+ MRV.

2.2 Methods

2.2.1 Study area

The study area covers approximately 20 000 km² at the southern extent of closed-canopy Amazon forests in the Brazilian state of Mato Grosso (Fig. 2-1). Mean annual precipitation (1895 mm) and temperature (25°C) support tropical forests and a diversity of land uses (Souza *et al* 2013). A four-month dry season (Fig. S 2-1) and periodic drought events (Chen *et al* 2011) contribute to the extent, duration, and severity of understory forest fires in the study region (Morton *et al* 2013, Brando *et al* 2014). Additionally, decades of agricultural expansion and selective logging (e.g. Asner *et al* 2005, Souza *et al* 2005, Matricardi *et al* 2007) have left a patchwork of fragmented and degraded forests in the study area, with few intact forests remaining outside of the Xingu Indigenous Reserve or Rio Ronuro Ecological Station (Fig. 2-1).

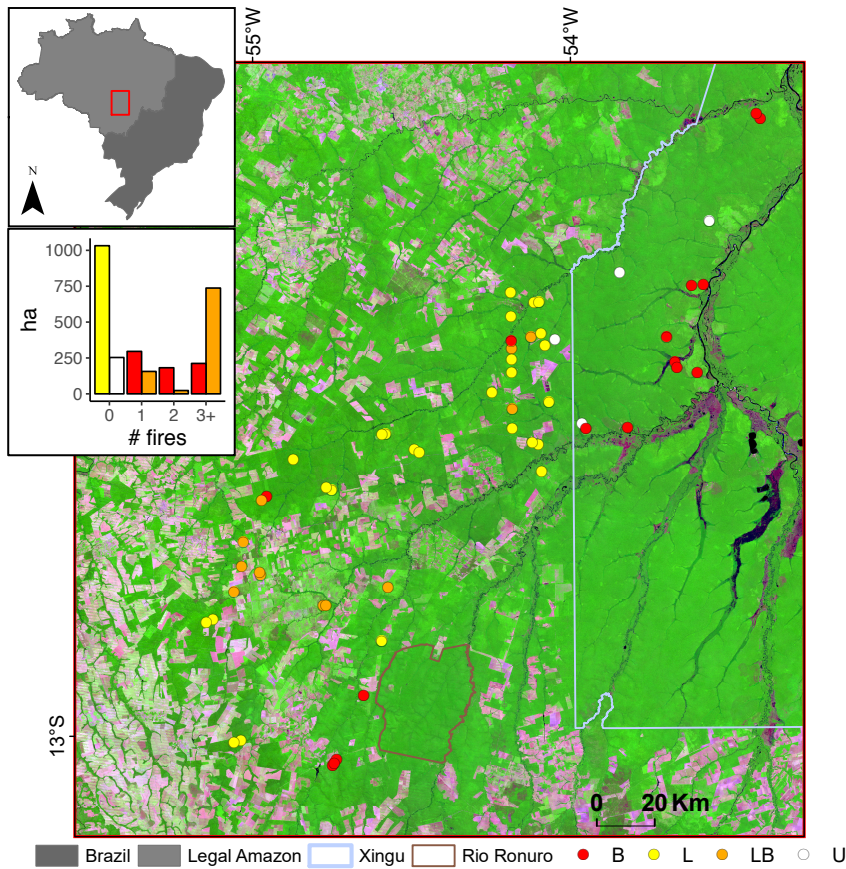


Figure 2-1. Degraded and intact forest stands were distributed across 20,000 km² in the Brazilian state of Mato Grosso (top inset). In the false-color composite image (2014 Landsat, bands 543), forest appears green, deforested areas appear pink, and wetland and open water appear purple. Circles indicating the centroid of forest stands with lidar coverage are color-coded by degradation history (U—undisturbed; L—logged; LB—logged and burned; B—burned). Airborne lidar data sampled frontier forests on private lands and within the Xingu Indigenous Park (light blue outline) and along a degradation gradient (bottom inset).

2.2.2 Data and analysis

We combined Landsat time series and airborne lidar data to quantify variability in forest structure and ACD across gradients of degradation type, frequency, severity, and timing. Degradation history for areas with lidar coverage was characterized using a two-tiered classification approach. First, the annual occurrence of logging, understory fires, and deforestation was mapped based on spatial, spectral,

and temporal information derived from annual time series of cloud-free Landsat mosaics for the early dry season months (June– August) of 1984–2016 (Fig. S 2-2; Text S 2-1). Understory fires and deforestation events were identified based on multi-year patterns of damage and recovery in Landsat Normalized Difference Vegetation Index (NDVI) (Morton *et al* 2011, Morton *et al* 2013). Logged forests were identified with an automated detection approach based on the spatial distribution of log landing decks (Asner *et al* 2004, Keller *et al* 2004). Mutually exclusive classification rules for the magnitude, duration, size, and shape of deforestation and degradation events avoided double counting errors common with the integration of independent products (Fig. S 2-2; Text S 2-1) (Morton *et al* 2011, Bustamante *et al* 2016). Second, forest stands of uniform degradation history were manually delineated within the extent of lidar coverage and visually validated to confirm the extent and timing of degradation events. Logging roads visible in multiple years of Landsat data were excluded from logged forest stands to control for the impact of logging infrastructure on estimated carbon stocks and recovery trajectories.

Airborne lidar data were used to estimate ACD in intact and degraded forest types stratified by degradation history. High-density airborne lidar data (minimum of 14 returns per m²) were collected as part of the Sustainable Landscapes Brazil project across a range of intact and degraded forests in a space-for-time substitution sampling design (Table S 2-1, data available from: www.paisagenslidar.cnptia.embrapa.br/webgis/). Based on the classification approach described above, the 2891.25 ha of lidar coverage were stratified into 58 forest stands (4.50– 498.50 ha; Table S 2-2).

A lidar-biomass model based on mean top of canopy height (TCH, m) (Longo *et al* 2016) was used to estimate ACD (kg C m^{-2}) in forest stands at 0.25 ha resolution:

$$\text{ACD}_{\text{TCH}} = 0.054 (\pm 0.012) \text{TCH}^{1.76(\pm 0.07)} \quad (1)$$

where the parenthetical values are the standard errors of the parameters.

Equation (1) assumes a biomass-to-carbon conversion factor of 0.5, following Baccini *et al* (2012). We selected the TCH model because of its simplicity, sensitivity to the lower range of the ACD distribution, and accurate representation of ACD in burned forests (Longo *et al* 2016). Equation (1) was developed using inventory and lidar data from intact and degraded Amazon forests. Here, we applied the model to a new set of lidar data sampled from the same regional context in which the Longo *et al* (2016) model was calibrated; about 8% of the lidar data set overlapped with the data used in model development.

Pixel-based uncertainty associated with modeled ACD was calculated from three sources of statistical uncertainty following the methods described in Longo *et al* (2016). A Monte Carlo approach with 10000 iterations was used to propagate the pixel-based uncertainty to the stand level by adjusting each biomass pixel with randomly distributed noise proportionate to its uncertainty before aggregating data at the stand level. The stand-level standard error was derived from the standard deviation of the simulated stand-level means.

Given the importance of canopy structure for wildlife habitat in tropical

forests (Bergen *et al* 2009), we also calculated two lidar-based measures of habitat structure. First, residual canopy cover was calculated using 1 m resolution lidar canopy height models (CHMs) as the proportion of the forest stand greater than or equal to the mean canopy height in intact forests (21 m). Second, clusters of one or more canopy trees (≥ 21 m) were identified using the 1 m CHMs with a maximum search radius of 10 m using a 3×3 pixel moving window (Silva *et al* 2015). These metrics provided complementary information on changes in forest structure from degradation and recovery processes to assess the drivers of ACD variability and the time-varying recovery of both carbon and habitat structure in degraded forests.

We used multiple linear regression to model the loss and recovery trajectories of ACD and canopy structure based on the chronosequence of lidar samples. Four least squares models were fit using the `lm` function in R version 3.3.0 (www.R-project.org). Model 1 estimated median ACD in degraded forest stands based on degradation type (burned or logged-only), timing (years since last degradation event), and fire frequency. Median ACD was selected as the measure of central tendency for each stand because of the skewed ACD distributions in degraded forests. Model 2 further stratified once-burned forests by fire severity, visible as rings of high- and low-severity canopy damage, based on the relative difference between the pre-fire and post-fire Landsat dry-season NDVI (RdNDVI). A fixed threshold of mean minus the standard deviation of RdNDVI was only used to stratify low and high-severity fire damages in once-burned stands because the spatial variability of fire damages was not well preserved following recurrent fire events. Models 3 and 4 used degradation type, timing, and frequency to predict residual canopy cover and density of canopy tree

clusters, respectively. In all four models, the variable for time since last degradation event was log-transformed to satisfy assumptions of normality and homoscedasticity (Vargas *et al* 2008, Becknell *et al* 2012). Additionally, to isolate the effect of forest recovery from the long-term impacts of logging infrastructure, logged forest stands were adjusted to exclude secondary roads and log landing decks. Interactions between degradation history (type, frequency, severity) and degradation timing were evaluated for significance and model performance in all four models. Lastly, differences across degradation strata were evaluated using pairwise Wilcoxon tests to accommodate the diversity of non-normal data distributions.

Consistent with recommendations from the Intergovernmental Panel on Climate Change (Penman *et al* 2003), an additional Monte Carlo procedure was used to propagate the effect of ACD uncertainty on model parameters and predictions by performing 10 000 realizations of the model fit on adjusted stand-level medians with normally distributed noise proportional to the stand-level standard error, or the standard deviation of the stand-level Monte Carlo aggregations.

2.3 Results

Degradation type, frequency, timing, and severity contributed to ACD variability in frontier forests. Lidar-based estimates of ACD in 58 Amazon forest stands varied by nearly two orders of magnitude between the most heavily degraded forest stand (median: 4.5 Mg C ha^{-1}), a stand that had been logged and burned three times, and the most carbon-dense intact forest stand (median: $114.3 \text{ Mg C ha}^{-1}$; Table S 2-2). At the pixel scale, median carbon density in degraded forests ($51.2 \text{ Mg C ha}^{-1}$

) was less than half of ACD in intact forests ($113.5 \text{ Mg C ha}^{-1}$). Degraded ACD was also more heterogeneous than intact ACD (coefficient of variation: 68.4% and 16.7% for degraded (2638.00 ha) and intact forest pixels (253.25 ha), respectively).

The variability in ACD following degradation could not be constrained by degradation type alone. ACD in pixels with a history of fire (median: $20.4 \text{ Mg C ha}^{-1}$; 1605.75ha) was significantly lower ($p < 0.05$) than ACD in logged-only pixels ($77.8 \text{ Mg C ha}^{-1}$; 1032.25 ha); however, ACD varied broadly within both degradation classes. At the stand level, there was considerable overlap between the ranges of median ACD in burned forests ($4.5\text{--}95.2 \text{ Mg C ha}^{-1}$) and logged-only forests ($39.0\text{--}117.3 \text{ Mg C ha}^{-1}$, Table S2-2).

Degradation timing was a critical factor for further differentiating ACD between and within logged and burned forest classes (Fig. S2-3; Table 2-1). Within two years of recovery, median ACD in burned pixels was 9.5 Mg C ha^{-1} , compared to $68.4 \text{ Mg C ha}^{-1}$ in logged-only pixels. Following 10 to 15 years of recovery, neither class recovered its estimated pre-disturbance ACD, and median ACD in burned pixels remained considerably lower than in logged pixels (difference: $17.5 \text{ Mg C ha}^{-1}$).

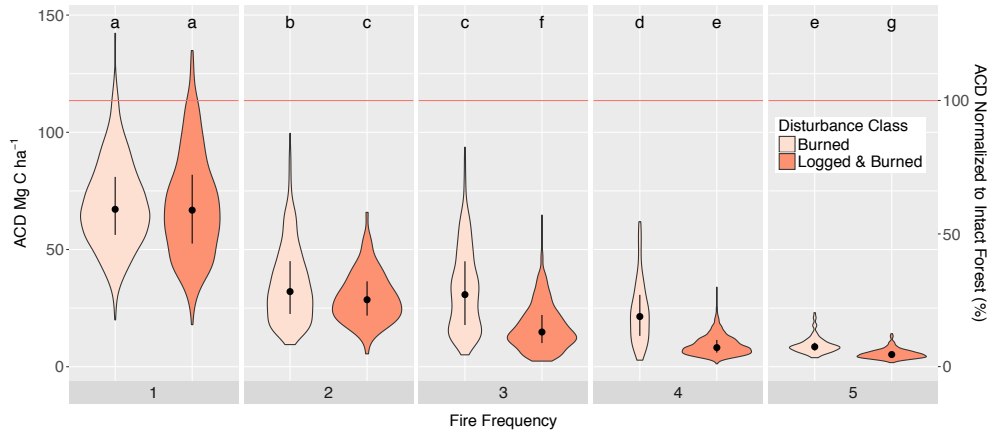


Figure 2-2. Forests affected by multiple fires had the largest differences in aboveground carbon density (ACD) compared to median ACD in intact forests (red line). Additionally, ACD distributions between burned and logged-and-burned forests were similar for once-burned forests. The violin plots summarize ACD distributions as a function of fire frequency and degradation class. The median and interquartile range of each group are indicated with the black circle and line. The tails of the violins are trimmed to the range of data, and all violins have the same area prior to trimming the tails. Distinct letters indicate significant differences among distributions from a pairwise Wilcoxon test with a Holm correction procedure to adjust α for multiple testing. See Fig. S2-4(a) for a comparison across burn frequency groups that also accounts for stand age.

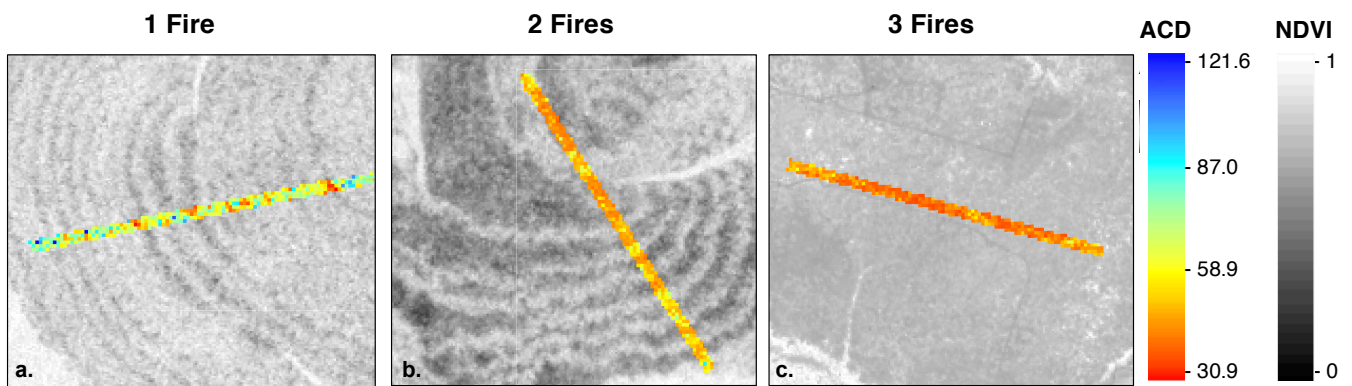


Figure 2-3. Ring patterns in burned forests indicate diurnal differences in fire line intensity, and increasing fire frequency results in a progressive loss of forest biomass and structural diversity. Lidar-based estimates of aboveground carbon density (ACD, Mg C ha⁻¹) at 0.25-hectare resolution for 5000 x 200 m transects are overlaid on post-fire Landsat NDVI for once-burned (a) twice-burned (b) and thrice-burned (c) forest stands. See Tables S 2-1 and S 2-2 for additional profile information associated with each stand (Stand IDs from left to right: 26, 13, and 8).

Fire frequency governed both the magnitude and the spatial pattern of residual forest carbon stocks (Figs. 2-2 and 2-3; Table 2-1). Repeated burning resulted in a non-linear decline in ACD, irrespective of logging history, with lowest ACD in forests subjected to three or more fires (Fig. 2-2). Forests affected by a single fire ($n = 10$) retained $67.0 \text{ Mg C ha}^{-1}$ (interquartile range [IQR] $\pm 26.4 \text{ Mg C ha}^{-1}$). Twice-burned forests ($n = 5$) contained less than half the carbon stocks in once-burned forests ($31.6 \pm 21.1 \text{ Mg C ha}^{-1}$). Forests burned three to five times ($n = 13$) retained few trees from the pre-fire forest stand; ACD was only one-sixth of that of once-burned forests ($10.3 \text{ Mg C ha}^{-1}$), with the narrowest IQR of all burn frequencies ($\pm 10.5 \text{ Mg C ha}^{-1}$). Importantly, the observed decrease in IQR with increasing fire frequency indicated a reduction in structural complexity from repeated burning (Figs. 2.2 and 2.3).

Unlike the impact of successive fires, there was no significant long-term impact on ACD recovery attributable to prior logging after controlling for fire frequency (Fig. S 2-4). Because the distinction between burned and logged-and-burned forests was not a statistically significant predictor of degraded forest ACD, nor did it improve model fit, logged-and-burned and burned forest stands were combined to model post-fire recovery of ACD.

Fire frequency and the time since the last degradation event explained the greatest variability in degraded ACD recovery (Model 1; adjusted $R^2 = 0.89$; F -statistic = 106.5 Fig. 2.4(a); Table S 2-3). The immediate reduction in ACD differed significantly for each degradation pathway (regression intercept; Table S 2-3). In the year following degradation, the modeled ACD for forests that had been logged, once-

burned, twice-burned, and subjected to three or more burns was 62.3, 52.0, 19.4, and 11.0 Mg C ha⁻¹, respectively. However, the rate of ACD recovery was similar for all classes, as interaction effects between fire frequency and time since degradation event were not statistically significant (Table S 2-3). Given these initial differences and the slow recovery in degraded forest ACD, the legacy of forest degradation was still evident 15 years following fire and logging (Table 2.2).

Initial fire severity was a statistically significant predictor of ACD recovery in once-burned forests (Model 2; Adjusted $R^2 = 0.88$; F -statistic = 87.87; Fig. 2.4(b); Tables 2-2 and S 2-3). In the year following fire, estimated high- and low-severity damages differed by 16% of intact ACD (Table 2.2). Modeled differences in ACD resulting from initial fire severity were preserved through time, with once-burned forests recovering between 57.6% and 73.9% of intact ACD after 15 years of recovery, depending on initial fire severity (Fig. 2.4(b); Table 2.2). Covariation of ACD with Landsat and lidar metrics of canopy density in burned forests provided additional insights into the contribution of fire severity to ACD variability within a single fire (Figs. S 2-6, S 2-7).

Changes in canopy structure from logging and fire were also persistent after 15 years of forest recovery (Fig. S 2-5; Table 2.1). Degradation timing and fire frequency explained the greatest variability in the recovery trajectory of residual canopy (Model 3; adjusted $R^2 = 0.74$; F -statistic = 38.85) and density of canopy trees (Model 4; adjusted $R^2 = 0.76$; F -statistic = 36.3; Fig. S 2-5; Table S 2-4). Understory fires resulted in the largest reduction of canopy tree clusters, particularly following recurrent fires. Logged forests retained more than twice as many canopy tree clusters

(46.5%) as once-burned forests (20.0%) when measured within 1–2 years of the degradation event. Forests burned three or more times retained only 4.7% the number of canopy tree clusters found in intact forests. After 14–15 years of regrowth, once-burned forests recovered only 80% of the canopy tree clusters present in logged forests. Further, these impacts to forest structure may persist even after ACD in degraded forests returns to pre-degradation levels. For example, after 14–15 years of regrowth, once-burned forests recovered a larger fraction of intact-forest ACD (80.2%) than canopy tree clusters (58.2%).

Table 2-1. Forest degradation from logging and fire alters ACD and stand structure relative to neighboring intact forests. Lidar-based estimates of the fraction of original canopy cover, number of canopy tree clusters, and the distribution of ACD in degraded forests. Degraded forests were partitioned along three axes of variability—degradation type, frequency, and timing. The lower, middle (median) and upper quartile of aboveground biomass density (Mg C ha⁻¹) are shown in ACD₂₅, ACD₅₀, and ACD₇₅, respectively.

	Intact	Logged (1-2 yrs)	Logged (4-5 yrs)	Logged (10-11 yrs)	Logged (14-15 yrs)	Logged (18-20 yrs)	Fire 1x (1-2 yrs)	Fire 1x (4-5 yrs)	Fire 1x (10-11 yrs)	Fire 1x (14-15 yrs)	Fire 2x	Fire 3x+
% Original	100	46.9	60.1	61.6	76.7	83.3	21.7	47.0	58.5	58.4	20.1	5.3
Canopy Clusters	170	79	104	111	127	145	34	78	92	99	31	8
ACD ₂₅	102.1	52.3	64.9	80.4	83.8	86.4	53.0	55.5	58.4	83.3	22.3	6.6
ACD ₅₀	113.5	68.4	76.8	89.7	98.8	105.5	64.3	65.6	74.0	91.0	31.6	10.3
ACD ₇₅	125.1	84.0	88.8	99.8	111.6	121.0	72.2	76.6	89.8	100.2	43.4	17.1

Table 2-2. Estimates based on the multiple linear regression models of aboveground carbon density predicted at four standard reporting periods following the most common logging and fire pathways. For each degradation class, modeled ACD and 95% confidence interval (in parentheses) are shown as the percentage of the intact forest reference (113.5 Mg C ha⁻¹). The confidence interval was calculated based on the mean of 10,000 confidence intervals generated from the Monte Carlo linear regressions, which were iteratively fit to the stand-level biomass estimates adjusted with noise proportionate to the stand-level standard errors. Model predictions for low- and high-severity fires are derived from model 2; all other predictions presented here are derived from model 1 (see Table S 2-2).

	Logged	Burned 1x (Average)	Burned 1x (Low)	Burned 1x (High)	Burned 2x	Burned 3x+
Y1	54.9 (49.4-60.2)	45.8 (38.0-53.6)	48.5 (41.0-56.1)	32.2 (24.1-40.2)	17.1 (8.5-25.8)	9.7 (4.5-14.9)
Y5	71.0 (67.5-74.5)	61.9 (56.3-67.6)	63.7 (58.0-69.2)	47.3 (41.0-53.5)	33.3 (25.2-41.4)	25.8 (20.0-31.7)
Y10	77.9 (73.6-82.3)	68.9 (63.1-74.7)	70.1 (64.4-75.8)	53.8 (47.5-60.2)	-	-
Y15	82.0 (76.9-87.1)	72.9 (66.8-79.1)	73.9 (67.9-80)	57.6 (51.0-64.2)	-	-

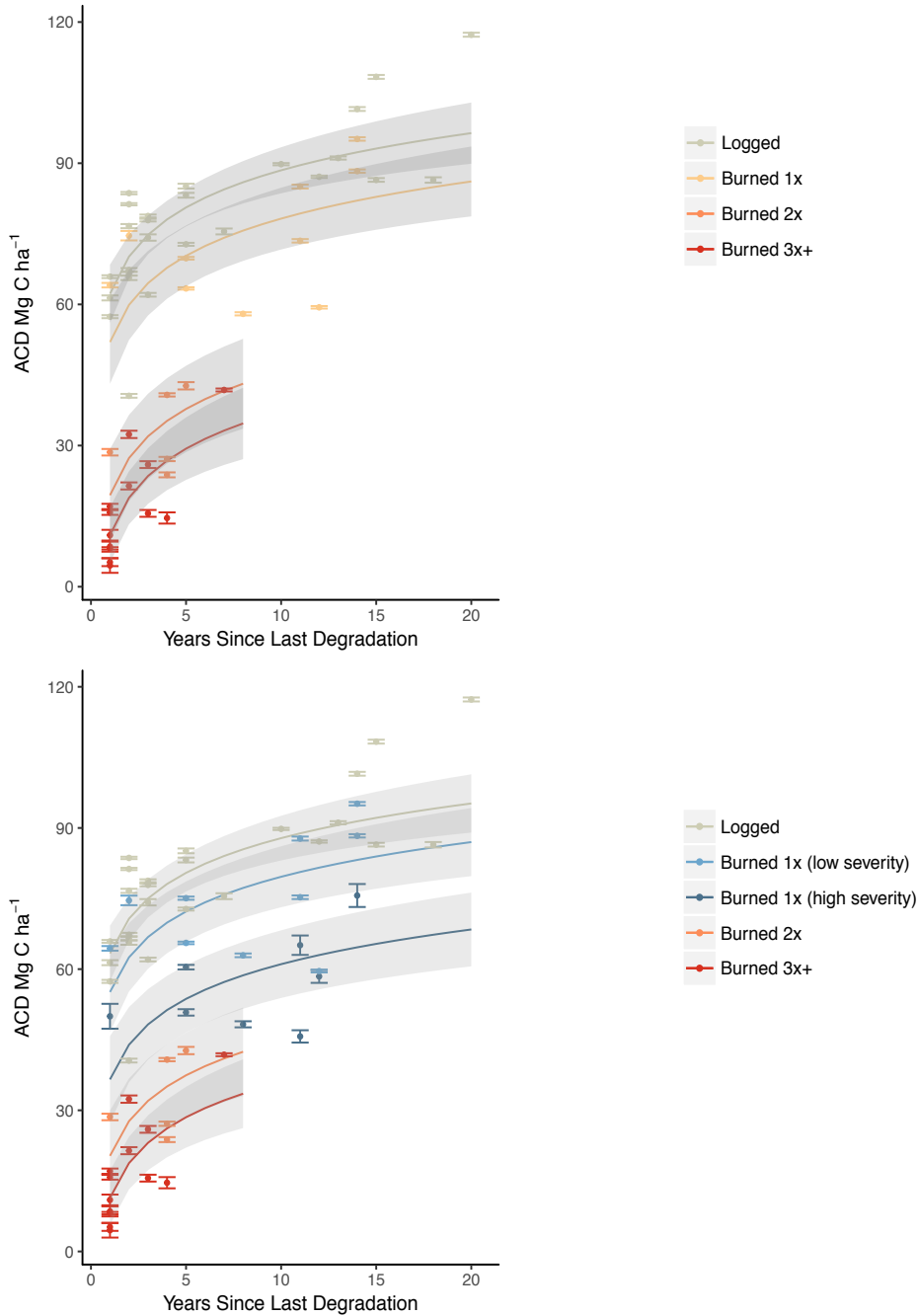


Figure 2-4. Patterns of aboveground biomass recovery following forest degradation highlight the magnitude and duration of ACD accumulation following fire. a) Relationship between ACD and stand age for logged, once-burned, twice-burned, and thrice-burned stands. b) Initial fire severity in once-burned forests further explains the heterogeneity in residual carbon stocks. Points correspond to estimated stand-level medians, error bars correspond to stand-level standard errors derived from 10,000 Monte Carlo stand-level aggregations, and the shaded bands represent the mean 95% confidence interval from 10,000 Monte Carlo simulations of the model fit. Model details are presented in Table S 2-3.

2.4 Discussion

Amazon forest degradation from logging and fire has a lasting impact on forest carbon stocks and canopy structure. The slow recovery of degraded forests underscores the need to address drivers of degradation to ensure the retention of carbon stocks and preserve complex canopy structure in frontier Amazon forests. Using a large sample of intact and degraded forests, we provide the first comprehensive look-up table of degradation emissions factors for Amazon forests to guide the incorporation of forest degradation within REDD+ MRV (tables 1 and 2). Our findings illustrate the persistence of degradation impacts beyond the time scales for REDD+ MRV and even REDD+ baselines (typically 10 years), providing the foundation for further investigations into the relative contributions from fire and logging to regional land-use emissions. ACD in degraded forests varied by two orders of magnitude across the study area (Table S 2-2), providing clear support for the creation of multiple classes of forest degradation within REDD+ or other carbon accounting frameworks based on degradation frequency, severity, and timing. Overall, understory fires led to larger and more persistent changes in ACD and forest structure than logging, consistent with previous findings from Longo *et al* (2016). Our results further demonstrate how fire severity and fire frequency contribute to non-linear declines in ACD and homogenization of degraded forest structure (Fig. 2-2, Tables 2-1 and 2-2). Collectively, these results address key data gaps that have hindered MRV of Amazon forest degradation.

Lidar-based estimates of carbon losses from fire were much larger than previous reports from experimental studies and forest inventories. For example, the reduction in ACD one year following a single burn in this study (54.2%) was

approximately three times larger than from experimental fires in the southeastern Amazon (Brando *et al* 2014). This discrepancy may reflect the improved capacity to characterize the heterogeneity of wildfire damages using airborne lidar or the difficulty for prescribed fires in experimental studies to replicate the emergent properties of wildfires, such as fire front intensity. Field studies have also reported smaller relative losses in ACD following fire (13.7%; Berenguer *et al* 2014). These differences may reflect the confounding influence of different age classes and burn frequencies, the challenges of capturing the length scales of spatial variability (see figure 3) using typical inventory plots (0.25–1.0 ha), or regional variability in fire intensity from climatic and forest-type specific responses to fire (e.g. Flores *et al* 2017). These broad discrepancies reinforce the need for large-scale studies of additional frontier landscapes to support emissions mitigation programs, including REDD+ MRV.

Reducing the incidence and frequency of understory forest fires would preserve both carbon stocks and habitat structure in frontier landscapes. The marginal carbon cost of recurrent fire events in this study suggests that avoiding just one additional fire in a previously burned forest would retain carbon stocks equivalent to one-third of the intact reference ACD. Notably, not all degradation sequences have the same cumulative impact. We contrast the non-linear impact of recurrent burns with the effect of selective logging before fire. In the case of recurrent burns, each fire leads to a greater proportional loss. However, logging before fire did not amplify the long-term carbon losses from fire, after accounting for fire frequency; nor was logging a significant predictor of carbon recovery, regardless of fire history. These

findings suggest that the distribution of fine litter (e.g. Balch *et al* 2008) may be a more important determinant of fire damage than large woody debris or canopy openings from logging.

The slow recovery of degraded ACD suggests that the continued omission of degradation from carbon accounting may result in substantial underreporting of forest carbon emissions. Relative to baseline periods, the frequency and severity of Amazon droughts (Boisier *et al* 2015, Duffy *et al* 2015) are projected to increase degradation risk in coming decades (Nobre *et al* 2016, Le Page *et al* 2017). The look-up table of proportional losses between degraded and intact forests developed in this study may facilitate the integration of carbon losses from fire and logging into REDD+ monitoring and reporting protocols. Further, accounting for carbon emissions from forest degradation may also reduce uncertainties in the Amazon carbon budget. Previous studies have either excluded a post-disturbance recovery term (Aragão *et al* 2014) or have combined secondary and degraded forests (Houghton *et al* 2000, Pan *et al* 2011), despite the diversity of loss and recovery pathways among degraded and secondary forest types (Poorter *et al* 2016).

Parallel ACD recovery curves in years 1–5 following logging and fire may reflect common site constraints, distinct mechanisms of forest growth, and model calibration. For example, different mechanisms of vegetation recovery and canopy closure may generate similar changes in estimated ACD, such as small gains in mean canopy height in logged forests and fast height growth of shorter resprouting or surviving trees in burned forests. Additionally, given that logging intensity is the single best predictor of ACD recovery time (Rutishauser *et al* 2015), evidence for

greater extracted wood volume of low-value species in frontier forests (Richardson and Peres 2016) than in interior forests and experimental logging sites may explain differences with previous estimates of ACD recovery in logged forests (e.g. Chambers *et al* 2004, Putz *et al* 2012, Andrade *et al* 2017). Further, moisture availability is a critical constraint on regeneration rates (Poorter *et al* 2016, Wagner *et al* 2016); moisture stress from the seasonality of the study site may limit recovery rates in both logged and burned forests. Additional observations in repeatedly burned forests are needed to constrain long-term estimates of recovery patterns (>5 years) in the more heavily degraded sites.

Airborne lidar captures details about 3D forest structure needed to quantify aboveground carbon stocks and advance quantitative reporting on biodiversity safeguards and other co-benefits of REDD+. Individual tree and plot-level data from airborne lidar provide insights into the mechanisms driving biomass variability and habitat impacts from forest degradation. The residual density of large canopy trees, which can be directly quantified using high-density airborne lidar, is an important driver of ACD variability in degraded forests (Slik *et al* 2013), and closely corresponds to the spatial patterns of fire-induced canopy mortality (Fig. S 2-7). In addition to ACD, the loss of canopy trees may also alter the forest micrometeorology, aerodynamic roughness, and successional success of grasses and lianas (Ray *et al* 2005, Silvério *et al* 2013). These changes, in turn, can increase vulnerability to windthrow and repeated fires, especially during drought years (e.g. Balch *et al* 2015). Canopy trees also serve as biodiversity refugia; the slower recovery of canopy tree clusters than carbon stocks in this study may suggest a more persistent impact of

degradation on biodiversity than biomass in the first decades following logging or fire, consistent with findings from Martin *et al* (2013). Characterizing the time-integrated effects of avoided degradation on forest structure is clearly an important step for policies and management that aim to promote the retention of both biomass and biodiversity. Measurement and monitoring capabilities to support REDD+ commitments to safeguard biodiversity and promote other co-benefits are not yet operational (Goetz *et al* 2015). This work highlights the potential of airborne lidar to advance REDD+ MRV for both carbon and non-carbon objectives.

Our findings provide a detailed characterization of the carbon and habitat changes following Amazon forest degradation, but additional measurements are needed to assess regional variability in degradation impacts. Additional lidar samples across gradients in land use, forest type, and climate may identify important differences in degradation impacts and ACD recovery. For example, previous work suggests that transitional forests along the southern extent of the Amazon may be more resilient to mortality from a single, low-severity fire during average weather conditions (Brando *et al* 2012) than interior forests. By contrast, forests in Central Amazon floodplains have exposed roots during dry periods, thin bark, and lack the ability to resprout, rendering them more vulnerable to fire-induced dieback (Flores *et al* 2017). Additionally, multi-temporal observations are needed to unequivocally attribute ACD losses to degradation, characterize delayed mortality, and investigate the potential for arrested succession (Barlow *et al* 2003). Multi-temporal studies may also help constrain interannual variability in fire damages (Brando *et al* 2014), consistent with the ~15% difference in ACD observed in this study between low and

high-severity damages within a single fire. Complementary field measurements may help characterize key aspects of degraded forest structure that are not well captured by airborne lidar, such as the species distribution of regeneration from seeds or sprouts and the selective impact of degradation on mean wood density (Bunker *et al* 2005, Longo *et al* 2016). Lastly, the strong correspondence between changes in Landsat surface reflectance and lidar-derived estimates of forest structure and ACD in burned forests may support regional estimates of carbon losses from understory fires using Landsat or similar moderate resolution imagery.

2.5 Conclusion

Forest degradation is ubiquitous in frontier Amazon forests, and damages from logging and fire were larger and longer lasting than previously reported for our southern Amazon study region. Combining the lookup table of emissions estimates from this study with activity data from satellite monitoring programs may allow for regional estimates of combined emissions from deforestation and forest degradation for REDD+. Understory fires—particularly, repeated burns—pose the greatest risk to forest carbon stocks and canopy structure along the Amazon arc of deforestation. Thus, avoiding additional fires in frontier landscapes may have an outsized benefit for carbon retention and habitat. Routine monitoring of frontier forests with airborne lidar may provide additional insights regarding the direct impacts of forest degradation on both carbon stocks and forest structure, including potential interannual variability from climate controls on fire severity or market influences on logging removals. Our approach to disentangle the complex legacy of degradation by combining forest

inventory, airborne lidar, and Landsat time series offers a blueprint to generate degradation emissions factors in other geographies and regional circumstances.

Acknowledgements

This work was partially supported by a National Science Foundation Doctoral Dissertation Research Improvement Grant (grant 1634168), a NASA Earth and Space Science Fellowship (D Rappaport), and NASA's Carbon Monitoring System program. Additional support was provided by the Brazilian National Council for Scientific and Technological Development (CNPq, grant 457927/2013-5) and Science Without Borders program (D Morton), and the São Paulo State Research Foundation (FAPESP, grant 2015/07227-6, M Longo). M Keller was supported as part of the Next Generation Ecosystem Experiments-Tropics, funded by the US Department of Energy, Office of Science, Office of Biological and Environmental Research. Support for data acquisition and M.N. dos-Santos was provided by the Sustainable Landscapes Brazil project, a collaboration of the Brazilian Agricultural Research Corporation (EMBRAPA), the US Forest Service, USAID, and the US Department of State. We gratefully acknowledge the assistance from Hyeungu Choi with lidar data processing.

References

- Aguiar A P D *et al* 2016 Land use change emission scenarios: anticipating a forest transition process in the Brazilian Amazon *Glob. Change Biol.* **22** 1821–40
- Alencar A, Nepstad D and Diaz M C V 2006 Forest understory fire in the Brazilian Amazon in ENSO and Non-ENSO years: area burned and committed carbon emissions *Earth Interact.* **10** 1–17
- Andrade R B, Balch J K, Parsons A L, Armenteras D, Roman-Cuesta R M and Bulkan J 2017

- Scenarios in tropical forest degradation: carbon stock trajectories for REDD+ *Carbon Balance Manage.* **12** 6
- Aragão L E O C and Shimabukuro Y E 2010 The incidence of fire in Amazonian forests with implications for REDD *Science* **328** 1275–8
- Aragão L E O C, Poulter B, Barlow J B, Anderson L O, Malhi Y, Saatchi S, Phillips O L and Gloor E 2014 Environmental change and the carbon balance of Amazonian forests *Biol. Rev.* **89** 913–31
- Asner G P, Keller M, Pereira R Jr, Zweede J C and Silva J N 2004 Canopy damage and recovery after selective logging in Amazonia: field and satellite studies *Ecol. Appl.* **14** 280–98
- Asner G P, Knapp D E, Broadbent E N, Oliveira P J, Keller M and Silva J N 2005 Selective logging in the Brazilian Amazon *Science* **310** 480–2
- Avitabile V *et al* 2016 An integrated pan-tropical biomass map using multiple reference datasets *Glob. Change Biol.* **22** 1406–20
- Baccini A *et al* 2012 Estimated carbon dioxide emissions from tropical deforestation improved by carbon-density maps *Nat. Clim. Change* **2** 182–5
- Balch J K, Nepstad D C, Brando P M, Curran L M, Portela O, De CARVALHO O and Lefebvre P 2008 Negative fire feedback in a transitional forest of southeastern Amazonia *Glob. Change Biol.* **14** 2276–87
- Balch J K *et al* 2015 The susceptibility of southeastern Amazon forests to fire insights from a large scale burn experiment *BioScience* **65** 893–905
- Barlow J, Peres C A, Lagan B O and Hugaasen T 2003 Large tree mortality and the decline of forest biomass following Amazonian wildfires *Ecol. Lett.* **6** 6–8
- Becknell J M, Kissing Kucek L and Powers L 2012 Aboveground biomass in mature and secondary seasonally dry tropical forests: a literature review and global synthesis *Forest Ecol. Manage.* **276** 88–95
- Berenguer E, Ferreira J, Gardner T A, Aragão L E O C, De Camargo P B, Cerri C E, Durigan M, Oliveira R C D, Vieira I C G and Barlow J 2014 A large-scale field assessment of carbon stocks in human-modified tropical forests *Glob. Change Biol.* **20** 3713–26
- Bergen K M, Goetz S J, Dubayah R O, Henebry G M, Hunsaker C T, Imhoff M L, Nelson R F, Parker G G and Radeloff V C 2009 Remote sensing of vegetation 3-D structure for biodiversity and habitat: Review and implications for lidar and radar spaceborne missions *J. Geophys. Res. Biogeosci.* **114**

- Boisier J P, Ciais P, Ducharne A and Guimberteau M 2015 Projected strengthening of Amazonian dry season by constrained climate model simulations *Nat. Clim. Change* **5** 656–60
- Brando P M, Nepstad D C, Balch J K, Bolker B, Christman M C, Coe M and Putz F E 2012 Fire-induced tree mortality in a neotropical forest: the roles of bark traits, tree size, wood density and fire behavior *Glob. Change Biol.* **18** 630–41
- Brando P M *et al* 2014 Abrupt increases in Amazonian tree mortality due to drought–fire interactions *Proc. Natl Acad. Sci.* **111** 6347–52
- Brazil 2014 Brazil’s submission of a Forest Reference Emission Level (FREL) for reducing emissions from deforestation in the Amazonia biome for REDD+ results-based payments under the UNFCCC
- Bunker D E, DeClerck F, Bradford J C, Colwell R K, Perfecto I, Phillips O L, Sankaran M and Naeem S 2005 Species loss and aboveground carbon storage in a tropical forest *Science* **310** 1029–31
- Bustamante M *et al* 2016 Toward an integrated monitoring framework to assess the effects of tropical forest degradation and recovery on carbon stocks and biodiversity *Glob. Change Biol.* **22** 92–109
- Canadell J G and Raupach M R 2008 Managing forests for climate change mitigation *Science* **320** 1456–7
- Chambers J Q, Higuchi N, Teixeira L M, Dos Santos J, Laurance S G and Trumbore S E 2004 Response of tree biomass and wood litter to disturbance in a Central Amazon forest *Oecologia* **141** 596–611
- Chen Y, Randerson J T, Morton D C, DeFries R S, Collatz G J, Kasibhatla P S, Giglio L, Jin Y and Marlier M E 2011 Forecasting fire season severity in South America using sea surface temperature anomalies *Science* **334** 787–91
- Duffy P B, Brando P, Asner G P and Field C B 2015 Projections of future meteorological drought and wet periods in the Amazon *Proc. Natl Acad. Sci.* **112** 13172–7
- Flores B M, Holmgren M, Xu C, van Nes E H, Jakovac C C, Mesquita R C G and Scheffer M 2017 Floodplains as an Achilles’ heel of Amazonian forest resilience *Proc. Natl Acad. Sci.* **114** 4442–6
- Friedlingstein P, Meinshausen M, Arora V K, Jones C D, Anav A, Liddicoat S K and Knutti R 2014 Uncertainties in CMIP5 climate projections due to carbon cycle feedbacks *J. Clim.* **27** 511–26
- Gatti L V *et al* 2014 Drought sensitivity of Amazonian carbon balance revealed by

- atmospheric measurements *Nature* **506** 76–80
- Goetz S J, Hansen M, Houghton R A, Walker W, Laporte N and Busch J 2015 Measurement and monitoring needs, capabilities and potential for addressing reduced emissions from deforestation and forest degradation under REDD+ *Environ. Res. Lett.* **10** 123001
- Griscom B W *et al* 2017 Natural climate solutions *Proc. Natl Acad. Sci.* **114** 11645–50
- Hansen A J, Phillips L B, Dubayah R, Goetz S and Hofton M 2014 Regional-scale application of lidar: variation in forest canopy structure across the southeastern US *Forest Ecol. Manage.* **329** 214–26
- Holdsworth A R and Uhl C 1997 Fire in Amazonian selectively logged rain forest and the potential for fire reduction *Ecol. Appl.* **7** 713–25
- Houghton R A, Skole D L, Nobre C A, Hackler J L, Lawrence K T and Chomentowski W H 2000 Annual fluxes of carbon from deforestation and regrowth in the Brazilian Amazon *Nature* **403** 301–4
- INPE 2015 Amazon program - monitoring the Brazilian Amazon by satellite: the Prodes, Deter, Degrad and Terraclass systems (www.inpe.br)
- Keller M, Asner G P, Silva J M N and Palace. M 2004 Sustainability of selective logging of upland forests in the Brazilian Amazon: carbon budgets and remote sensing as tools for evaluation of logging effects *Working Forests in the American Tropics: Conservation Through Sustainable Management?* ed D J Zarin, J Alavalapati, F E Putz and M Schmink (New York: Colombia University Press) pp 41–63
- Le Page Y, Morton D, Hartin C, Bond-Lamberty B, Pereira J M C, Hurtt G and Asrar G 2017 Synergy between land use and climate change increases future fire risk in Amazon forests *Earth Syst. Dyn.* **8** 1237
- Le Qué'ré' C, Andrew R M, Canadell J G, Sitch S, Korsbakken J I, Peters G P, Manning A C, Boden T A, Tans P P and Houghton R A 2016 Global carbon budget 2016 *Earth Syst. Sci. Data* **8** 605
- Longo M, Keller M M, dos-Santos M N, Leitold V, Pinagé' E R, Baccini A, Saatchi S, Nogueira E M, Batistella M and Morton D C 2016 Aboveground biomass variability across intact and degraded forests in the Brazilian Amazon *Glob. Biogeochem. Cycles* **30** 1639–60
- Martin P A, Newton A C and Bullock J M 2013 Carbon pools recover more quickly than plant biodiversity in tropical secondary forests *Proc. R. Soc. B* **280** 20132236
- Matricardi E A T, Skole D L, Cochrane M A, Pedlowski M and Chomentowski W 2007 Multi-temporal assessment of selective logging in the Brazilian Amazon using Landsat

- data *Int. J. Remote Sens.* **28** 63–82
- Mertz O *et al* 2012 The forgotten D: challenges of addressing forest degradation in complex mosaic landscapes under REDD+ *Geografisk Tidsskrift-Danish J. Geogr.* **112** 63–76
- Morton D C, DeFries R S, Nagol J, Souza Jr. C M, Kasischke E S, Hurtt G C and Dubayah R 2011 Mapping canopy damage from understory fires in Amazon forests using annual time series of Landsat and MODIS data *Remote Sens. Environ.* **115** 1706–20
- Morton D C, Page Y L, DeFries R, Collatz G J and Hurtt G C 2013 Understorey fire frequency and the fate of burned forests in southern Amazonia *Phil. Trans. R. Soc. B Biol. Sci.* **368** 20120163
- Nobre C A, Sampaio G, Borma L S, Castilla-Rubio J C, Silva J S and Cardoso M 2016 Land-use and climate change risks in the Amazon and the need of a novel sustainable development paradigm *Proc. Natl Acad. Sci.* **113** 10759–68
- Pan Y *et al* 2011 A large and persistent carbon sink in the world's forests *Science* **333** 988–93
- Penman J *et al* 2003 *Good Practice Guidance for Land Use, Land-Use Change and Forestry* (Kanagawa: IPCC National Greenhouse Gas Inventories Programme, Institute for Global Environmental Strategies)
- Pereira D, Santos D, Vedoveto M, Guimarães J and Ver'issimo A 2010 *Fatos Florestais* (Imazon: Belém, PA)
- Poorter L *et al* 2016 Biomass resilience of Neotropical secondary forests *Nature* **530** 211–4
- Putz F E *et al* 2012 Sustaining conservation values in selectively logged tropical forests: the attained and the attainable *Conserv. Lett.* **5** 296–303
- Ray D, Nepstad D and Moutinho P 2005 Micrometeorological and canopy controls of fire susceptibility in a forested Amazon landscape *Ecol. Appl.* **15** 1664–78
- Richardson V A and Peres C A 2016 Temporal decay in timber species composition and value in Amazonian logging concessions *PLoS ONE* **11** e0159035
- Rutishauser E *et al* 2015 Rapid tree carbon stock recovery in managed Amazonian forests *Curr. Biol.* **25** R787–8
- Sato L Y, Gomes V C F, Shimabukuro Y E, Keller M, Arai E, dos-Santos M N, Brown I F and e Cruz de Aragã'o L E O 2016 Post-fire changes in forest biomass retrieved by airborne LiDAR in Amazonia *Remote Sens.* **8** 839
- Slik J W F *et al* 2013 Large trees drive forest aboveground biomass variation in moist lowland forests across the tropics *Glob. Ecol. Biogeogr.* **22** 1261–71
- Silva C A, Crookston N L, Hudak A T and Vierling L A 2015 rLiDAR: An R package for reading, processing and visualizing LiDAR (Light Detection and Ranging) data,

version 0.1

- Silvério D V, Brando P M, Balch J K, Putz F E, Nepstad D C, Oliveira-Santos C and Bustamante M M C 2013 Testing the Amazon savannization hypothesis: fire effects on invasion of a neotropical forest by native cerrado and exotic pasture grasses *Phil. Trans. R. Soc. B Biol. Sci.* **368** 20120427
- Souza C M, Roberts D A and Monteiro A 2005 Multitemporal analysis of degraded forests in the southern Brazilian Amazon *Earth Interact.* **9** 1–25
- Souza A P, Mota L L, Zamadei T, Martin C C, Almeida F T and Paulino J 2013 Classificação climática e balanço hídrico climatológico no estado de Mato Grosso *Nativa* **1** 34–43
- Uhl C and Vieira I C G 1989 Ecological impacts of selective logging in the Brazilian Amazon: a case study from the Paragominas region of the state of Pará *Biotropica* 98–106
- van der Werf G R, Morton D C, DeFries R S, Olivier J G, Kasibhatla P S, Jackson R B, Collatz G J and Randerson J T 2009 CO₂ emissions from forest loss *Nat. Geosci.* **2** 737–8
- Vargas R, Allen M F and Allen E B 2008 Biomass and carbon accumulation in a fire chronosequence of a seasonally dry tropical forest *Glob. Change Biol.* **14** 109–24
- Wagner F H *et al* 2016 Climate seasonality limits leaf carbon assimilation and wood productivity in tropical forests *Biogeosci. Katlenburg-Lindau* **13** 2537–62

2.6 Supplemental Materials

2.6.1 Degradation and deforestation classification methods

Degradation and deforestation were classified using distinct spatial, spectral, and temporal attributes in time series of annual Landsat data from 1984-2016 for three Landsat scenes (225/068; 226/068; 226/069) (Fig. 2.6.1). Contiguous patches of forest change ≥ 1 ha were divided between deforestation and understory forest fires based on the multi-year trajectory of damage and recovery (Morton *et al* 2011, Morton *et al* 2013). The transition from forest to non-forest in two or more consecutive years was considered deforestation, based on dry-season normalized difference vegetation index (NDVI) thresholds for forest (>0.75) and non-forest (<0.65). Understory forest fires exhibit an intermediate loss of dry-season NDVI, followed by one or more years of recovery in dry-season NDVI (Fig. 2.6.1).

We used evidence for larger logging infrastructure, including logging roads and log landing decks (patios, small clearings where harvested wood is stacked before being transported to saw mills), to map the extent of annual logging activity. Logging infrastructure is easily identifiable at the scale of a Landsat pixel (Asner *et al* 2004). Previous studies have also identified logging damages using spectral mixture models to evaluate sub-pixel changes in canopy reflectance (Asner *et al* 2004, 2005, Souza *et al* 2005). However, these approaches typically require greater radiometric resolution, which is only possible with Landsat 7 or more recent instruments. Given the interest in this study in degradation dynamics during the 1980s and 1990s, periods when only Landsat Thematic Mapper data are available, we used a classification approach based on the unique spatial pattern of logging damages that could be identified in data from all Landsat sensors.

Logging patios were initially identified using a 3x3-pixel moving window approach to locate candidate center pixels with large changes in NDVI between years, surrounded by forest (mean NDVI of neighboring pixels >0.6). Candidate patios were ranked based on the magnitude of NDVI change between years, using an iterative process to select and classify center pixels with NDVI differences of 0.06 to >0.12 .

Three spatial filters were used to evaluate and group candidate patio detections into logging areas. First, the highest confidence pixel was selected from all candidate patios using an 11-pixel window (330 m). This search radius was selected based on previous studies of patio density in conventional logging operations (e.g. Matricardi *et al* 2007). Second, we identified road features that were initially classified as candidate patios using two tests. Linear arrangements of candidate pixels within a 1 degree angle tolerance and >10 pixels within a 150-pixel linear distance were discarded as road or edge features. Third, we eliminated isolated patio detections based on a neighborhood search for clusters of high-confidence patio detections. The search algorithm calculated the median distance between neighboring patio detections. Pixels with a median distance >6 and <14 pixels and a low standard deviation of neighbor distance (<6 pixels) were retained as clusters corresponding to recent logging activity. Finally, we estimated the logged area associated with each cluster of logging patios by creating a convex polygon encompassing each cluster of patio detections.

References

- Asner, G.P., Keller, M., Pereira Jr., R., Zweede, J.C., 2002. Remote sensing of selective logging in Amazonia: Assessing limitations based on detailed field observations, Landsat ETM+, and textural analysis. *Remote Sensing of Environment* 80, 483–496.
[https://doi.org/10.1016/S0034-4257\(01\)00326-1](https://doi.org/10.1016/S0034-4257(01)00326-1)
- Asner, G.P., Knapp, D.E., Broadbent, E.N., Oliveira, P.J., Keller, M., Silva, J.N., 2005. Selective logging in the Brazilian Amazon. *Science* 310, 480–482.
- Matricardi, E.A.T., Skole, D.L., Cochrane, M.A., Pedlowski, M., Chomentowski, W., 2007. Multi-temporal assessment of selective logging in the Brazilian Amazon using Landsat data. *International Journal of Remote Sensing* 28, 63–82.
<https://doi.org/10.1080/01431160600763014>
- Morton, D.C., DeFries, R.S., Nagol, J., Souza Jr., C.M., Kasischke, E.S., Hurtt, G.C., Dubayah, R., 2011. Mapping canopy damage from understory fires in Amazon forests using annual time series of Landsat and MODIS data. *Remote Sensing of Environment* 115, 1706–1720.
<https://doi.org/10.1016/j.rse.2011.03.002>
- Morton, D.C., Page, Y.L., DeFries, R., Collatz, G.J., Hurtt, G.C., 2013. Understorey fire frequency and the fate of burned forests in southern Amazonia. *Philosophical Transactions*

of the Royal Society B: Biological Sciences 368, 20120163.

<https://doi.org/10.1098/rstb.2012.016>

Souza, C.M., Roberts, D.A., Monteiro, A., 2005. Multitemporal Analysis of Degraded Forests in the Southern Brazilian Amazon. *Earth Interact.* 9, 1–25. <https://doi.org/10.1175/EI132.1>

2.6.1 Supplemental figures and tables

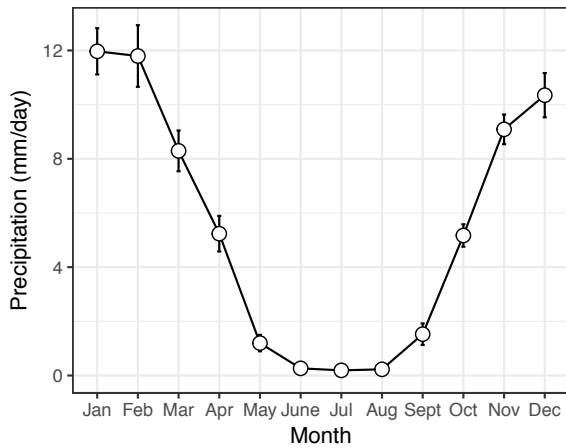


Figure S 2-1. Climatology of mean monthly precipitation for the study region based on 0.25° data for 2007-2017 from the Tropical Rainfall Measuring Mission (TRMM, 3B43v7). Error bars correspond to the monthly standard error derived from the 10-year time series.

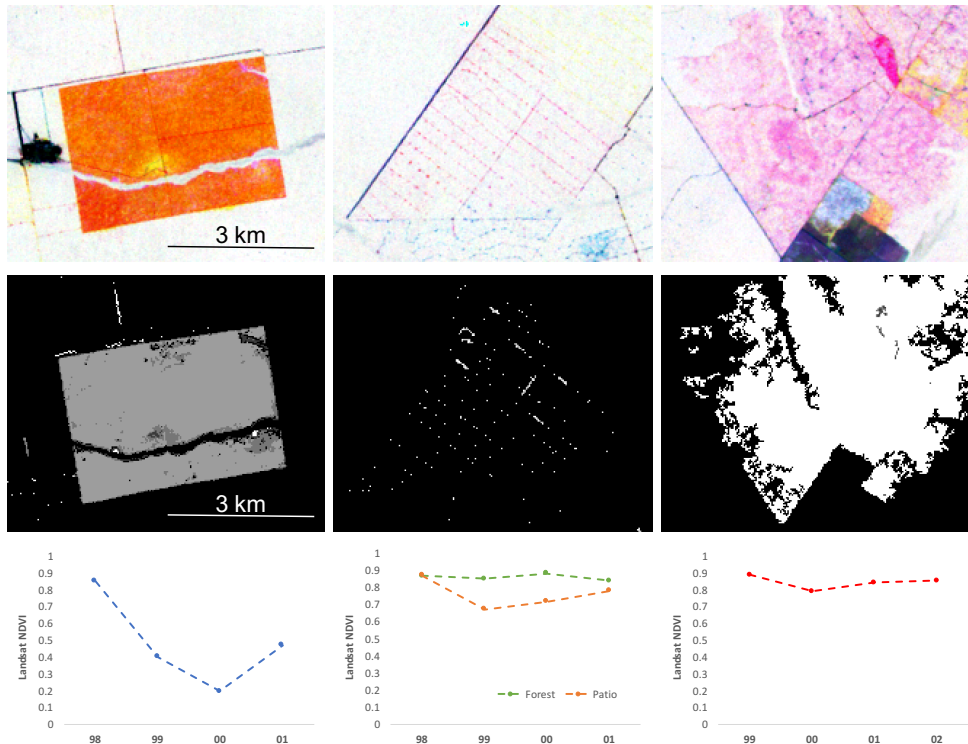


Figure S 2-2. The spatial, spectral, and temporal patterns of forest damage and recovery were used to separate deforestation, selective logging, and understory forest fire damages in Amazon forests. Patch size, shape, and the magnitude of forest damages were the first set of criteria for classification, followed by tests for the multi-year NDVI trajectory (third row) to separate deforestation from selective logging and understory forest fires. Small patches typical of logging infrastructure (1-3 Landsat pixels) were evaluated based on tests for spatial clustering.

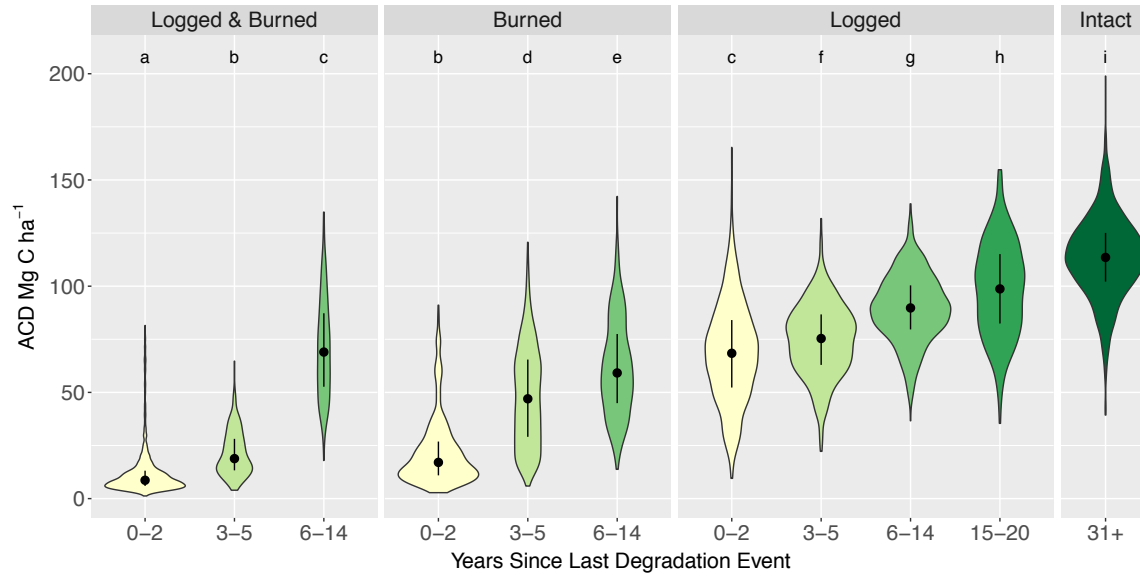


Figure S 2-3. The recovery of aboveground carbon density over time for logged and burned forests. Although biomass accumulates with increasing time since last disturbance, the carbon consequences of both logging and fire were persistent. The median and interquartile range of each group are indicated with the black circle and line. The tails of the violins are trimmed to the range of data, and all violins have the same area prior to trimming the tails. Distinct letters indicate significant differences among distributions from a pairwise Wilcoxon test with a Holm correction procedure to adjust α for multiple testing.

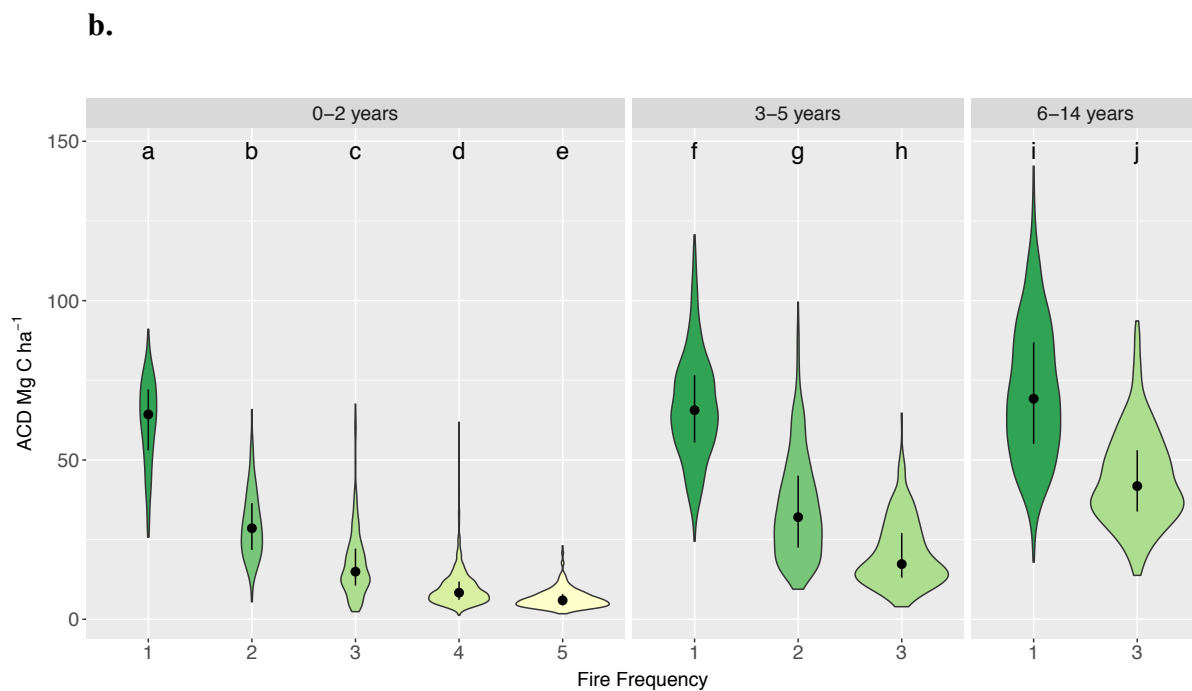
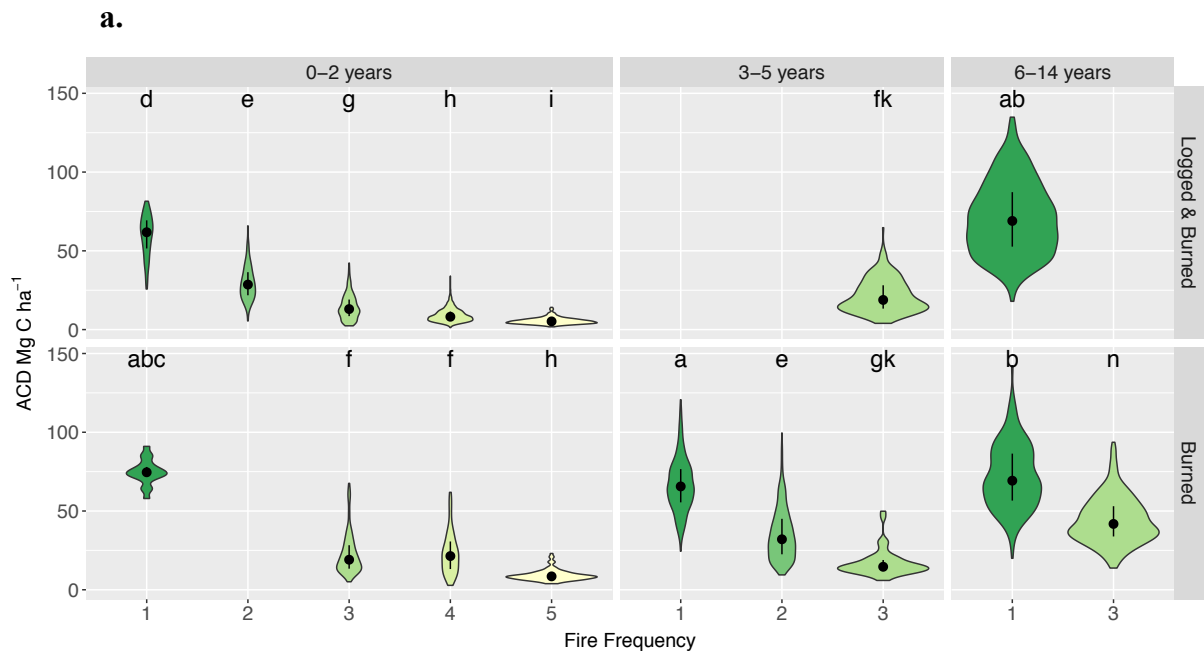


Figure S 2-4. Fire frequency and time since last fire were more important than logging history for ACD variability in degraded forests. In these two figures, burned forest ACD is separated by fire frequency for three age classes of years since last degradation event. The top panel (a) separates logged and burned forests from burned forests, whereas the bottom panel (b) presents data for all burned forests, regardless of logging history. The historical presence of logging does not influence the long-term (>3 years) cumulative effect of multiple fire events, once fire frequency and age are considered. Distinct letters indicate significant differences among distributions from a pairwise Wilcoxon test with a Holm correction procedure to adjust α for multiple testing.

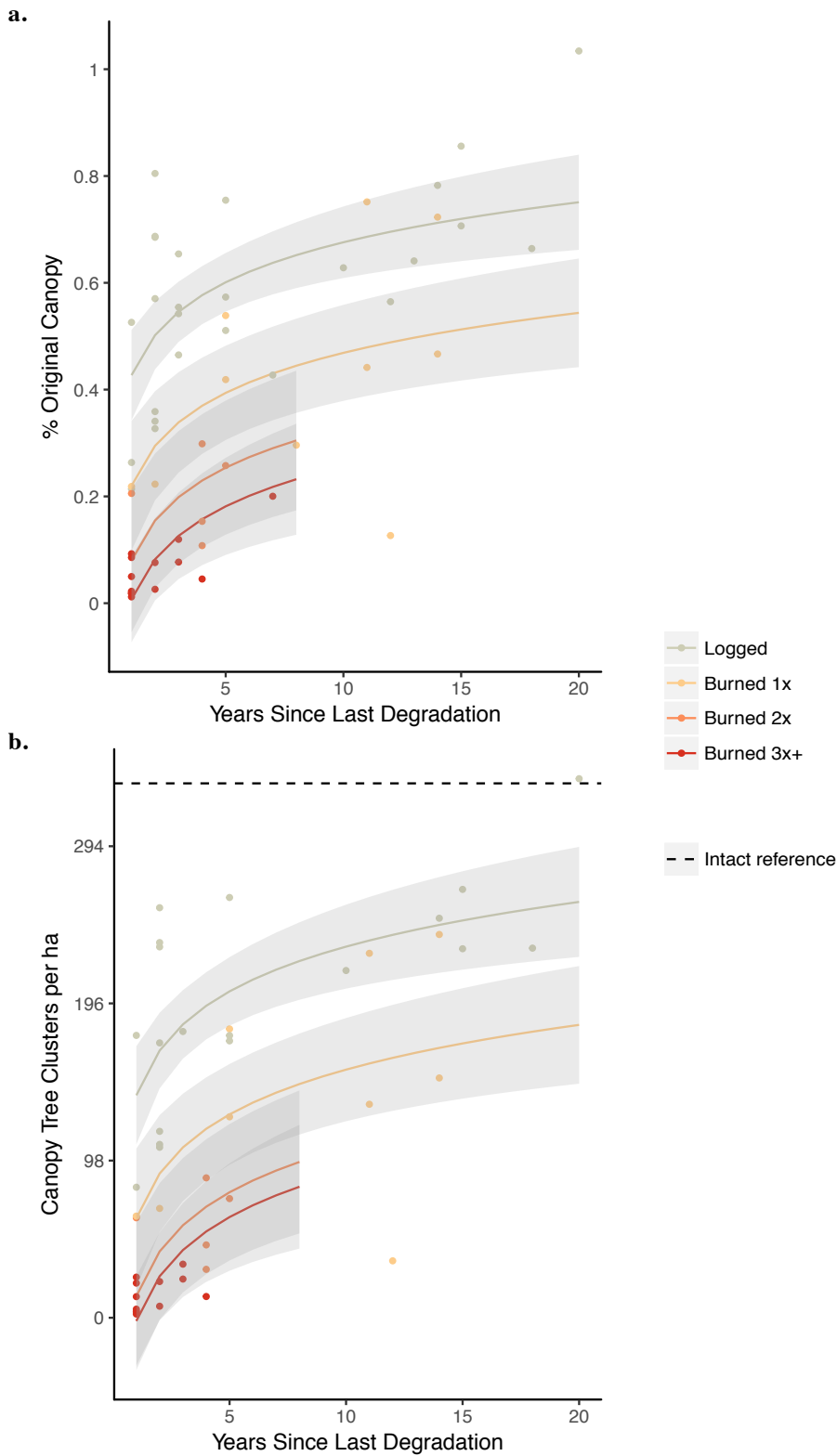


Figure S 2-5. The recovery trajectories for canopy structure following logging, single, and recurrent fires complement ACD information regarding the restoration of ecosystem function following forest degradation. The trajectory of two complementary indices derived from lidar, % residual canopy (a) and density of canopy trees per hectare (b) indicate that fire results in the largest and most persistent alterations to canopy structure. The curves correspond to the best-fit regression lines presented in table S4.

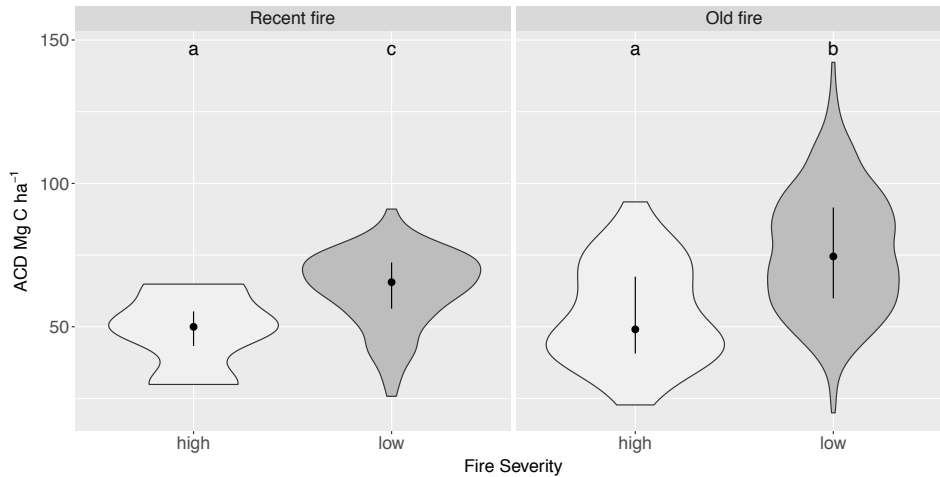


Figure S 2-6. Within-fire differences in ACD from initial fire severity were evident more than a decade following fire damages. Violin plots show ACD distributions following single burns for recent fires (≤ 2 years) and older fires (11-14 years). Distinct letters indicate statistically significant differences (Wilcoxon test with $p < 0.05$).

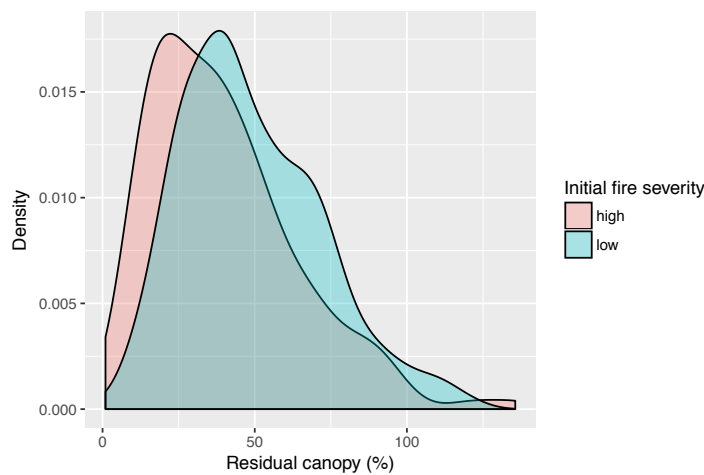


Figure S 2-7. Patterns of canopy mortality following a single fire event are not uniform. Post-fire variability in canopy structure following high- and low-severity damages can help explain the observed variability in post-fire ACD. The density plots compare distributions of the residual canopy structure aggregated at 0.25 ha for the once-burned forests burned in the 2010 drought year, where intra-stand differences from initial fire severity were most preserved. The two distributions are significantly different (Wilcoxon test with $p < 0.05$).

Table S 2-1. The lidar data were collected by Sustainable Landscapes Brazil, and can be freely accessed from: <https://www.paisagenslidar.cnptia.embrapa.br/webgis/>. Acquisition dates, names and corresponding stand IDs are listed below. Additional stand-level information can be derived from Table S2.

Date	Name	Stand ID
8/12/2013-8/13/13	FNA	3
8/15/13	FN1	18, 57
8/15/13	FN2	12, 44, 47, 48, 51, 53, 54, 58
6/22/2015-7/06/2015	FN3	1-2, 4-11, 13-17, 19-43, 45-46, 49-50, 52, 55-56

Table S 2-2. Attributes of 58 forest stands derived from the combination of Landsat and lidar data, including aboveground carbon density (ACD, Mg C ha⁻¹), frequency, and age since last degradation event. The distribution of estimated carbon stocks in each stand are summarized using ACD25—lower quartile; ACD50—median; SE—standard error derived from 10,000 Monte Carlo simulations for stand-level aggregation; ACD75—upper quartile; Δ ACD—% difference relative to median ACD in nearby intact stands. History Classes: U—undisturbed; L—logged once; L(2x)—logged twice; LB—logged and burned; B—burned.

Stand ID	History	Fire freq.	Last fire	Last logging	Age	Stand area (ha)	ACD25	ACD50	SE	ACD75	% Intact
1	LB	3	2014	2007	1	19.5	3.8	4.5	1.6	5.6	3.9
2	LB	5	2014	2000	1	63.3	4.1	5.2	0.8	6.5	4.6
3	LB	4	2012	2010	1	498.5	6.0	8.2	0.2	11.4	7.2
4	B	5	2014	NA	1	25.0	6.9	8.5	1.1	10.2	7.5
5	LB	3	2014	2010	1	18.3	8.2	11.0	1.1	14.3	9.6
6	B	3	2011	NA	4	12.3	11.9	14.6	1.2	18.9	12.9
7	LB	3	2012	1999	3	39.8	11.4	15.1	0.7	21.1	13.3
8	LB	3	2014	2010	1	75.5	11.8	16.3	0.5	21.7	14.4
9	B	3	2014	NA	1	50.3	13.0	17.1	0.6	22.5	15.0
10	B	4	2013	NA	2	27.5	13.2	21.4	0.8	30.7	18.9
11	B	2	2011	NA	4	43.8	16.2	23.8	0.5	38.3	20.9
12	LB	3	2010	2002	3	22.5	21.7	26.2	0.7	34.5	23.1
13	B	2	2011	NA	4	56.0	20.5	27.1	0.4	34.4	23.9
14	L(2x)	2	2012	2014	1	23.0	21.8	28.6	0.7	36.4	25.2
15	B	3	2013	NA	2	17.5	24.0	32.4	0.8	45.2	28.5
16	L	0	NA	2013	2	56.0	28.5	39.0	0.4	51.3	34.4
17	B	2	2011	NA	4	69.5	30.3	40.8	0.3	53.6	35.9
18	B	3	2006	NA	7	79.5	33.8	41.8	0.3	53.1	36.8
19	B	2	2010	NA	5	12.5	35.4	42.7	0.8	50.5	37.6
20	L(2x)	0	NA	2014	1	62.0	44.9	57.3	0.3	70.0	50.5
21	LB	1	2007	2004	8	51.5	46.2	57.9	0.3	69.0	51.0
22	B	1	2003	NA	12	79.3	50.6	59.4	0.3	68.2	52.3
23	L(2x)	0	NA	2014	1	23.5	51.4	61.0	0.5	67.0	53.7
24	LB	1	2014	2011	1	27.8	51.5	61.8	0.5	69.4	54.4
25	L	0	NA	2012	3	37.0	50.6	62.0	0.4	75.1	54.6
26	B	1	2010	NA	5	86.5	54.1	63.4	0.3	73.7	55.8
27	L	0	NA	2013	2	24.8	54.0	65.5	0.5	75.4	57.7
28	L	0	NA	2014	1	63.0	51.8	65.9	0.3	78.5	58.0
29	L	0	NA	2013	2	26.8	58.6	66.6	0.4	74.3	58.6
30	LB	1	2004	1997	11	48.3	52.9	69.3	0.4	81.6	61.1
31	B	1	2010	NA	5	64.3	57.5	69.8	0.3	82.1	61.5
32	L	0	NA	2010	5	46.8	62.5	72.8	0.3	84.3	64.1
33	B	1	2013	NA	2	4.5	72.3	74.6	1.0	78.0	65.7

34	L	0	NA	2013	2	54.8	60.7	75.4	0.4	89.0	66.4
35	L	0	NA	2012	3	10.5	67.0	75.4	0.7	88.8	66.4
36	L(2x)	0	NA	2008	7	11.5	62.9	75.5	0.6	91.4	66.5
37	L(2x)	0	NA	2013	2	25.3	62.7	76.5	0.4	87.8	67.4
38	L(2x)	0	NA	2012	3	59.0	63.5	77.9	0.3	87.5	68.6
39	L	0	NA	2012	3	47.0	68.5	78.8	0.3	86.5	69.4
40	L	0	NA	2013	2	82.8	67.8	81.3	0.2	97.9	71.6
41	L	0	NA	2010	5	17.0	71.2	83.2	0.5	95.9	73.3
42	L(2x)	0	NA	2013	2	71.3	72.4	83.6	0.2	95.2	73.7
43	B	1	2004	NA	11	29.0	69.5	84.6	0.4	98.7	74.5
44	L	0	NA	2008	5	16.5	71.7	85.1	0.5	92.7	75.0
45	L	0	NA	1997	18	12.3	77.3	86.4	0.6	98.0	76.1
46	L	0	NA	2000	15	28.3	73.9	86.8	0.4	98.0	76.4
47	L	0	NA	2001	12	66.0	78.9	87.0	0.2	95.8	76.6
48	B	1	1999	NA	14	32.3	82.4	88.3	0.3	95.2	77.8
49	L	0	NA	2005	10	84.8	80.4	89.7	0.2	99.8	79.0
50	L	0	NA	2002	13	36.5	80.2	90.9	0.3	101.3	80.1
51	LB	1	1999	1993	14	28.5	85.2	95.2	0.4	108.2	83.8
52	U	0	NA	NA	NA	5.0	85.5	99.0	0.9	104.8	87.2
53	L	0	NA	1999	14	31.0	89.9	104.3	0.4	113.2	91.9
54	L	0	NA	1998	15	20.3	98.1	108.3	0.4	119.2	95.4
55	U	0	NA	NA	NA	10.8	99.0	108.6	0.6	119.8	95.6
56	U	0	NA	NA	NA	9.3	102.0	113.5	0.6	119.6	100.0
57	U	0	NA	NA	NA	228.3	102.9	114.3	0.1	125.7	100.7
58	L	0	NA	1993	20	18.0	105.5	117.3	0.4	127.0	103.3

Table S 2-3. Best-fit regression equations to predict time-dependent recovery of aboveground carbon density (Mg-C ha⁻¹) of logged stands and stands burned once, twice, and three or more times. *Model 1* considers once-burned stands as a single class, while *Model 2* further partitions once-burned stands into low- or high-severity areas based on post-fire changes in canopy reflectance. Age represents years since the last logging or fire disturbance. Uncertainty in model parameters are presented in parentheses as 95% confidence intervals derived from 10,000 Monte Carlo model fits with added noise to stand-level ACD proportionate to stand-level uncertainty. Mean standard error is presented.

1)		Coefficient (β)		SE
	Intercept (logging)	62.259 (61.969-62.548)	***	3.077
	ln(age)	11.395 (11.2202-11.566)	***	1.644
	Class fire (1x)	-10.268 (-10.613- (-9.918))	**	3.809
	Class fire (2x)	-42.813 (-43.347- (-42.293))	***	4.938
	Class fire (3x+)	-51.251 (-51.755- (-50.748))	***	3.728
	Model fit statistics			
	Adjusted R ²	0.89		
	F-statistic	106.5	***	
2)		Coefficient (β)		SE
	Intercept (logging)	63.347 (62.900-63.798)	***	2.946
	ln(age)	10.637 (10.342-10.933)	***	1.531
	Class fire (1x low severity)	-8.211 (-8.578 - (-7.835))	*	3.778
	Class fire (1x high severity)	-26.785 (-27.988- (-25.590))	***	4.108
	Class fire (2x)	-43.026 (-43.569- (-42.489))	***	4.905
	Class fire (3x+)	-51.936 (-52.490- (-51.378))	***	3.670
	Model fit statistics			
	Adjusted R ²	0.88		
	F-statistic	87.87	***	

* P value < 0.001

** P value < 0.001

*** P value < 0.0001

Table S 2-4. Best-fit regression equations to predict time-dependent recovery of residual canopy (*Model 3*) and density of canopy trees (*Model 4*) of logged stands and stands burned once, twice, and three or more times.

3)		Coefficient (β)	SE
	Intercept (logging)	0.214 ***	0.021
	ln(age)	0.054 ***	0.011
	Class fire (1x)	-0.104 ***	0.026
	Class fire (2x)	-0.174 ***	0.034
	Class fire (3x+)	-0.210 ***	0.255
	Model fit statistics		
	Adjusted R ²	0.74	
	F-statistic	38.85 ***	
4)		Coefficient (β)	SE
	Intercept (logging)	70.770 ***	7.733
	ln(age)	20.537 ***	4.173
	Class fire (1x)	-39.128 ***	9.707
	Class fire (2x)	-63.910 ***	11.86
	Class fire (3x+)	-71.798 ***	9.485
	Model fit statistics		
	Adjusted R ²	0.76	
	F-statistic	36.3 ***	

*** P value < 0.0001

3 Acoustic space occupancy: Combining ecoacoustics and lidar to model biodiversity variation and detection bias across heterogeneous landscapes²

Abstract

There is global interest in quantifying changing biodiversity in human-modified landscapes. Ecoacoustics may offer a promising pathway for supporting multi-taxa monitoring, but its scalability has been hampered by the sonic complexity of biodiverse ecosystems and the imperfect detectability of animal-generated signals. The acoustic signature of a habitat, or soundscape, contains information about multiple taxa and may circumvent species identification, but robust statistical technology for characterizing community-level attributes is lacking. Here, we present the Acoustic Space Occupancy Model, a flexible hierarchical framework designed to account for detection artifacts from acoustic surveys in order to model biologically relevant variation in acoustic space use among community assemblages. We illustrate its utility in a biologically and structurally diverse Amazon frontier forest landscape, a valuable test case for modeling biodiversity variation and acoustic attenuation from vegetation density. We use complementary airborne lidar data to capture aspects of 3D forest structure hypothesized to influence community composition and acoustic signal detection. Our novel analytic framework permitted us to model both the assembly and detectability of soundscapes using lidar-derived estimates of forest

² The material in this chapter was accepted for publication by the journal *Ecological Indicators* (co-authors: Danielle Rappaport, Andy Royle, Douglas Morton).

structure. Our empirical predictions were consistent with physical models of frequency-dependent attenuation, and we estimated that the probability of observing animal activity in the frequency channel most vulnerable to acoustic attenuation varied by over 60%, depending on vegetation density. There were also large differences in the biotic use of acoustic space predicted for intact and degraded forest habitats, with notable differences in the soundscape channels predominantly occupied by insects. This study advances the utility of ecoacoustics by providing a robust modeling framework for addressing detection bias from remote audio surveys while preserving the rich dimensionality of soundscape data, which may be critical for inferring biological patterns pertinent to multiple taxonomic groups in the tropics. Our methodology paves the way for greater integration of remotely sensed observations with high throughput biodiversity data to help bring routine, multi-taxa monitoring to scale in dynamic and diverse landscapes.

3.1 Introduction

Biodiversity loss as a direct and indirect result of human activity represents a major threat to life on Earth (e.g., Cardinale et al., 2012). Operational capacity to monitor known biodiversity is extremely limited, resulting in incomplete species inventories (Troutet et al., 2017) and sparse data coverage (Meyer et al., 2015). There is broad international interest in improving biodiversity monitoring, including efforts by the Group on Earth Observations Biodiversity Observation Network (GEO BON) to harmonize biodiversity measurements across space and time as essential biodiversity variables (EBVs). The success of EBVs for expanding the scope of

routine monitoring fundamentally depends on advances in distributed monitoring technology with increased taxonomic coverage, including DNA metabarcoding, camera traps, and ecoacoustic surveys. Since most of Earth's taxonomic diversity is not visible from air or space, such high-throughput biodiversity observations may complement spatially extensive Earth observations to monitor biodiversity trends at policy-relevant extents (Bush et al., 2017). Scaling up biodiversity observations on the level needed to support global conservation commitments will also require advances in computational methods designed to adjust for data sparsity and other sampling artifacts that could otherwise confound estimates of biodiversity trends.

Strategies for routine monitoring of biodiversity confront a range of trade-offs related to taxonomic coverage and sampling bias. The existing body of biodiversity data is strongly skewed towards popular taxa (e.g. plants, vertebrates), resulting in data gaps for invertebrates and other organisms (Troudet et al., 2017). These data disparities also reflect limitations in taxonomic expertise, especially in biodiverse tropical forests, which harbor over 50% of Earth's species, many of which are not readily identifiable. Even birds, the most well-studied taxa, suffer from high rates of imperfect detection and species classification errors in tropical forests, where over 95% of individuals are heard but not seen by surveyors tasked with discriminating among hundreds of species with rich vocal repertoires in dark forest understories (Robinson et al., 2018). Additionally, there is seldom enough information about species distributions to establish sampling protocols that account for key sources of sample bias from spatial variability and habitat heterogeneity, especially in tropical forests where visibility is limited, canopy structure is complex, and extents are large.

Emerging remote sensing tools, such as lidar and ecoacoustics, may support goals to expand the scope of biodiversity monitoring by collecting biodiversity variables across taxonomic, spatial, and temporal domains in a cost-effective and non-invasive manner. Lidar, short for Light Detection and Ranging, provides detailed, three-dimensional (3D) information on habitat structure, and lidar-derived measures of forest structure have been used to assess patterns of species diversity and abundance in forested environments (e.g., Goetz et al., 2007; Bergen et al., 2009). High-density airborne lidar data capture fine-scale changes in forest structure from human activity, with 3D data over hundreds to thousands of hectares needed to support landscape-scale investigations (Longo et al., 2016; Rappaport et al., 2018). Ecoacoustic surveys offer a complementary perspective by providing direct observations of the animal community over diurnal, seasonal, and interannual time scales. Remote acoustic surveys have the potential to track many animal taxa (e.g. birds, amphibians, insects, mammals, bats), and, unlike traditional field methods (e.g. point-counts), the acoustic environment can be surveyed simultaneously at multiple sites with concurrent recorders covering large spatial extents (Gibb et al., 2019). These remote sensing tools have been used independently for biodiversity monitoring, but they have rarely been used together, despite known associations between habitat structure, habitat use, and acoustic signal transmission (Pekin et al., 2012; Royle, 2018).

Three primary developments are needed to enable widespread use of ecoacoustics for routine biodiversity monitoring. First, acoustic analysis techniques that derive information about multiple taxa while bypassing the need for species

identification are critical to enable rapid, replicable, and scalable assessments of biodiversity change. The sonic signature of a site, or “soundscape,” encodes information about the resident animal community, and the 3D structure of the soundscape defined by time, frequency, and amplitude represents a valuable opportunity to capture multiple taxa. As taxonomic groups emit acoustic signals (vocalizations, stridulations) at routine periods of the day and at standard frequency ranges, the soundscape can be regarded as an abstracted representation of the animal community, comprised of acoustic transmission channels in time-frequency space that are occupied by distinct species composites (Aide et al., 2017).

Second, analytic methods are needed to handle the data complexity of soundscapes from biodiverse environments in a manner that is robust across time scales, sensors, and acoustic conditions (Gibb et al., 2019). A diversity of acoustic indices have been developed by collapsing the 3D soundscape into measures of energy distribution along either the time or frequency dimensions, but seldom both (as reviewed by Sueur et al., 2014). Such indices have been used to predict species richness in low-diversity temperate ecosystems dominated by a single vocal taxon, but predictive performance has been less stable in tropical forests, which are characterized by diverse signaling assemblages, multi-taxa choruses, and constant background noise (e.g. routine rainfall, insect stridulations) (Eldridge et al., 2018). Retaining the time and frequency dimensions may be crucial for capturing the complex patterns of acoustic energy in biodiverse tropical systems (Eldridge et al., 2016, 2018; Aide et al., 2017). Furthermore, preserving the spectral-temporal structure of soundscapes is conceptually consistent with the hypothetical link between

biodiversity and acoustic diversity, originally introduced in the Acoustic Niche Hypothesis (ANH; Krause, 1978). The ANH purports that acoustic space is partitioned into spectral-temporal ‘niches’ through evolutionary processes and competitive interactions that minimize signal overlap among co-existing species. Whether taxa do in fact occupy coherent acoustic niches is an area of active research, and, while much remains to be learned about the factors that structure acoustic transmission space (Pijanowski et al., 2011), the proportion of that space occupied by biota has been found to be an effective proxy for species richness in tropical forests (Aide et al., 2017). Exploiting this spectral-temporal structure—referred to henceforth as “acoustic space occupancy”—may open up new analytic pathways for rapid and replicable assessments of biodiversity.

Third, statistical solutions must be developed to account for observation bias in soundscape recordings. The likelihood of detecting a soniferous species occupying a site depends not only on whether it is acoustically active during a given survey, but also on a myriad of factors that influence the detectability of its acoustic signals, such as interference with vegetation, obfuscating abiotic noise, signal amplitude and frequency, distance of the animal to the recorder, micrometeorology, and survey effort, among others (Wiley & Richards, 1982). Nonetheless, most soundscape analysis methods do not adjust for sampling artifacts and detectability, despite the fact that imperfect detection can skew ecological inferences (Royle, 2018). For example, vegetation selectively limits the propagation of certain frequencies due to the physics of sound attenuation in forested environments (Wiley & Richards, 1982),

so unless properly addressed by statistical methods, raw soundscape observations are likely to underestimate the extent of occupied acoustic space in dense forest habitats.

Here, we accommodated these three methodological objectives using a novel analytic framework for capturing signals relevant to multiple taxa while accounting for sources of detection bias in remote audio surveys. Our methodological approach, the Acoustic Space Occupancy Model (ASOM), assumes that the observed soundscape is not a perfect characterization of the acoustic community, and therefore the modeling framework reconstructs the true, latent soundscape in a manner that is directly analogous to the ‘occupancy model’ framework for estimating species occurrence probability (e.g. MacKenzie et al., 2002). ASOM is a hierarchical model with explicit covariate effects to separate the ecological process (i.e., acoustic space occupancy) from the observation process (i.e., acoustic space detection) and quantify parameter uncertainties. Furthermore, its flexible framework can accommodate a range of extensions and study designs (MacKenzie et al. 2018).

We applied ASOM to ecoacoustic and airborne lidar data from a frontier forest mosaic in the southern Brazilian Amazon to illustrate the utility of our model and investigate hypothesized synergies between 3D observations of acoustic space-filling and physical space-filling. The enormous structural diversity of the study region represents a valuable test case for evaluating the role of forest structure in explaining variability in acoustic community assembly between sites and informing models of detection failure.

3.2 Materials and Methods

3.2.1 Case study region

We collected ecoacoustic and lidar data in the municipalities of Nova Ubiritã and Feliz Natal, Mato Grosso, near the southern extent of closed-canopy forests in the Brazilian Amazon (Fig. 3-1). More than 40 years of agricultural expansion, selective logging, and understory fires have given rise to a mosaic of fragmented and degraded forests with a diversity of canopy structures (Rappaport et al., 2018). The non-forest matrix is dominated by large-scale commodity agriculture, including soy, corn, and cattle ranching. The largest area of intact forest remaining in the region is in the adjacent Xingu Indigenous Park; airborne lidar acquisitions include intact forest areas for reference.

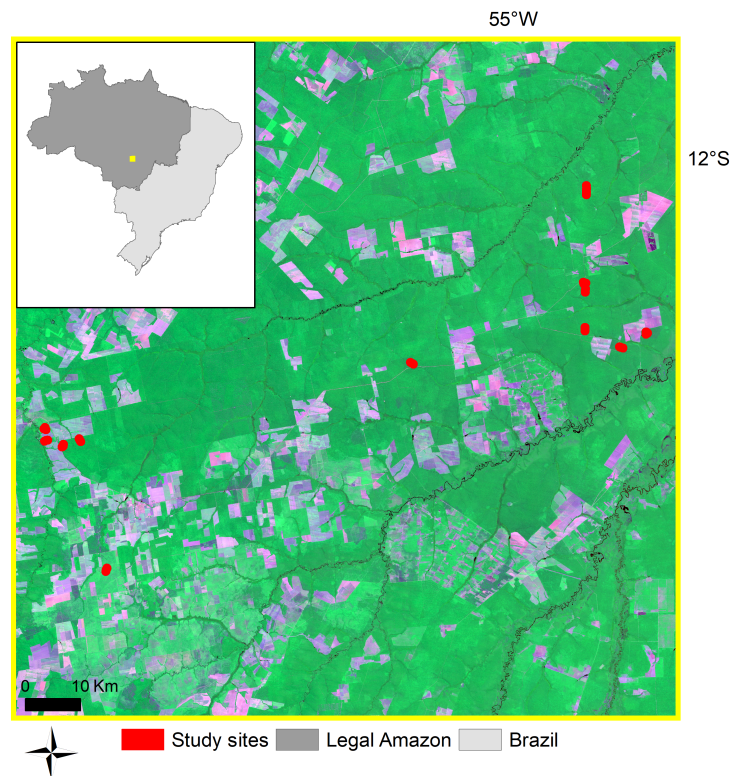


Figure 3-1. The locations of the ecoacoustic and lidar surveys (red polygons; $n = 34$) shown in relation to the case study landscape (2014 Landsat composite, bands 543) and broader regional context (map inset).

3.2.2 Lidar surveys and analysis

High-density airborne lidar surveys (≥ 14 returns per m^2) were conducted by the Sustainable Landscapes Brazil project between 2013 and 2016 to target a range of intact and degraded forest conditions in the region. Within the lidar coverage, 34 sites (forest patches ≥ 300 m in radius) with uniform degradation history were identified (Rappaport et al., 2018). Sites were spaced at least 300 m from one another and from the non-forest matrix to avoid edge effects and establish spatial independence (Fig. 1). Standard lidar metrics were calculated for each site following methods developed for NASA Goddard's Lidar, Hyperspectral, and Thermal (G-LiHT) Airborne Imager (Cook et al., 2013; Table 1), and biomass was estimated using a regional lidar-biomass model based on mean top of canopy height (Longo et al., 2016).

3.2.3 Acoustic surveys and analysis

We deployed passive acoustic recording sensors at the center of each site to survey the spatiotemporal patterns of acoustic communities between August and October 2016. ARBIMON acoustic sensors (Aide et al., 2013) were installed at breast height (1.37 m) to record all activity between 0 and 22 kHz. The acoustic environment was sampled for one minute every five minutes for a minimum of five days at each site, totaling more than 1100 hours of acoustic survey data.

Three preprocessing steps were used to convert the recording archive into soundscape matrices of acoustic space use following previous methods (Aide et al., 2013). First, the ARBIMON analysis platform was used to transform each one-minute recording into a graphical representation of its spectral components, known as a

spectrogram (constructed with 512 samples per temporal interval). Second, a supervised machine learning-based model (Aide et al., 2013) was applied to the entire volume of spectrograms to classify rain-contaminated spectrograms, which were removed to isolate the biotic contribution to the soundscape. Manual validation of the rainfall screening procedure (n=100) yielded no false negatives and a precision of 0.93 (7% false positives). Third, the spectrograms collected at each site (n=34) and during each day (n=5) were aggregated by hour (24 hours) and frequency (0-22 kHz; bin size: 344 Hz). For each of the constituent 1536 acoustic channels (24 hours x 64 frequency bands), a binary detection history was generated based on an amplitude threshold of 0.02 (Aide et al., 2013). The resulting 3D matrix (x=hour, y=frequency, z=evidence of biotic activity) represented the synoptic signature of the acoustic community for each site and each daily survey.

3.2.4 Acoustic space occupancy model

We developed the ASOM framework to predict acoustic variability relevant to multiple taxa while accounting for biologically irrelevant variability due to observation bias. The model was adapted from the standard single season occupancy model (MacKenzie et al., 2002) to account for the fact that the occupancy status of an acoustic channel is not perfectly observable and that failure to detect acoustic space occupancy may result from inactivity of the constituent species or factors that limit signal propagation and detection (e.g. survey effort, sound attenuation).

Table 3-1. Lidar and ecoacoustic covariates evaluated for models of detection and occupancy. The only candidate covariates not fit to both model components were n and $(C_n + S_n)$, which were exclusively used as detection and observation covariates, respectively.

Data source	Covariates	Description
Lidar surveys	all_mean	Mean of all return heights (m)
	all_kurtosis	Kurtosis of all return heights (m)
	all_skewness	Skewness of all return heights (m)
	all_stdev	Standard deviation of all return heights (m)
	all_p10...all_p100	Height percentiles (10% increments) of all returns (m)
	tree_fract	Fraction of all returns classified as tree* (m)
	tree_fcover	Fraction of first returns intercepted by tree* (m)
	tree_iqr	Interquartile range (p75-p25) of returns classified as tree* (m)
	shrub_mean	Mean height of returns classified as shrub** (m)
	shrub_stdev	Standard deviation of return heights classified as shrub** (m)
	biomass	Aboveground carbon density (Mg C ha ⁻¹) (Longo et al., 2016)
residual_canopy	The percentage of the site with canopy heights \geq intact reference (21m) (Rappaport et al., 2018)	
Acoustic surveys	freq	The frequency associated with a given transmission channel (Hz)
	n	Sample density, corresponding to the number of rain-free acoustic samples aggregated for each hour bin
	$(C_n + S_n)$	The sine-cosine pairs for the harmonic regression used to approximate the multimodal patterns in acoustic activity over a 24-hour period ($n = 1: 4$)

*Tree returns: returns > 1.37 m

**Shrub returns: non-ground returns < 1.37 m

Table 3-2. The model with the most substantial level of empirical support is shown with coefficients (SE) presented separately for the detection and occupancy components. Covariate descriptions are provided in Table 1.

Probability of acoustic space detection		
$Y_{nik} (*) \rho_{nik}(freq^2 + n + biomass + shrub_stdev)$		
Intercept	-10.08	(0.35)
biomass	0.46	(0.03)
freq	-9.87	(0.47)
freq ²	-2.75	(0.15)
n	0.07	(0.01)
shrub_stdev	0.13	(0.03)
Probability of acoustic space occupancy		
$\Psi_{ni} (freq \cdot (C_1 + S_1 + C_2 + S_2 + C_3 + S_3 + C_4 + S_4) \cdot tree_fract + shrub_stdev^2)$		
Intercept	-4.69	(0.41)
shrub_stdev	-0.07	(0.05)
shrub_stdev ²	0.24	(0.04)
C ₁	1.93	(0.53)
C ₂	-1.75	(0.47)
C ₃	-0.69	(0.48)
C ₄	1.27	(0.34)
S ₁	-4.96	(0.51)
S ₂	-1.62	(0.52)
S ₃	1.72	(0.44)
S ₄	-0.89	(0.35)
tree_fract	-1.59	(0.44)
freq	-0.81	(0.21)
C ₁ :tree_fract	-0.88	(0.76)
C ₂ :tree_fract	1.09	(0.60)
C ₃ :tree_fract	0.69	(0.49)
C ₄ :tree_fract	0.49	(0.39)
S ₁ :tree_fract	0.73	(0.48)
S ₂ :tree_fract	0.58	(0.48)
S ₃ :tree_fract	0.57	(0.46)
S ₄ :tree_fract	-1.25	(0.40)
C ₁ :freq	0.07	(0.26)
C ₂ :freq	-0.67	(0.23)
C ₃ :freq	-0.18	(0.23)
C ₄ :freq	0.47	(0.17)
S ₁ :freq	-1.87	(0.24)
S ₂ :freq	-0.87	(0.25)
S ₃ :freq	0.73	(0.22)
S ₄ :freq	-0.36	(0.17)
tree_fract:freq	-0.58	(0.23)
C ₁ :tree_fract:freq	-0.23	(0.39)
C ₂ :tree_fract:freq	0.29	(0.31)
C ₃ :tree_fract:freq	0.52	(0.25)
C ₄ :tree_fract:freq	0.17	(0.20)
S ₁ :tree_fract:freq	0.49	(0.24)
S ₂ :tree_fract:freq	0.31	(0.24)
S ₃ :tree_fract:freq	0.19	(0.24)
S ₄ :tree_fract:freq	-0.49	(0.21)

Formally, let z_{ni} be the true occupancy status of acoustic channel n at sample location (“site”) i . Each acoustic channel n is comprised of a frequency/time coordinate $n = (f, t)$ such that n is analogous to a “site” in the classical occupancy modeling vernacular. Thus, acoustic channel n is the unit of occupancy in our study, whereas we use the term “site” to represent higher-level structure across which acoustic space occupancy might vary, such as a geographic stratum (e.g., forest patch), which is analogous to some type of blocking structure in classical occupancy modeling vernacular. Let y_{nik} denote the observed occupancy for acoustic channel n , site i , and sample occasion k .

Here, the five daily soundscapes ($k = 1:5$) for each site were treated as temporal replicate observations of each acoustic channel. We used a maximum likelihood estimation framework to build separate models for the observation process (i.e., acoustic space detection) and the true state process (i.e., acoustic space occupancy).

The true latent occupancy state of an acoustic channel (z_{ni}) can be modeled as a Bernoulli process described as:

$$(1) \quad z_{ni} \sim \text{Bernoulli}(\Psi_{ni})$$

where Ψ_{ni} is the probability of occupancy of acoustic channel n at site i . We modeled the probability of occupancy as a function of covariates using a logistic model. For example, with a single covariate the model has the form:

$$(2) \quad \text{logit}(\Psi_{ni}) = \beta_0 + \beta_1 x_{ni}$$

where x_{ni} is a measured covariate that varies by dimensions of the acoustic soundscape (frequency and time) or varies across the different sample sites.

The observation process can be modeled as another Bernoulli random variable conditional on the state process:

$$(3) \quad y_{nik} | z_{ni} \sim \text{Bernoulli}(z_{ni} p_{nik})$$

where y_{nik} is the realized detection of acoustic channel n at site i during survey j , and p_{nik} is the detection probability. We also modeled measured covariates on detection probability according to a logistic model, e.g., with one covariate:

$$(4) \quad \text{logit}(p_{nik}) = \alpha_0 + \alpha_1 x_{nik}$$

where x_{nik} is a measured covariate that varies by frequency, time of day, survey occasion or sample location.

We used Akaike's information criterion (AIC) to select the best-supported models for inference (Burnham & Anderson, 2003), and performed model selection stepwise. First, the top-ranked models ($\Delta\text{AIC} \leq 2$) were identified for the detection component, p , by assuming the null model for the occupancy component, Ψ . Then, the best-approximating models were identified for Ψ assuming the previously

selected covariate set for p . The R program *unmarked* was used for ASOM model fitting and selection (R Development Core Team 2018; Fiske & Chandler, 2011).

The ASOM framework allows covariate effects in the spectral or temporal dimensions of the soundscape, which can be used to model variability in either acoustic space occupancy or detection probability. In all candidate models, frequency was included either in linear or quadratic form as a fixed covariate for both Ψ and p to account for possible curvilinear effects of frequency-dependence on occupancy and sound transmission. Note that the frequency covariate (f) was transformed to facilitate model convergence ($f-12/4$ kHz) and models were fit to a frequency subset containing the central mass of the data (1.4-10 kHz) to avoid issues with data sparsity at the frequency extremes. Sample density (i.e. usable recordings per hour) was also included as a fixed covariate for p to account for detection bias due to variability in survey effort. Additionally, harmonic regression terms were used to model the multimodal peaks in occupancy from the diurnal periodicity in acoustic activity (Weir et al., 2005), estimated as:

$$(5) \quad \text{logit}(\Psi_{ni}) = \beta_0 + \beta_1 \cos\left(\frac{2\pi t f_c}{24}\right) + \beta_2 \sin\left(\frac{2\pi t f_c}{24}\right)$$

where β_1 and β_2 represent the sinusoidal amplitude and phase during the diurnal period, t represents the sampling time period, and f_c represents the frequency of the sinusoid, with up to 4 cycles per day ($c = 1:4$) considered within each candidate model.

The ASOM framework also permits covariate effects to vary across the sites in which the soundscapes were observed. We used 22 lidar metrics to account for

variability in forest structure across sites (Table 3-1). Covariate selection was guided by *a priori* hypotheses regarding the influence of habitat structure on biotic community assembly and signal attenuation, and our previous findings on the lidar metrics most useful for discriminating among complex Amazon forest structures (Longo et al., 2016; Rappaport et al., 2018). The lidar metrics were calculated using a 50 m radius from the location of the recording devices, and they were scaled and centered to assist with model convergence. We constructed candidate models with ≤ 2 lidar metrics for Ψ and p using an exhaustive model-fitting procedure (R package *MuMIN*; Barton, 2018), which evaluated linear combinations of predictors in the stepwise fashion described above. All variable pairs with Pearson correlation coefficients ≥ 0.6 were excluded from consideration to address potential issues with multicollinearity.

We evaluated three ecologically viable interactions among covariates selected in the top-ranked model: 1) An interaction between the lidar metrics and signal frequency in p to test the influence of habitat structure on frequency-dependent attenuation; 2) an interaction between the sinusoids and frequency in Ψ to account for the expected variability in diurnal activity across frequency bands (i.e. pseudo-taxa); and 3) an interaction between the lidar metrics and the sinusoids in Ψ to account for the hypothesized influence of 3D habitat structure on diurnal activity (i.e. from differences in community composition).

The model was calibrated with 33 of the 34 sites, and its predictive capacity was evaluated using cross validation with the remaining site. To assess classification accuracy, we calculated the area under the receiver operator curve at the site level

(AUC) following Sadoti et al. (2013). AUC ranges from 0.5 to 1.0, and values above 0.80 indicate adequate discriminatory power.

Lastly, we used the top-supported model to generate predictions over the sampled range of degraded forest structures to support interpretation of covariate effects, as well as covariate ranges derived from the intact reference forests in the Xingu Indigenous Park to illustrate the utility of the ASOM framework for predicting outside of the immediate zone of study and forecasting conservation outcomes.

3.3 Results

There was large spectral-temporal variability in detected acoustic activity within and among the surveyed sites. The observed site-level proportion of occupied acoustic space, or ‘naive’ occupancy, ranged between 2-17% (mean: 7%). There was a marked influence of time of day on the observed utilization of frequency channels, and the diurnal patterning was not uniform across sites (Fig. 3-2). On average, naive occupancy was highest during the dusk to pre-dawn period (17:00-3:00), with detections progressively decreasing from a peak in activity during the dusk chorus. The largest gaps in utilized acoustic space were detected during the dawn to pre-dusk period (6:00-15:00) and only a small subset of sites contributed to aggregate detections at those hours (Fig. 3-2). On average, naive occupancy was highest at the middle frequencies (3-8 kHz) and lowest at the low (< 3 kHz) and high frequencies (> 8 kHz) (Fig. 3-3). At the high-frequency range, the relative proportion of detections in closed versus open forests progressively decreased with increasing frequency, and

detections > 10 kHz were exclusively registered in degraded forests with open canopies (Fig. 3-3).

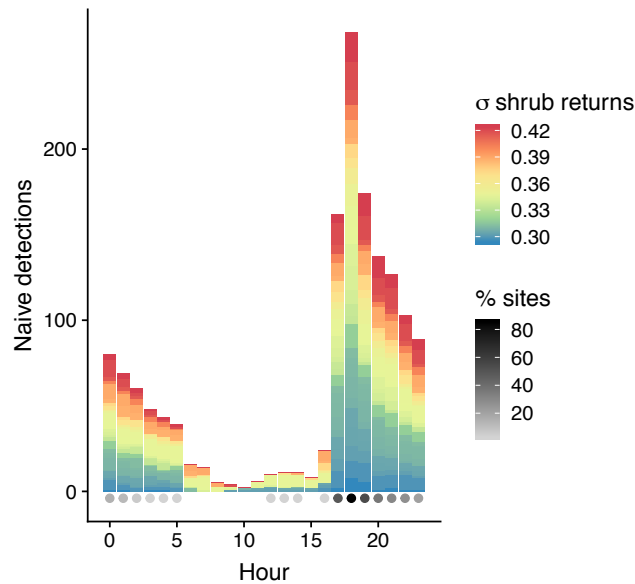


Figure 3-2. Naive observations per hour for the 33 sites used for model calibration. Colors correspond to the degree of canopy openness of the corresponding sites (higher values of shrub standard deviation indicate greater canopy loss from degradation). The greyscale indicates the percentage of sites with ≥ 5 detections.

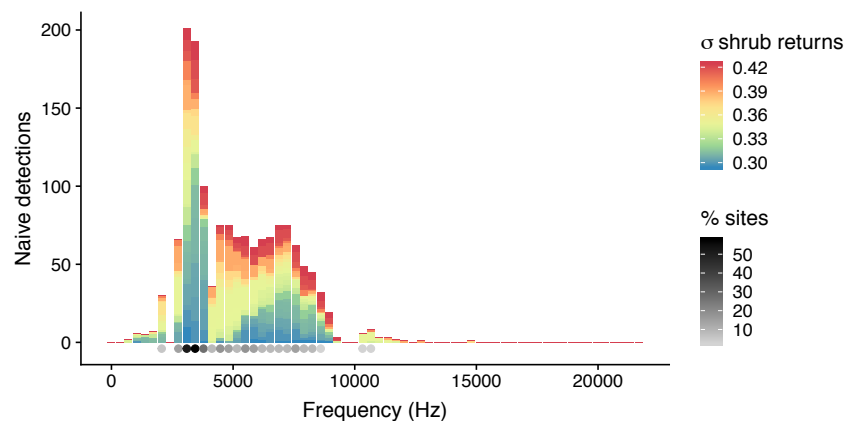


Figure 3-3. Naive observations per frequency band. Colors correspond to the degree of canopy openness and the greyscale corresponds to the percentage of sites with ≥ 5 detections.

By accounting for the factors that influence signal detection, the ASOM framework permitted us to estimate latent soundscape structure that would have otherwise been unobservable from the naive detections alone. The top-ranked model (Table 3-2) showed evidence of good predictive accuracy (AUC = 0.91), and results for the observation process (p) and state process (Ψ) model components will be presented in turn.

The sub-model for p revealed a strong frequency dependence of detection bias. The likelihood of detecting acoustic activity peaked around 5 kHz, and was governed by a quadratic effect of frequency (Fig. 3-4). The requisite sampling effort needed to maximize p also varied as a function of frequency, and high frequencies were predicted as being most susceptible to detection failure regardless of sample density (Fig. 3-5). In an average forest, the likelihood of detecting the lowest, average, and highest frequency bands was 8%, 39% and 1%, respectively, assuming maximum temporal coverage from our study design (12 samples/hour). At the most intensive sampling protocol theoretically possible (60 samples/hour), it increased to 77%, 96%, and 21%, respectively.

Our frequency-dependent predictions of detection probability were improved by including estimates of forest structure to account for signal interference with vegetation. Two lidar covariates were selected in the top-ranked model for p , aboveground biomass and the standard deviation of shrub heights (Table 3-2). When predicted over the entire sampled distribution of degraded forest structure, maximum estimates of p increased compared to the estimates above, exceeding 60% for the lowest, average, and highest frequency channels (assuming sample density of 12

recordings/hour). In each case, maximum p was predicted for heavily degraded forests that ranked in the top 10th percentile of sampled shrub standard deviation, a lidar metric that indicates more heterogeneous vegetation cover from 0-1.3 m, typical of degraded Amazon forests with low fractional tree cover. This suggests that acoustic signals were more readily detectable in heavily altered and open forest environments (Fig. 3-4).

Forest structure was also important for explaining variation in acoustic space occupancy. Based on model selection of the state process component (Table 3-2), variability in Ψ was best approximated by a three-way interaction between four sinusoids, frequency, and the lidar-derived covariate, tree fractional cover, which allowed the diurnal patterns of acoustic activity to vary across the frequency and habitat domains. The top-ranked model also included shrub standard deviation as a quadratic effect, which further constrained variability in Ψ as a function of forest structure. Patterns of predicted and observed occupancy were in close agreement over the sampled habitat distribution. In most cases, transmission channels that were predicted as having a high likelihood of occupancy were also registered by the acoustic surveys (Fig. 3-6). Divergence between modeled and observed occupancy occurred primarily for predictions in dense forest conditions and frequency bands estimated as most vulnerable to attenuation (Figs. 3-3, 3-6).

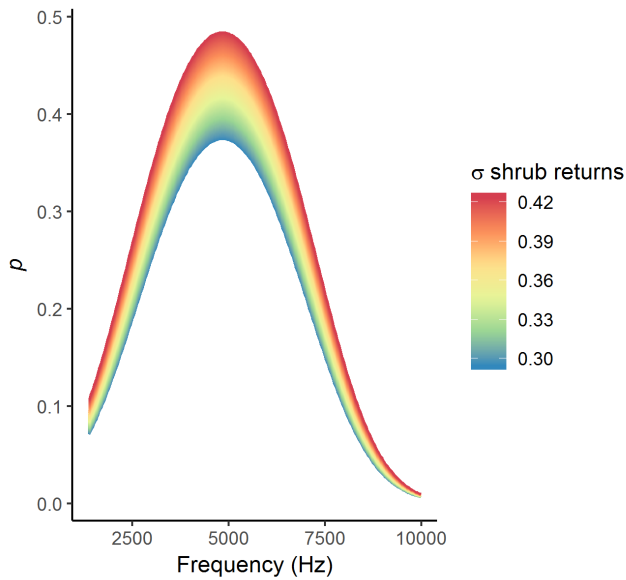


Figure 3-4. The combined effects of signal frequency and forest structure, indicated by the standard deviation of shrub-classified lidar returns, on top-ranked model predictions of detection probability (p), assuming 12 samples/hour and mean values for other detection covariates (not shown).

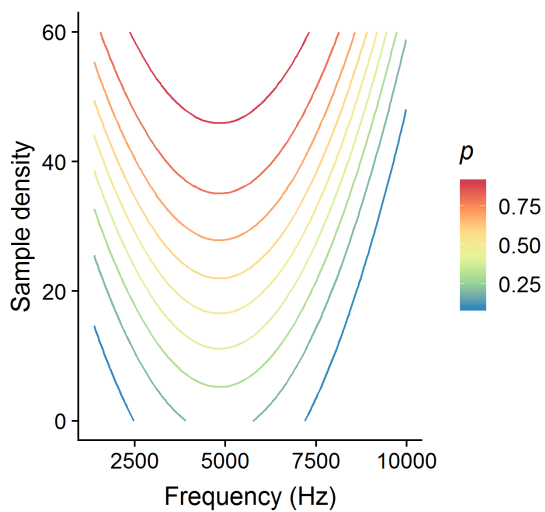


Figure 3-5. The influence of sample density on frequency-dependent detection probability (p) predicted from the top-ranked model, assuming average forest characteristics and a maximum sample density of 60 one-minute recordings per hour.

Estimates of Ψ revealed a diversity of acoustic community assemblages with distinct occupancy patterns across the time and frequency domains, and notable differences between intact and degraded habitats. When predicted for the average degraded forest and mean frequency, the largest peak in Ψ (mean acoustic space occupancy: 56%) occurred during the early evening hours of the insect chorus (18:00-19:00) (Fig. 3-7). The diurnal peaks in acoustic activity varied within each frequency channel. Often, the low and high frequencies had contrasting patterns of occupancy. For example, within the same two-hour time interval associated with the onset of the insect chorus, acoustic space occupancy ranged between 7% and 97% in the lowest and highest frequency channels, respectively. The opposite dynamic was observed for the pre-dawn/dawn period (24:00-7:00), during which low frequencies predominated (33%) and high frequencies were virtually absent (1%). The differences in model predictions between intact and degraded forest habitats were large, particularly for the same two contrasting time intervals (Figs 3-6, 3-7). For example, estimates of Ψ during the pre-dawn/dawn period (24:00-7:00) ranged between 23% and 85% for the most utilized frequency channel (1.4 kHz), depending on whether canopy structure was closed or open, respectively (Fig. 3-7).

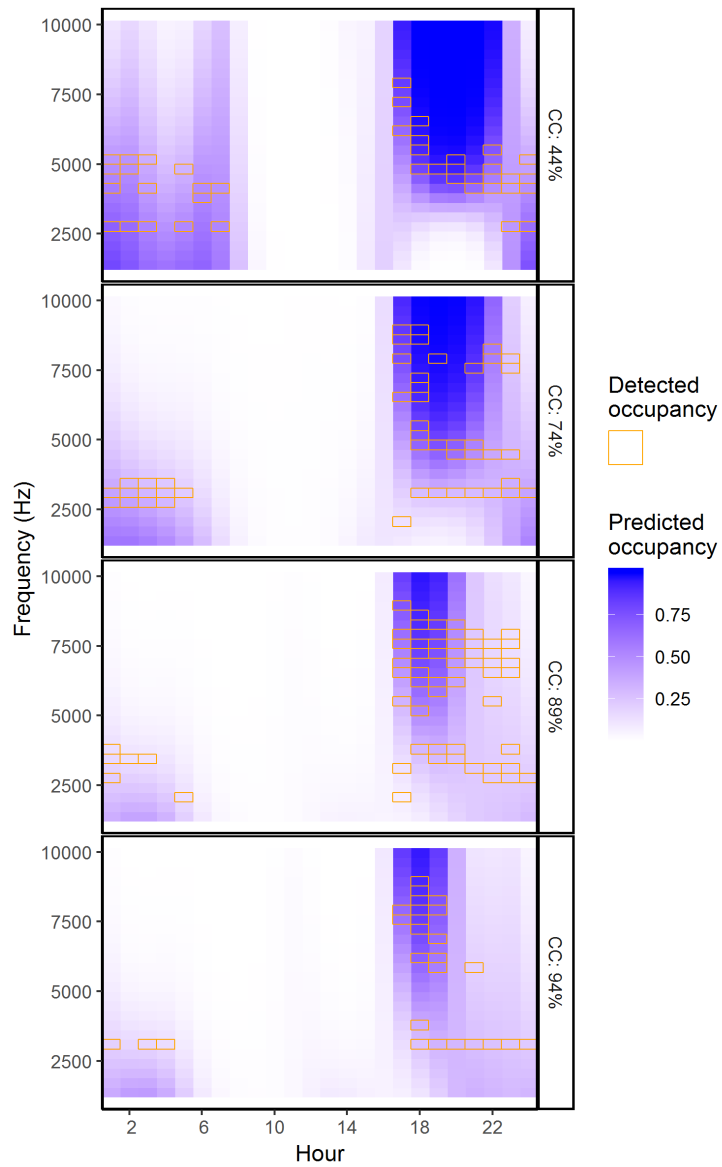


Figure 3-6. Predicted occupancy (blue scale) overlaid with naive detected occupancy aggregated over five days (orange outline) for four study sites with differing fractional canopy cover (CC).

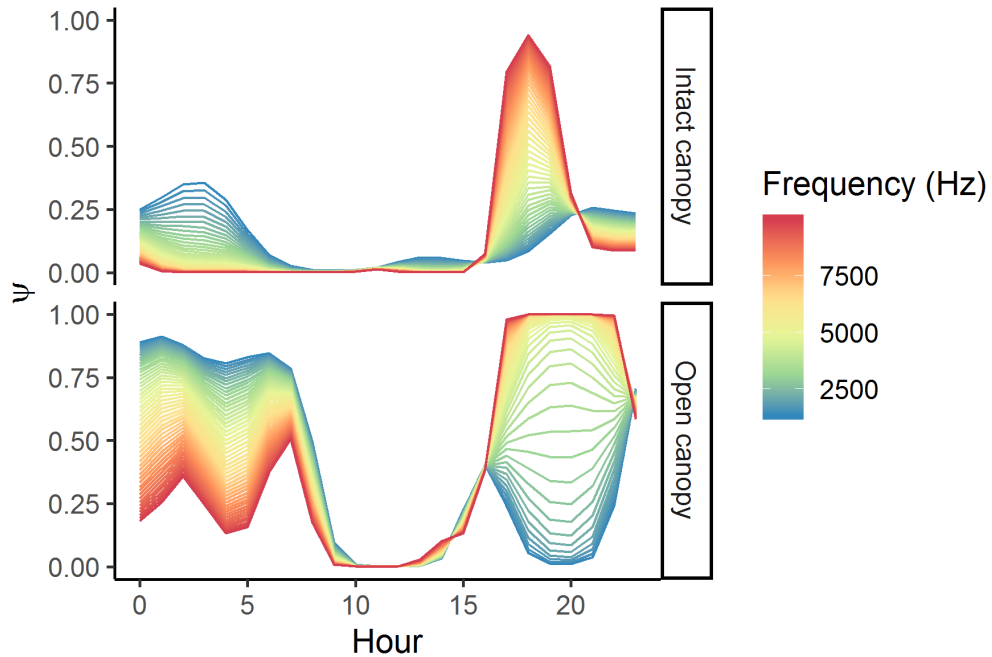


Figure 3-7. Predicted occupancy probability (Ψ) over the 24-hour cycle and frequency spectrum for two divergent habitats, a heavily degraded forest (44% canopy cover), and an intact forest (93% canopy cover).

3.4 Discussion

We developed a flexible methodological framework for capturing biologically plausible variation in acoustic quantities while accounting for sampling artifacts and failure in detecting animal-generated signals. Application of ASOM to a complex tropical forest mosaic illustrated four key attributes of our analytic framework. First, in assuming that the true underlying acoustic community is an unobservable structure, ASOM provides a clear coherent linkage between the observed soundscape and the true latent soundscape, the object of inference. Second, the flexible hierarchical structure of our modeling framework allows the factors that govern the ecological process and the observation process to be modeled separately. We provide clear evidence that the likelihood of detecting biotic signals varies across degraded forest

environments, which could otherwise confound inferences about the legacy of habitat degradation on biodiversity. Third, by retaining the multidimensional structure of the community-level acoustic signature, ASOM captures multiple taxa, even in tropical forests where sonic space is shared by simultaneous biotic signals and noisy abiotic processes. Lastly, ASOM provides a flexible framework for predicting the assemblage of acoustic communities, and we demonstrate its use for making predictions for intact forests beyond the sampled distribution of degraded habitats and for populating data-poor regions of the soundscape.

Hierarchical models that combine 3D observations of physical space filling and acoustic space filling provide a path forward for handling detection bias in soundscape studies. Existing analysis methods regard soundscapes as unbiased representations of the underlying animal community, yet soundscapes are intrinsically imperfect and vulnerable to the same issues of detection bias that affect species distribution modeling in general (e.g., MacKenzie et al., 2002). Even within an individual site, there are important sources of detection heterogeneity, including minor variations in the expression of biotic signals over time (e.g. weather, phenology, etc.). Fortunately, multi-day soundscape surveys capture temporal heterogeneity by design, and hierarchical occupancy models are uniquely equipped to model the effects responsible for observed heterogeneity. Our hierarchical framework also provides estimates of between-site detection heterogeneity. By drawing upon the synergies between ecoacoustics and airborne lidar to capture aspects of the physical interactions between sound and structure, our empirical predictions of frequency-dependent detection failure were consistent with expectations from physics. We

estimated that the risk of detection failure was greatest for high frequencies (> 8 kHz), slightly lower for low frequencies (< 3 kHz), and lowest for middle frequencies (3-8 kHz), similar to physical models of the forested environment that account for sound attenuation from interference with vegetation and ground (e.g. Wiley & Richards, 1982). It is not surprising, then, that the mode of our naive observations was in the most-detectable middle-frequency zone, or that the majority of our high-likelihood predictions that were not registered by our recorders were in the high-frequency zone, which is most vulnerable to attenuation from scattering (Wiley & Richards, 1982). Similarly, only samples from heavily degraded sites with only a few trees remaining to scatter sound contained detections with frequencies above 10 kHz. It should be noted that scattering is also caused by non-stationary heterogeneities (e.g., atmospheric turbulence), which mediate the effect of habitat on sound transmission (Wiley & Richards, 1982) and cannot be captured by lidar alone, but could perhaps be better approximated with physical models of acoustic attenuation. Signal transmission may also be better parameterized with alternative estimates of the structural environment, such as tree diameter distributions retrievable from terrestrial laser scanning or forest inventory data.

Formalized procedures for characterizing uncertainty, such as the ASOM framework, also provide a means to guide sampling effort allocation and adjust for data sparsity. We demonstrated the utility of our model for informing study design by predicting detection uncertainties over a range of sampling protocols. For example, we estimated that in an average forest, the probability of detecting acoustic activity in the least detectable frequency channel would not exceed 10%, even when increasing

sample density to 50% daily coverage, a probability which may or may not be considered adequate depending on the uncertainty thresholds and objectives of the monitoring program in question. Optimizing predictive power amidst resource constraints requires a clear understanding of sampling tradeoffs (e.g. spatial vs. temporal replicates). Hierarchical occupancy models are uniquely suited to inform such assessments through simulation-based exercises (Bailey et al., 2007). Further, as acoustic monitoring networks expand in scale (Gibb et al., 2019), there will be an increasing need to obtain accurate confidence intervals on ecological inferences derived from sparse and complicated ecoacoustic datasets.

Since the multidimensional soundscape reflects the taxonomic complexity of the biodiversity process (Aide et al., 2017), its constituent ‘channels’ may offer sufficient resolution for monitoring change. Assessing differences between soundscapes (β diversity) is even more challenging than estimating biodiversity within soundscapes, and the current set of β -diversity methods require perfect homologies that are often impractical, even for simultaneous recordings (Sueur et al., 2014), and readily confounded by environmental variation and noise (Buxton et al., 2018). By abstracting the soundscape into a map of spectral-temporal transmission channels, our analytic framework permitted us to model differences between biotic community assemblages across a complex forest landscape mosaic with variable sources of background noise and signal interference. Since the coarseness of the channels and number of diurnal replicates are effectively model assumptions, exploring the synoptic scale of the soundscape to address underlying heterogeneity should be a logical extension of this work. Targeting soundscape regions that

represent peak activity of particular taxa could also be informative and possibly more tractable than modeling the full diurnal signal. Our findings from disaggregating the community-level response curves suggest that the signal of Amazon forest degradation may be most evident in the transmission channels predominantly occupied by insects (e.g. midnight), warranting targeted investigations into their potential role as acoustic indicators of habitat change.

We anticipate a range of methodological developments to extend the applicability of the ASOM framework. A Bayesian implementation could allow for greater flexibility in capturing the fine-scale structure and dependencies in time-frequency space than what can be approximated with sinusoidal functions and low-order polynomials. A Bayesian framework would more easily allow for flexible spatial surface modeling using GAMs (Carroll et al., 2010) or computationally efficient methods used in high-dimensional space-time applications such as Empirical Orthogonal Functions (EOFs, Wike & Cressie, 1999). More sophisticated techniques could be used to adjust for the abiotic occupancy of acoustic space, including Poisson processes to differentiate true and false positives from continuous detection information on the z-axis (e.g. Chambert et al., 2018). Moreover, collapsing the z-axis into binary presence-absence values, as required by the traditional binomial model, may not be the most efficient use of the 3D soundscape. For example, the relative abundance of soundscape quantities could be used with N-mixture models (e.g. Royle, 2004) to investigate how metapopulation dynamics are reflected in acoustic assemblages. Lastly, the ASOM framework could also be readily extended to track longitudinal dynamics (e.g. MacKenzie et al., 2003).

3.5 Conclusion

Ecoacoustics represents an exciting pathway for routine biodiversity monitoring on the scale needed to support the derivation of essential biodiversity variables (EBVs). Yet, its operational potential depends on statistical solutions for characterizing multiple taxa, handling data complexity, and addressing observation bias—methodological criteria that have proven most challenging in biodiverse tropical forests (Eldridge et al., 2018; Gibb et al., 2019). By applying our analytic framework to a dynamic Amazon forest frontier, we show its potential for meeting these objectives while addressing knowledge gaps from chronically under-sampled taxa, such as insects. Our findings also underscore important synergies between lidar and ecoacoustics for informing models of occupancy and detection, and supporting future investigations into the role of habitat structure in shaping habitat use. Our flexible framework can be readily extended to other forest types and regional contexts to account for observation bias from imperfect detection of forest pseudo-taxa likely to be affected by sound attenuation.

Acknowledgements

Support was provided by the NASA Earth and Space Science Fellowship program (D. I. Rappaport), a National Science Foundation Doctoral Dissertation Research Improvement Grant (D. I. Rappaport, grant 1634168), and NASA's Carbon Monitoring System program. Sustainable Landscapes Brazil collected the lidar data, and Maiza Dos-Santos and Hyeungu Choi provided assistance with data processing. We also thank biologist Eveline Salvático for her valuable support in the field during

acoustic data collection.

References

- Aide, T. M., Corrada-Bravo, C., Campos-Cerqueira, M., Milan, C., Vega, G., & Alvarez, R. (2013). Real-time bioacoustics monitoring and automated species identification. *PeerJ*, *1*, e103. doi:10.7717/peerj.103
- Aide, T. M., Hernández-Serna, A., Campos-Cerqueira, M., Acevedo-Charry, O., & Deichmann, J. L. (2017). Species Richness (of Insects) Drives the Use of Acoustic Space in the Tropics. *Remote Sensing*, *9*(11), 1096. doi:10.3390/rs9111096
- Bailey, L. L., Hines, J. E., Nichols, J. D., & MacKenzie, D. I. (2007). Sampling design trade-offs in occupancy studies with imperfect detection: examples and software. *Ecological Applications*, *17*(1), 281–290.
- Barton, K. (2018). *Package 'MuMIn'*. *R package version 1.40.4*.
- Bergen, K. M., Goetz, S. J., Dubayah, R. O., Henebry, G. M., Hunsaker, C. T., Imhoff, M. L., ... Radeloff, V. C. (2009). Remote sensing of vegetation 3-D structure for biodiversity and habitat: Review and implications for lidar and radar spaceborne missions. *Journal of Geophysical Research: Biogeosciences*, *114*(G2). doi:10.1029/2008JG000883
- Burnham, K. P., & Anderson, D. R. (2003). *Model selection and multimodel inference: a practical information-theoretic approach*. Springer Science & Business Media.
- Bush, A., Sollmann, R., Wilting, A., Bohmann, K., Cole, B., Balzter, H., ... Yu, D. W. (2017). Connecting Earth observation to high-throughput biodiversity data. *Nature Ecology & Evolution*, *1*(7), 0176.
- Buxton, R. T., McKenna, M. F., Clapp, M., Meyer, E., Stabenau, E., Angeloni, L. M., ... Wittemyer, G. (2018). Efficacy of extracting indices from large-scale acoustic

- recordings to monitor biodiversity. *Conservation Biology*, 32(5), 1174–1184.
doi:10.1111/cobi.13119
- Cardinale, B. J., Duffy, J. E., Gonzalez, A., Hooper, D. U., Perrings, C., Venail, P., ...
Naeem, S. (2012). Biodiversity loss and its impact on humanity. *Nature*, 486(7401), 59–
67. doi:10.1038/nature11148
- Carroll, C., Johnson, D. S., Dunk, J. R., & Zielinski, W. J. (2010). Hierarchical Bayesian
Spatial Models for Multispecies Conservation Planning and Monitoring. *Conservation
Biology*, 24(6), 1538–1548.
- Chambert, T., Waddle, J. H., Miller, D. A., Walls, S. C., & Nichols, J. D. (2018). A new
framework for analysing automated acoustic species detection data: Occupancy
estimation and optimization of recordings post-processing. *Methods in Ecology and
Evolution*, 9(3), 560–570.
- Cook, B. D., Nelson, R. F., Middleton, E. M., Morton, D. C., McCorkel, J. T., Masek, J. G.,
... others. (2013). NASA Goddard's LiDAR, Hyperspectral and Thermal (G-LiHT)
Airborne Imager. *Remote Sensing*, 5(8), 4045–4066.
- Eldridge, A., Casey, M., Moscoso, P., & Peck, M. (2016). A new method for ecoacoustics?
Toward the extraction and evaluation of ecologically-meaningful soundscape
components using sparse coding methods. *PeerJ*, 4, e2108. doi:10.7717/peerj.2108
- Eldridge, A., Guyot, P., Moscoso, P., Johnston, A., Eyre-walker, Y., & Peck, M. (2018).
Sounding out ecoacoustic metrics: avian species richness is predicted by acoustic indices
in temperate but not tropical habitats. *Ecological Indicators*.
- Fiske, I., & Chandler, R. (2011). Unmarked: an R package for fitting hierarchical models of
wildlife occurrence and abundance. *Journal of Statistical Software*, 43(10), 1–23.
- Gibb, R., Browning, E., Glover-Kapfer, P., & Jones, K. E. (2019). Emerging opportunities
and challenges for passive acoustics in ecological assessment and monitoring. *Methods
in Ecology and Evolution*, 10(2), 169-185.

- Goetz, S., Steinberg, D., Dubayah, R., & Blair, B. (2007). Laser remote sensing of canopy habitat heterogeneity as a predictor of bird species richness in an eastern temperate forest, USA. *Remote Sensing of Environment*, *108*(3), 254–263.
doi:10.1016/j.rse.2006.11.016
- Krause, B. (1987). Bioacoustics, habitat ambience in ecological balance. *Whole Earth Review*, *57*, 14–18.
- Longo, M., Keller, M. M., dos-Santos, M. N., Leitold, V., Pinagé, E. R., Baccini, A., ... Morton, D. C. (2016). Aboveground biomass variability across intact and degraded forests in the Brazilian Amazon. *Global Biogeochemical Cycles*, 2016GB005465.
doi:10.1002/2016GB005465
- MacKenzie, D. I., Nichols, J. D., Hines, J. E., Knutson, M. G., & Franklin, A. B. (2003). Estimating site occupancy, colonization, and local extinction when a species is detected imperfectly. *Ecology*, *84*(8), 2200–2207.
- MacKenzie, D. I., Nichols, J. D., Lachman, G. B., Droege, S., Andrew Royle, J., & Langtimm, C. A. (2002). Estimating site occupancy rates when detection probabilities are less than one. *Ecology*, *83*(8), 2248–2255.
- Meyer, C., Kreft, H., Guralnick, R., & Jetz, W. (2015). Global priorities for an effective information basis of biodiversity distributions. *Nature Communications*, *6*, 8221.
doi:10.1038/ncomms9221
- Pekin, B. K., Jung, J., Villanueva-Rivera, L. J., Pijanowski, B. C., & Ahumada, J. A. (2012). Modeling acoustic diversity using soundscape recordings and LIDAR-derived metrics of vertical forest structure in a neotropical rainforest. *Landscape Ecology*, *27*(10), 1513–1522.
- Pijanowski, B. C., Villanueva-Rivera, L. J., Dumyahn, S. L., Farina, A., Krause, B. L., Napoletano, B. M., ... Pieretti, N. (2011). Soundscape Ecology: The Science of Sound in the Landscape. *BioScience*, *61*(3), 203–216. doi:10.1525/bio.2011.61.3.6

- Rappaport, D. I., Morton, D. C., Longo, M., Keller, M., Dubayah, R., & dos-Santos, M. N. (2018). Quantifying long-term changes in carbon stocks and forest structure from Amazon forest degradation. *Environmental Research Letters*, *13*(6), 065013. doi:10.1088/1748-9326/aac331
- Robinson, W. D., Lees, A. C., & Blake, J. G. (2018). Surveying tropical birds is much harder than you think: a primer of best practices. *Biotropica*.
- Royle, J. A. (2004). N-Mixture Models for Estimating Population Size from Spatially Replicated Counts. *Biometrics*, *60*(1), 108–115. doi:10.1111/j.0006-341X.2004.00142.x
- Royle, J. A. (2018). Modelling sound attenuation in heterogeneous environments for improved bioacoustic sampling of wildlife populations. *Methods in Ecology and Evolution*, *9*(9), 1939–1947. doi:10.1111/2041-210X.13040
- Sadoti, G., Zuckerberg, B., Jarzyna, M. A., & Porter, W. F. (2013). Applying occupancy estimation and modelling to the analysis of atlas data. *Diversity and Distributions*, *19*(7), 804–814.
- Sueur, J., Farina, A., Gasc, A., Pieretti, N., & Pavoine, S. (2014). Acoustic indices for biodiversity assessment and landscape investigation. *Acta Acustica United with Acustica*, *100*(4), 772–781.
- Troudet, J., Grandcolas, P., Blin, A., Vignes-Lebbe, R., & Legendre, F. (2017). Taxonomic bias in biodiversity data and societal preferences. *Scientific Reports*, *7*(1), 9132. doi:10.1038/s41598-017-09084-6
- Weir, L. A., Royle, J. A., Nanjappa, P., & Jung, R. E. (2005). Modeling anuran detection and site occupancy on North American Amphibian Monitoring Program (NAAMP) routes in Maryland. *Journal of Herpetology*, *39*(4), 627–639.
- Wikle, C. K., & Cressie, N. (1999). A dimension-reduced approach to space-time Kalman filtering. *Biometrika*, *86*(4), 815–829.

Wiley, R. H. and D. G. Richards. 1982. Adaptations for acoustic communication in birds: sound transmission and signal detection. In *Acoustic Communication in Birds* (D. Kroodsma, E. H. Miller, and H. Ouellet, eds.), pp. 131–181. New York: Academic Press.

4 Animal soundscapes reveal key markers of Amazon forest degradation from fire and logging³

Abstract

Safeguarding tropical forest biodiversity requires tractable solutions for monitoring the impact of human activity on a diversity of ecosystem services. Logging and fire reduce Amazon forest carbon stocks and alter forest composition, but the long-term consequences of forest degradation for animal biodiversity remain unclear, especially for lesser-known taxa. Here, we combined data from diurnal acoustic surveys, airborne lidar, and satellite time series covering logged and burned forests (n=39) in the southern Brazilian Amazon to identify acoustic markers of degradation, and confront the *Acoustic Niche Hypothesis* (ANH) using an array of statistical and network-based analyses. Our findings contradicted expectations from the ANH that more structurally intact habitats support animal communities that consistently occupy more acoustic ‘niche’ space, even during dawn and dusk chorus. Instead, we found biomass was not a consistent proxy for biodiversity recovery, due to soundscape differences between logged and burned forests. Going a step beyond cumulative occupancy to analyze the topology of animal communication networks provided complementary insights into the distinct patterns of biotic assembly following logging and fire, and possible taxonomic drivers. Communication networks highlighted a stark and sustained shift in community structure after multiple fires: animal communities in forests burned two or more times were quieter, less connected, and

³ The research in this chapter was co-authored. Collaborators included Doug Morton, Bill Fagan, Anshuman Swain, Andy Royle, Ralph Dubayah, and Matt Hansen.

more homogenous than logged or once-burned forests. Broadband cicadas and insect choruses characteristic of tropical forests may be driving the dominant time-dependent acoustic signals of degradation (e.g. mid-morning, noon and nighttime). Networks revealed clustering patterns between neighboring sets of pseudo-taxa, “cliques,” as well as consistent coordination along degradation and recovery trajectories following fire and logging. Soundscape data covering multiple taxa highlight large potential biodiversity co-benefits to protecting Amazon forests from recurrent fire activity. Complementary species-level and multi-temporal observations are needed to further develop acoustic indicators of community composition and strengthen ecological attribution to enhance the viability of routine, large-scale monitoring of tropical forest biodiversity.

4.1 Introduction

Biological diversity is disappearing rapidly in response to human activity, especially in tropical forests, home to well over half of Earth’s terrestrial biodiversity (Gardner et al. 2009). Global concern over greenhouse gas emissions from tropical deforestation and degradation (Van der Werf et al. 2009) has led to international efforts such as REDD+. Yet, carbon-focused conservation may not result in a commensurate win for tropical forest biodiversity (Ferreira et al. 2018). Quantifying these tradeoffs in the tropics is further complicated by the large data gaps on species distributions and human impacts on biodiversity (Meyer et al. 2015).

Addressing the tropical biodiversity crisis therefore requires an efficient, distributed monitoring system to assess species abundance and diversity. Traditional,

ground-based biodiversity inventories are logistically prohibitive to conduct at scale, and limited taxonomic expertise perpetuates large data discrepancies for lesser-known taxa, such as insects, which constitute the bulk of tropical biodiversity (Meyer et al. 2013). Advances in the emerging discipline of ecoacoustics may permit large-scale biodiversity monitoring for multiple taxa, including unidentifiable species, based on the aggregate sound signature of the animal community, or *soundscape* (Gibb et al. 2018).

The *Acoustic Niche Hypothesis* (ANH) (Krause 1987) is a core premise of ecoacoustics and the chief organizing principle for assessing species richness (Aide et al. 2017) and beta diversity (Burivalova et al. 2018, 2019) from sound. The ANH posits that more biodiverse habitats should feature finer niche partitioning of available transmission space, as described by frequency and time, and thus, greater acoustic space occupancy (ASO). The corollary is that more degraded habitats support less acoustic infilling due to vacant ‘acoustic niches’ from local species extirpations (e.g., Dumyahn and Pijanowski 2011). Ecoacoustics approaches have great potential in the hyperdiverse tropics, where competition for acoustic space is strongest (Planqué and Slabbekoorn 2008). Still, large uncertainties remain as to whether acoustic space infilling can be used as a robust proxy for ecosystem intactness to monitor human-altered landscapes (Eldridge et al. 2018). Most previous efforts to utilize acoustic data for biodiversity monitoring have focused on detecting known vocalizations associated with individual species (Aide et al. 2013), but there is broad interest in evaluating whether the collection of all vocalizations and stridulations, or soundscapes, may serve as a proxy of ecosystem integrity. In

contrast to previous efforts to measure acoustic diversity using single metrics that consider variation in acoustic energy as a function of either time or frequency (e.g., Sueur et al. 2014), we evaluated the full diurnal profile of 2D matrices of acoustic space use (Aide et al. 2017) from 3-8 kHz to identify the time periods and acoustic pseudo-taxa that differentiated degraded forest sites (see Methods).

The Brazilian Amazon has high rates of forest degradation from fire and logging, which may double biodiversity loss from deforestation alone (Barlow et al. 2016). However, the enormous heterogeneity of degraded forests in terms of canopy damage and regeneration complicates our understanding of the cumulative effect of fire and logging on animal communities. Time dependence may explain some of the apparent contradictions in previous studies of logging impacts on birds, the most well studied Amazonian taxa. Insectivores, for example, show immediate sensitivity to changes in habitat from logging and continue declining in the long term, whereas nectarivores increase in abundance immediately after logging but ultimately decline (Burivalova et al. 2015). By simultaneously surveying multiple taxa across multiple sites, sound surveys may reduce the effort and cost associated with large-scale and long-term monitoring and permit standardized assessments of community-level variation and ecosystem condition (Gibb et al. 2018).

Here, we conducted the first test of the ANH across logged and burned forests in the southern Brazilian Amazon to identify acoustic markers of forest degradation. We collected coincident high-density airborne lidar data and acoustic surveys in 39 forests with different times since logging (4-23 years) and histories of fire activity (1-5 fires) before 2016 to characterize threshold effects and time dependence on the

composition and connectivity of animal acoustic networks. We collected 1192.5 hours of diurnal acoustic recordings during the peak month of bird breeding activity. Sites were stratified based on a 32-year time series of annual Landsat imagery and coincident, high-density airborne lidar (Rappaport et al. 2018). We used space-for-time substitution to evaluate the biodiversity legacy of degradation as a function of disturbance timing, frequency, and severity. We used two complementary analytic approaches to capture the complexity of degraded forest soundscapes. First, we calculated ASO for each site at hourly and one-minute time steps to test the ANH and to quantify the magnitude, variability, and persistence of shifts in community structure following forest degradation. Second, we used a network-based approach to quantify system-level patterns of the ‘acoustic guild’ as well as compositional differences in acoustic pseudo-taxa, as described by time and frequency. Our findings revealed distinct acoustic soundscapes following fire and logging, providing further support for the utility of acoustic monitoring despite the complexity of patterns that characterize tropical forests and the diversity of biota they support.

4.2 Methods

4.2.1 Study site

A 33-year Landsat time series (1984-2017) was used to select 39 sites representing the continuum of Amazon forest degradation from fire and logging across a 9,400 km² frontier landscape encompassing the municipalities of Nova Ubiritã and Feliz Natal in Mato Grosso, Brazil (11°50'0"S, 55°0'00"W) (Fig. 4-1; Rappaport et al, 2018). Logged sites (n=24) were sampled between 4 and 23 years

post-disturbance, once-burned sites were sampled between 5 (n=3) and 17 (n=3) years post-disturbance, and recurrently burned sites were affected 2 (n=3), 3 (n=3) and 5 (n=3) times during the study period. Sites had at least 300 m of uniform degradation history and spacing between one another and from the forest edge. Most degradation strata contained three spatially proximate sites to capture the characteristic heterogeneity in forest structure at short length scales associated with logging infrastructure and fire severity (Rappaport et al., 2018), which we measured between 2013 and 2016 using coincident high-density airborne lidar data (≥ 14 returns per m^2) (data available from: www.paisagenslidar.cnptia.embrapa.br/webgis/). A regional model calibrated with frontier forests converted canopy height estimates from lidar to aboveground biomass (Longo et al. 2016).

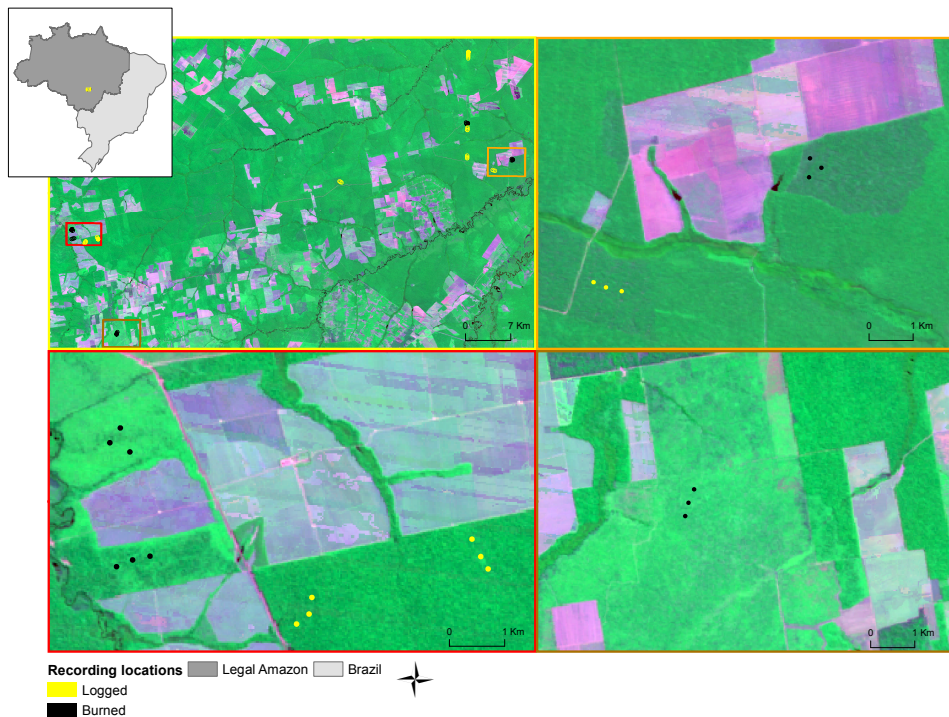


Figure 4-1. Triplicate recording sites were installed in 39 locations distributed across 9,400 km^2 in northern Mato Grosso to characterize acoustic communities following forest degradation. The three close-up panels show the characteristic variability in degraded vegetation as seen from satellite imagery (2014 Landsat, 543-RGB), and the distribution of sampling effort designed to capture this heterogeneity.

4.2.2 Acoustic processing and acoustic space use

Passive ARBIMON recorders (Aide et al. 2013) were installed at the center of each site to survey the acoustic community continuously for one minute every five minutes over 2-8 days during September 2016, totaling over 1100 hours of data. Acoustic surveys were aggregated into three-dimensional soundscapes (site-level summaries of acoustic space use) by binning recordings into frequency (bin size: 83.13 Hz) and time channels. Two sets of soundscapes were generated based first on the native minute resolution and second on hourly resolution. Analyses were constrained to frequencies between 3-8 kHz, which represent the greatest spectral overlap among birds, insects, and anurans (Aide et al., 2017), and have been shown to be most robust to detection bias from acoustic attenuation (Rappaport et al., in review). Based on the two scales of aggregation, we evaluated 16992 channels (x-axis = 288 minute bins, y-axis = 59 frequency bins) and 1416 channels (x-axis = 24 hour bins, y-axis = 59 frequency bins). An amplitude-filtering threshold of 0.2 was used to account for abiotic noise when evaluating the occupancy status of each time-frequency channel (z-axis = binary presence/absence of biotic activity). Acoustic space occupancy (ASO) was calculated based on the proportion of occupied time-frequency channels for each time step (mean ASO for soundscapes at native resolution and cumulative ASO for hourly soundscapes). A correlation analysis was used to evaluate habitat and ASO relationships at the scale of the day and constituent time intervals.

4.2.3 Network analyses

Similar to the acoustic recording analyses mentioned above, network construction and analyses were limited to frequencies between 3-8 kHz. We constructed weighted bipartite networks with sound frequency bins and sound hour bins as two classes of nodes. Frequency bins consisted of 60 nodes (3-8 kHz with bin size of 83.13 Hz) and time bins had 24 nodes (each depicting a 1-hour time interval during the day). Links between the two classes of nodes depicted presence of a given sound frequency bin during a noted sound hour bin and were weighted according to average number of observations for the link per day. Two levels of network metrics were constructed for each of the 39 sites in the dataset. Global-level analyses summarized the overall time-frequency topology of acoustic communication networks at a given site (Alatalo interaction evenness, Muller et al. 1999), and local-level analyses (node/class) unmixed ASO into the constituent elements that drive overall differences in network structure and connectivity (clustering coefficient, Watts and Strogatz 1998) partner diversity, generality, and vulnerability). The network analyses were performed with the aid of the following packages in R: ‘igraph’ (Csardi & Nepusz 2006), ‘vegan’ (McGlenn et. al., 2019) and ‘bipartite’ (Dormann et al., 2008; Dormann, 2011).

Alatalo interaction evenness measures heterogeneity in interactions across the network. Here, we focus on the frequency bins as total n entries, with p_k are proportions of interactions of bin k , and calculate the metric as:

$$AIE = \frac{(\sum_n p_k^2)^{-1} - 1}{\prod_n p_k^{p_k} - 1}$$

Clustering coefficient can be calculated for the whole network, the class level and the node level. Here, we evaluated the clustering coefficient separately for sound frequency bins and sound hour bins by averaging the clustering coefficients of all nodes in a given class (i.e. rows and columns separately). It refers to the degree to which adjacent nodes in a graph tend to cluster together; i.e., if a frequency bin is present in two or more time bins, how many other frequency bins also share the same and vice-versa. It is based on the idea of triplets (Watts & Strogatz, 1998), which consist of three nodes that are joined either via two (open triplet) or three (closed triplet) undirected ties. The clustering coefficient is defined as:

$$CC = \frac{\text{number of closed triplets}}{\text{total number of triplets}}$$

Partner diversity (PD) is the Shannon diversity of the number of interactions for a given node:

$$PD_k = - \sum_m p_i \ln(p_i)$$

where, PD_{kl} is the partner diversity of node k of a given class, which has m weighted connections from the other class of nodes, each of which has a proportion of interaction p_i for a node i from the other bipartite node class. This value of PD can be calculated as prescribed for a node and then averaged for a given class, weighted by their marginal totals – and is termed as generality (when calculated for sound frequency bins) and vulnerability (sound hour bins). PD can also be calculated for the entire network by weighted average of all the nodes' PD values (see Dormann, 2011).

4.3 Results

Soundscapes sampled in degraded Amazon forests did not support the ANH (Fig. 4-2). Instead, acoustic analyses showed contrasting impacts on community structure from two distinct processes of habitat utilization following fire and logging. After fire, daily ASO increased with biomass, but did not follow biomass distributions after logging. Importantly, ASO-degradation relationships did not hold when stratified by hourly time intervals (Fig. 4-2; Fig. S 4-3).

Insects were the dominant acoustic markers of changing community composition in burned forests. ASO during insect-dominated periods of the day (e.g. mid-morning, noon, nighttime) strongly differentiated burned forests as a function of both biomass (max $|r| = 0.9$ at 22-23:00) and fire frequency (max $|r| = -0.82$ at 20-21:00), and these time periods governed the overall daily trend (Fig. 4-2; Fig. S 4-1). Notably, ASO relationships with biomass and fire frequency were weakest during the 05:00-06:00 dawn chorus typical of bird surveys ($p > 0.05$; Fig. 2). In the logging case, the only window that exhibited a moderately strong relationship with logging age (22:00-23:00; $r = -0.61$) showed an unexpected decline in ASO with increasing regeneration. ASO and biomass in logged forests were not correlated for any time period. Relationships between ASO and degradation history were consistent at hourly and minute time scales (Fig. S 4-4).

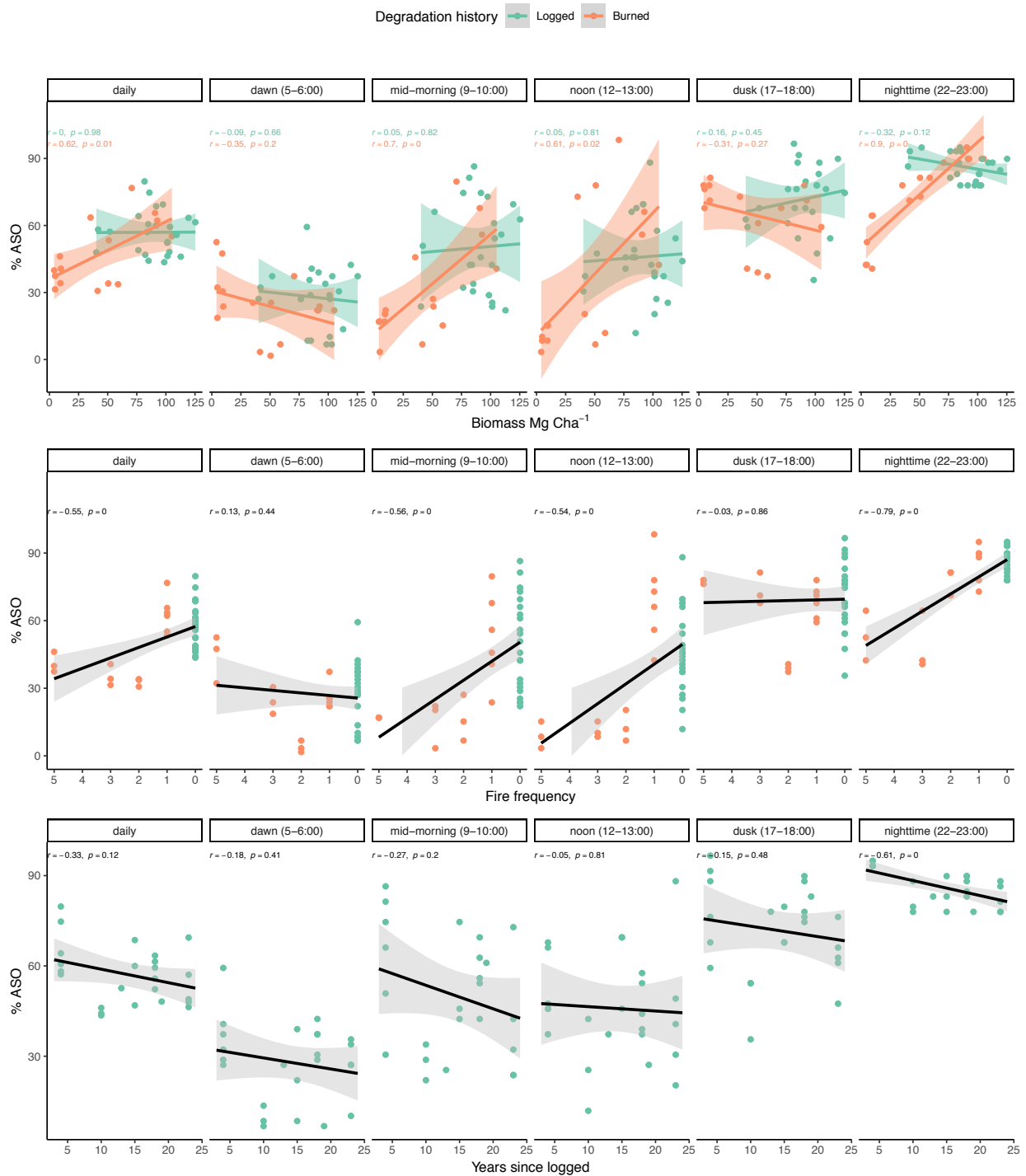


Figure 4-2. Patterns of acoustic space infilling do not conform to expectations from the Acoustic Niche Hypothesis when evaluated in terms of structural intactness (biomass) and degradation history (fire frequency, logging age). The contradictory responses to fire (green) and logging (orange) by acoustic communities indicate no predictable variability in acoustic space occupancy (ASO) with time since logging, despite the important role of degradation history in governing the recovery of ecosystem structure. The cumulative proportion of ASO aggregated hourly is presented for the full daily cycle and for specific time windows of biological relevance for birds and insects to pinpoint the likely taxonomic contributions to daily trends. See Fig. S 4-4 for ASO relationships aggregated at 1-minute resolution.

When considering the full 24-hour cycle, the diurnal signature of acoustic space occupancy varied markedly among burned forests as a function of fire history, in contrast to the less obvious variation among logged forest soundscapes (Fig. 4-3). Similarities in daily ASO curves were observed among logged forests, despite a 50% difference in forest carbon stocks, 4-23 years of forest succession, and potential impacts of logging infrastructure (e.g. skid trails, tree-fall gaps) on community composition (Fig. 4-1). Acoustic activity peaks were similar in magnitude and timing between logged and once-burned forests; both exhibited greater diurnal variability and cumulative ASO than recurrently burned forests. Acoustic communities in recurrently burned forests occupied the least amount of frequency space during all time periods except dusk, which was the most heavily occupied time window for all degradation classes (17-18:00). 24-hour soundscapes were least filled at dawn for all except the most heavily degraded classes burned 3 or more times.

Differences in ASO after logging and fire reflect distinct assemblages of pseudo-taxa. With the exception of middle range (~ 3.7-5.2 kHz), most frequencies were sounded in a greater diversity of hours after logging and a single fire than after multiple burns (Fig. 4-4). However, the pseudo-taxa that best differentiated burned forests (~3.5 kHz, 6.5-7.5 kHz) were not the same that best differentiated logged forests (~4.2 kHz), which was confirmed using a frequency-specific measure of diversity, which is comparable to frequency-agnostic ASO (Fig. S 4-1). In the logging case, most frequency bins were associated with a higher average diversity of sound hours in the lowest biomass class (with only 4 years of regeneration) than in the older more structurally intact classes (Fig. 4-4). Surprisingly, between 4 and 10 years of

regeneration, logged forests exhibited rapid changes in partner diversity for most spectra, which shifted from maximum to minimum values, respectively. Still, the dynamic range among logged classes was much subtle than among burned classes.

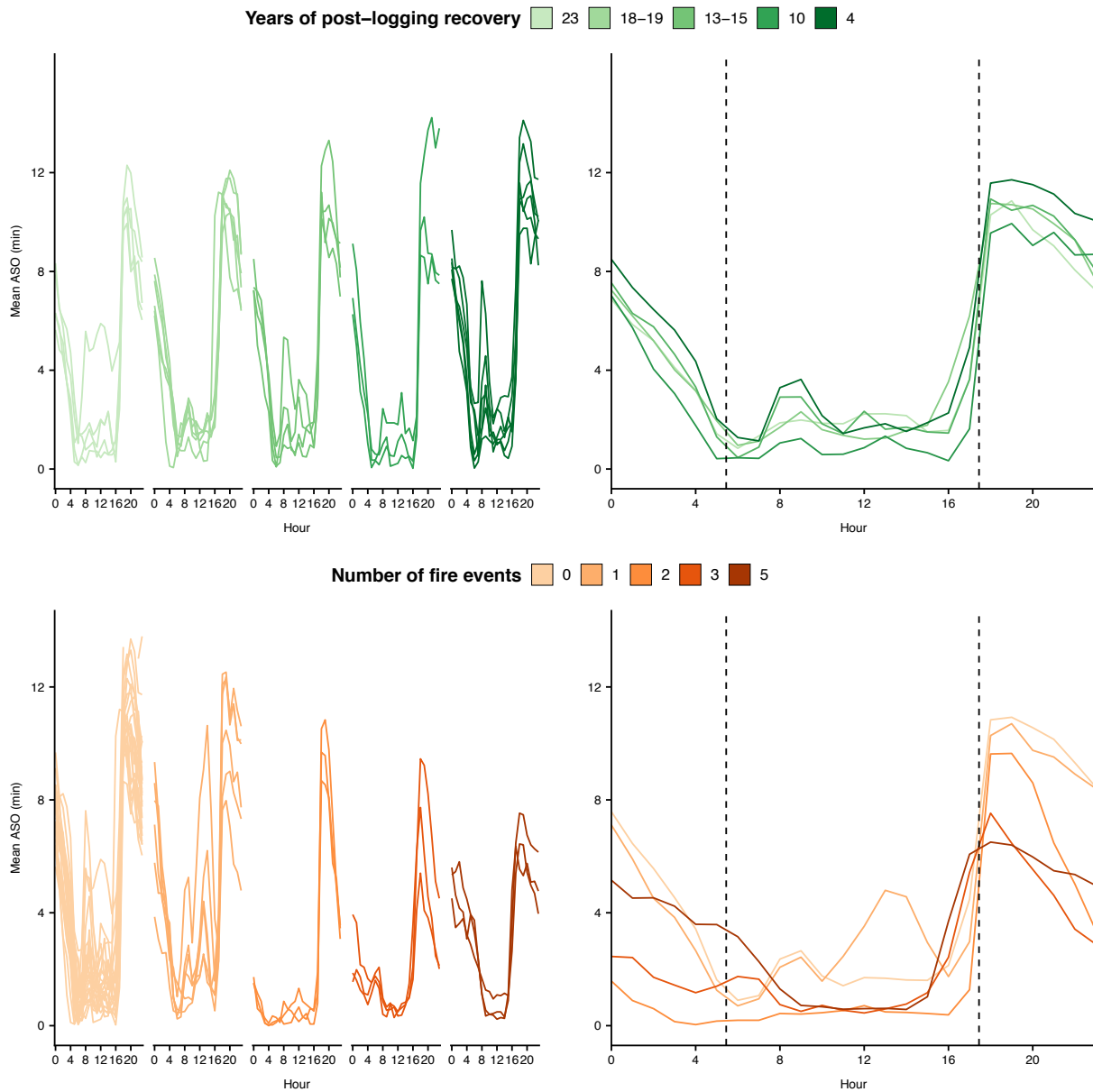


Figure 4-3. Diurnal patterns of ASO reveal a non-linear biological response to changes in structure associated with recurrent fire events (orange), and a relatively homogenous response to logging, irrespective of post-disturbance recovery (green). Mean responses per site are shown on the left and average responses per degradation stratum are overlaid on the right. Together, they show consistency within treatments and provide comparison across treatments. Sunrise and sunset are indicated with dashed lines.

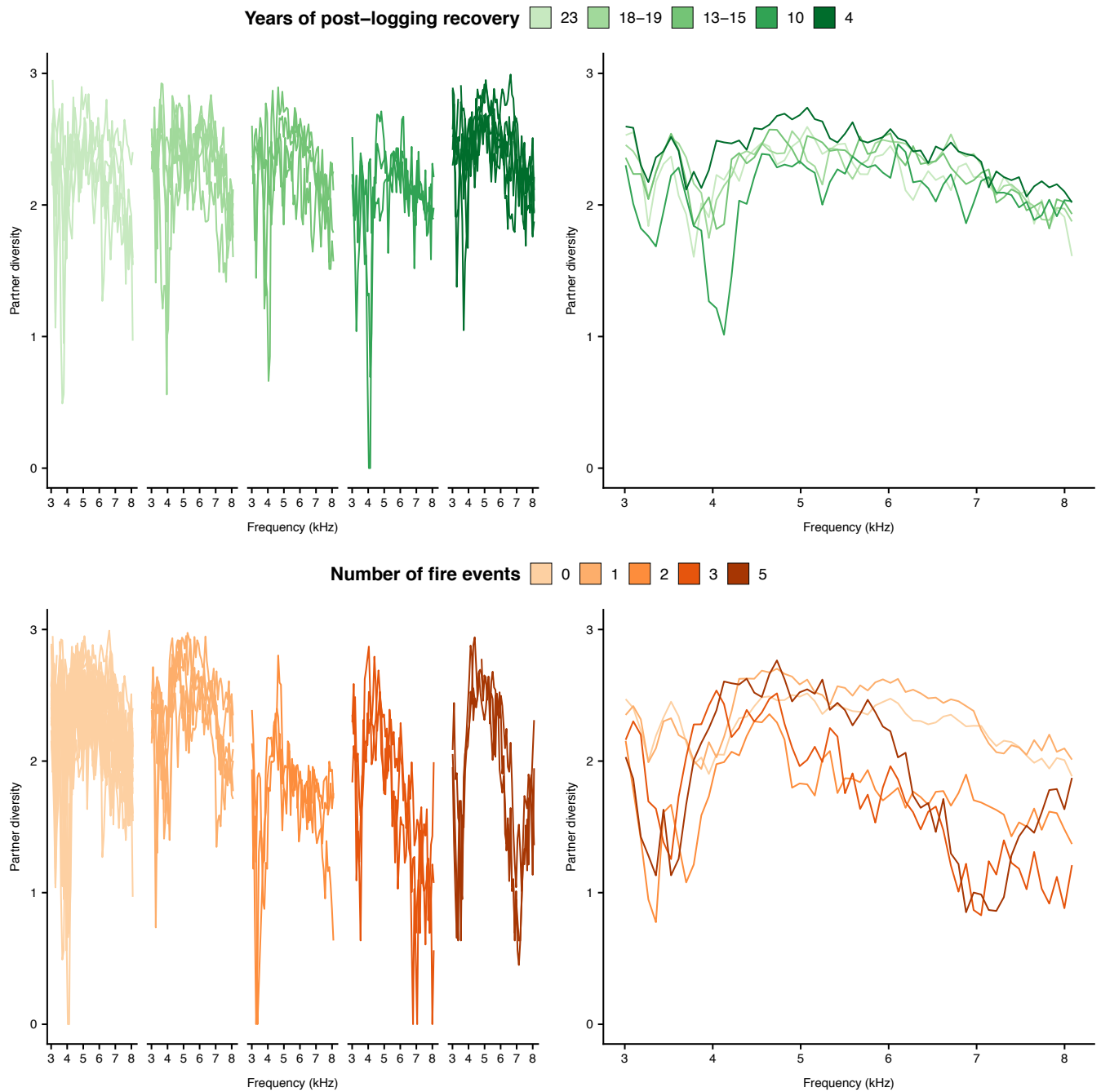


Figure 4-4. Mean partner diversity shows the frequency dependence of soundscape differences among individual site replicates (left) and degradation strata (right) after logging (top) and fire (bottom). After recurrent burns, there is an overall reduction in partner diversity, but the sharpest declines in specific pseudo-taxa do not coincide with the strongest source of deviation in an otherwise comparable pattern among logged forests.

We identified a breakpoint in community composition between forests burned once and forests with two or more fires. A non-linear threshold effect from fire recurrence manifested as a sustained reduction in ASO from late morning through late afternoon (10:00-15:00; Fig. 3). Notably, differences from initial fire severity were also most evident during that same time period, reflecting localized responses by acoustic communities, even along short length scales within the same burn scar (300 m, S 4-5). In contrast to the non-linear shifts observed midday, ASO declined linearly with increasing fire frequency around dusk (Fig. 4-2).

Overall, fire resulted in more missingness across the diurnal soundscape; more pseudo-taxa were conserved along the successional gradient of logging damages (Fig. 4-5). Soundscape transitions showed distinct patterns of pseudo-taxa loss and reassembly along gradients of logging timing, and fire frequency and severity. Many of the time-frequency niches that went silent between 4 and 10 years after logging were re-occupied between 10 and 23 years. By contrast, soundscapes in burned forests showed evidence of major organizational change with increasing fire damages; sets of pseudo-taxa were lost and not regained between 1-2 fires and 1-5 fires. In all transitions, losses and gains were clustered in time-frequency space. One large cluster of losses between forests burned 1 and 5 times covered the late morning to late afternoon hours (10:00-15:00), the same time period shown in Figure 2 that clearly differentiated forests by fire frequency.

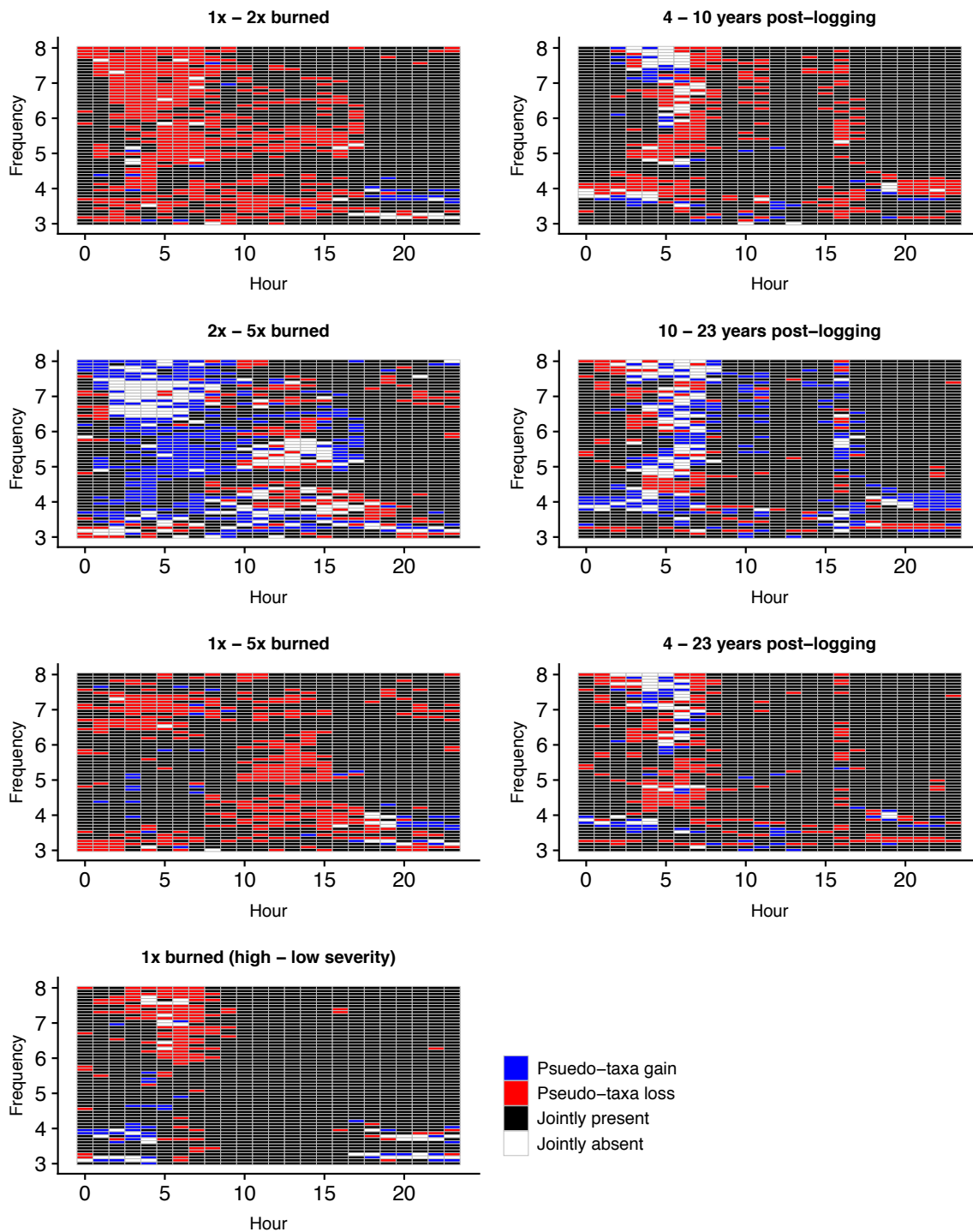


Figure 4-5. Soundscape transitions show coordinated losses and gains of pseudo-taxa after fire and logging as a function of degradation frequency, timing, and severity. 2D soundscape matrices show distinct trajectories of biotic assembly after fire versus logging, and capture localized heterogeneity from burn damages even within a single fire, most obvious as coordinated silences during the early morning period.

Animal communication networks became more acoustically homogenous with increasing fire recurrence. Alatalo evenness, which measures the global spread of signals across time-frequency space, increased linearly with increasing fire frequency, and within-class variance also declined linearly with each successive fire event (Fig. 6). The evenness of sound signals also helped explain variation in successional recovery after fire. Alatalo evenness was consistently lower in younger once-burned stands than older stands, reflecting an increased dominance of fewer sets of sounds.

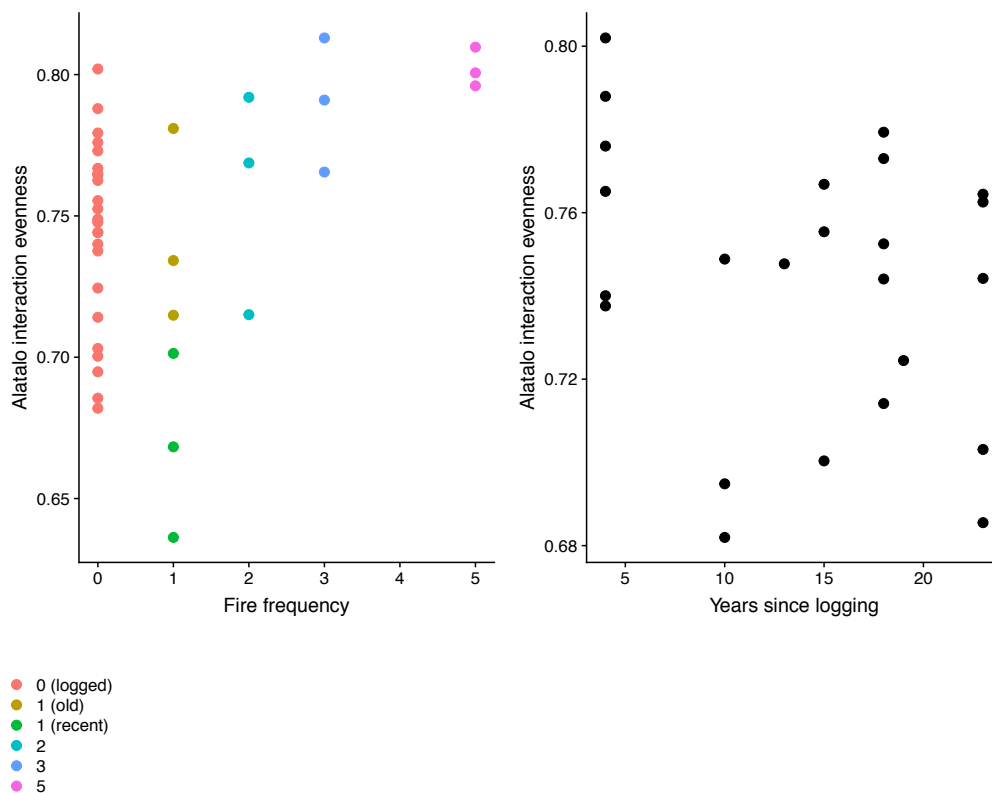


Figure 4-6. The increased evenness of the spread of links from 1 to 5 fires indicates that recurrent fire results in a soundscape that is more homogenous and composed of fewer dominant and rare links. The non-linear patterns of evenness with increasing regeneration after logging are not clearly differentiated by logging history.

Multiple fire events led to a restructuring of animal communication networks in Amazon forests. Local-scale network metrics, like clustering coefficient, offer a more synthetic understanding of the component processes that drive system-level patterns, including evenness and ASO, by tracking the ‘cliquishness’ of adjacent pseudo-taxa and formation of closely clustered sound groups. The large drop in the frequency cluster coefficient between once and twice-burned forests was consistent with a disintegration of time-synchronized cliques (Fig. 4-7). The subsequent increase in the frequency cluster coefficient from 2 to 5 fires involved the formation of cliques at new frequencies, rather than a replacement of cliques that were lost between 1 to 2 fires. By contrast, network properties after logging were more suggestive of community-level recovery than reorganization. A decline in evenness and the clustering coefficient of sound hours and sound frequency bands between 4 and 10 years of recovery after logging provided further indication of possible time-dependent or disturbance-dependent shifts in community assembly.

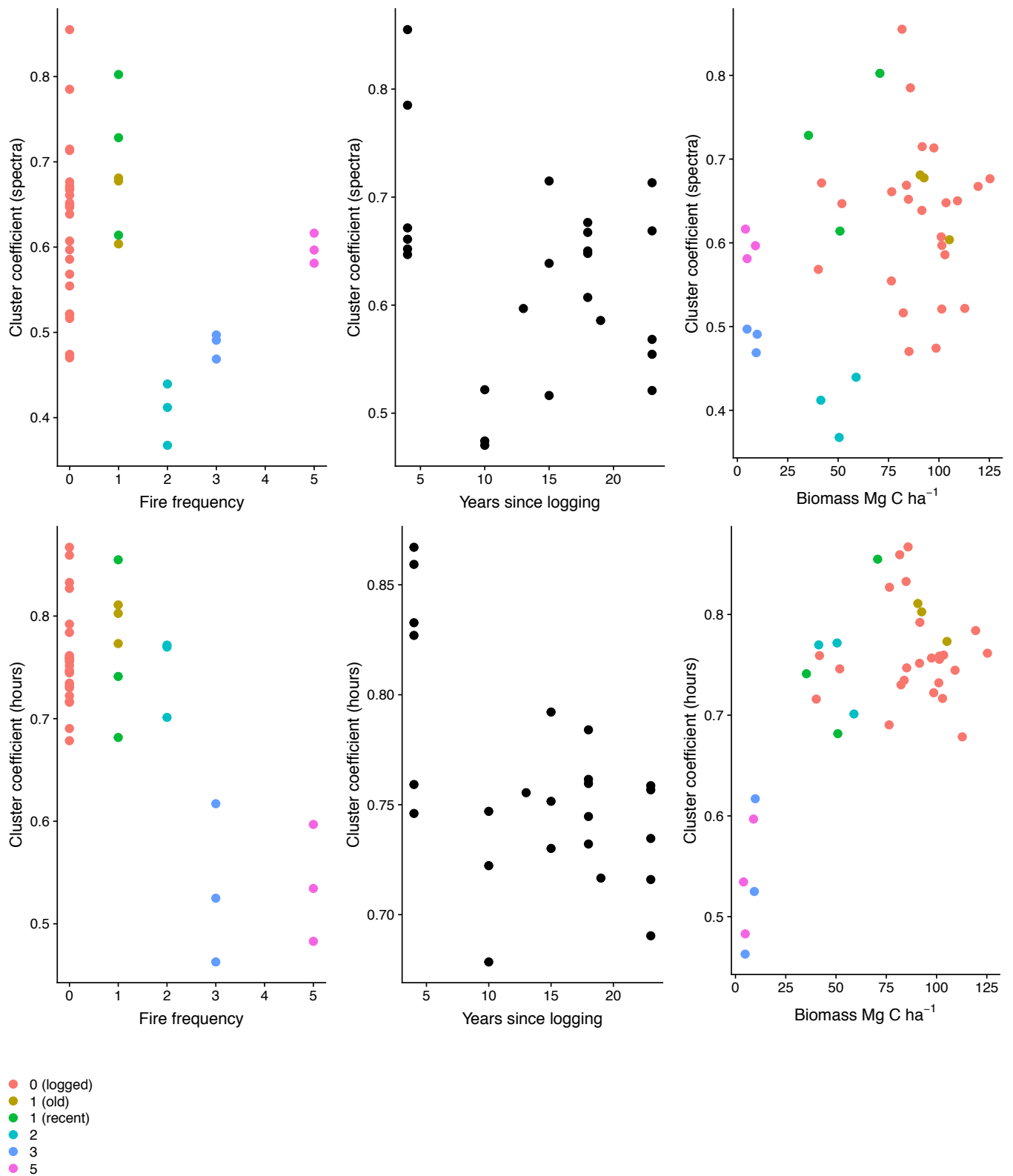


Figure 4-7. The clustering of adjacent nodes, as indicated by the cluster coefficient at the level of sound frequencies (top) and sound hours (bottom), shows that fire recurrence directly affects the connectedness of the soundscape and the likelihood that adjacent pseudo-taxa coordinate activity as part of a larger clique.

4.4 Discussion

Tropical forest soundscapes revealed strong and sustained shifts in animal community composition following fire and a decoupling of biotic and biomass recovery following logging. Animal communities in more degraded habitats did not consistently have more gaps in acoustic niche space, providing limited evidence for the Acoustic Niche Hypothesis (ANH). When disaggregated by hour, the most obvious acoustic markers of degradation coincided with insect-dominated periods of the day (e.g. midday, nighttime), yielding important insights for ecosystem monitoring. Network analyses unmixed the composite soundscape signal to better understand the ecological processes that contributed to patterns of missingness and reorganization of the soundscape. The acoustic signatures of degraded Amazonian forests featured both time-dependent impacts and thresholds from human activity. The imprint of logging recovery was most evident in the short-term, reflected in the loss and subsequent recovery of acoustic pseudo-taxa. Degradation from fire had lasting impacts on community reassembly: after multiple fires, soundscape networks became quieter, less connected, and more homogenous.

We conducted the first test of the ANH in logged and burned Amazon forests, and did not find a consistent positive relationship between ASO and habitat intactness along the day or the sampled range of degraded forest conditions. In burned Amazon forests, ASO varied with residual aboveground biomass, and thus, with fire frequency, severity, and timing, with the strongest linear relationships during 20:00-23:00. By contrast, the daily patterns of ASO in logged forests showed non-linear responses to habitat; structural differences from logging damages and recovery do not

generally translate into predictable linear changes in ASO. Our findings provide at best meager support for the ANH. Though we cannot ascertain absolute magnitude of ASO change because of the absence of remaining intact forests in our study region, ANH predicts a positive linear relationship between ASO and habitat intactness throughout the day and across the full range of state space (from degraded to intact), including this limited domain that lacks an intact reference. Importantly, acoustic data provide an opportunity to work with full annual datasets to account for variation from phenology. Future work should evaluate these relationships outside of the targeted breeding bird period to test ANH during the wet season when sensitivity to anurans is higher.

One explanation for the observed decoupling of ASO and habitat condition in degraded Amazon forests is that a diversity of mechanisms are important for structuring the soundscape in the short-term as organisms adapt to changing environmental constraints, such as for thermoregulation, predator avoidance, and transmission efficacy ([Rabin and Greene 2002](#)). Field-based analyses of the dawn chorus in Amazon forests found that avian species from related lineages use overlapping signals in time-frequency space to mediate communication and help with defending resources and territories ([Tobias et al. 2014](#)). However, birds are only a minor component of the soundscape ([Aide et al. 2017](#)), and there are numerous mechanisms that structure ASO, especially during time periods when insects dominate acoustic niche space. Broadband cicada stridulations and multi-taxa insect choruses leave some of the most obvious imprints in the Amazon forest soundscape. Cicadas, which often overlap spectrally, instead stratify acoustic space vertically from

the canopy top to the ground to minimize signal masking (Sueur 2002, Schmidt, Römer, and Riede 2012). Consequently, individual cicada species have evolved to occupy narrow thermal niches based on structural position, which may make them immediately responsive to fine-scale changes in structure (Sueur 2002, Schmidt, Römer, and Riede 2012). Furthermore, the onset of the noisy cicada chorus is governed by temperature conditions, and it, in turn, governs acoustic activity by other species (Stanley et al 2016). It follows, then, that the same features that make insect choruses obvious markers in the acoustic record may also help explain why they contribute more than birds as the dominant acoustic signal of Amazon forest degradation. This may also help explain why forest disturbances appear to strongly affect the modularity of soundscape networks and interactions among sound sources.

The time-resolved periods of greatest habitat separability highlights the potential value of arthropods as acoustic indicators of change. After dusk, ASO in burned forests declined linearly with increasing fire frequency. The persistence of this pronounced signal from nightfall through early morning (18:00-1:00) makes it unlikely to be due to changes in bird-dominated dusk choruses. In Papua New Guinea, acoustic activity peaks associated with dawn and dusk bird choruses were the most effective predictors of habitat intactness (Burivalova et al. 2017). However, such peaks disappear in response to even moderate perturbations to forest cover (Burivalova et al. 2018), and thus they may have limited utility in differentiating among more heavily degraded forests. In Borneo, nighttime activity was one of the most conspicuous acoustic markers of degradation; logged forests were considerably noisier at night than never-logged forests, which Burivalova et al. (2019)

hypothesized may be due to an influx of generalist nocturnal species following logging. Likewise, here, the only strong linear relationship between ASO and time since logging was at night (22:00) and nighttime ASO was greater in the more degraded logged forests.

Although network analyses have not previously been applied to acoustic data, we demonstrate that frequency-specific and clustering metrics from network theory complement existing tools in ecoacoustics research. Network analyses revealed a coordinated gain and loss of sets of sounds that represent distinct patterns of biotic reorganization in repeatedly burned Amazon forests. For example, compared to once-burned forests, twice-burned forests feature further declines in acoustic pseudo-taxa and the loss of time-synchronized ‘cliques’ of spectrally similar sounds broke apart, most obviously at midday. The subsequent transition, involving an increase in ASO from 2 to 5 fires, is of a fundamentally different character, as new spectral cliques appeared, which coincided little with the acoustic niches lost between 1 to 2 fires (Fig. 4-7). By tracking the coordinated gain and loss of adjacent pseudo-taxa, the cluster coefficient may be a useful proxy for biological mechanisms that occupy broad swaths of soundscape space, such as interacting sets of taxa (e.g. insect choruses) or individual taxa with broadband signals (e.g. cicadas); both appear to be conspicuous markers of degradation in this study region. The spectral-temporal incongruence of acoustic guild composition in forests subjected to 1-5 fires may reflect distinct extinction filters that result in successional divergence and novel biotic assemblages after each recurrent fire event ([Arroyo-Rodríguez et al. 2017](#)). However, complementary information is needed to unequivocally attribute spectral-temporal

features to specific incidents of species gain and loss at the soundscape scale. Furthermore, the linear relationship between Alatalo evenness and fire frequency confirms that ASO loss after fire is an indicator of increasing biotic homogenization.

By contrast, the nonlinearity in the structure of communication networks after logging appears to reflect community recovery rather than reorganization. Like fire, logging damages also reduced the clustering tendency of pseudo-taxa and partner diversity per sound frequency band, but only in the short term. Furthermore, the sound frequency bands that differentiated logged forest classes were distinct from those that best differentiated burned forest classes. In the absence of intact reference landscapes for comparison, we cannot rule out extensive recovery of the acoustic community during the period of regrowth prior to sampling. However, our lidar measurements in nearby protected forests show a nearly 40% reduction in biomass in logged forest even after 4 years of recovery (Rappaport et al. 2018), suggesting a sizable, lingering effect of logging on ecosystem condition. Furthermore, we see substantial time-dependent shifts in network structure between 4 to 10 years after logging, followed by increased soundscape homogeneity between 10 and 23 years, which may be evidence of time-lagged responses and subsequent payment of extinction debt (Rappaport et al. 2015). Several obvious pseudo-taxa appear and disappear with logging recovery (~ 4 kHz); however, most pseudo-taxa are conserved during recovery (4-23 years post-disturbance) (Fig. 4-5).

By pinpointing the changing dominance and identity of acoustic communities, soundscapes provide a much needed alternative to biomass as a metric of forest community impact, and a promising avenue for routine monitoring of biodiversity

over time (Su et al. 2004, de Castro Solar et al. 2016, Hillebrand et al. 2018). The acoustic community may be a particularly promising surrogate of biodiversity that satisfies the need for metrics of community composition (i.e., similarity, turnover) instead of species richness as indicators of forest disturbance (Su et al. 2004, de Castro Solar et al. 2016, Hillebrand et al. 2018). Soundscapes are likely to be more inclusive surrogates of biotic communities than species-specific field surveys (Aide et al. 2017), and appear to register differences in functional diversity within shorter sampling periods than estimates of species diversity in the Amazon (de Camargo et al. 2019). Furthermore, based on likely co-evolving feedbacks between acoustic composition and floristic composition, acoustic sensor networks may provide insight into the time scales of community recovery. Recent findings from a multi-year study in the Amazon confirms our space-for-time assessment by identifying soundscapes as long-term “memory banks”, which may register habitat alterations as enduring acoustic imprints even years after the initial disturbance (de Camargo et al. 2019). Permanent acoustic monitoring stations represent a cost-effective solution for longitudinal monitoring to enable operational continuity. Future research should evaluate whether soundscapes can be mined for early warning signals of impending compositional reassembly following habitat modification as might occur through extinction debts and colonization time-lags (Rappaport et al. 2015).

Further elucidation of the links between soundscape structure, species composition, and floristics will help us better understand what drives the breakpoint following recurrent fire events, and further investigate time-scales for recovery. Furthermore, we recommend that future sampling campaigns consider co-deploying a

rainfall monitoring system to account for false positives from abiotic noise to meet the statistical assumptions for modeling observation bias. We opted not to statistically correct for detection bias because of the technological challenges in filtering out rain-contaminated recordings, so we restricted our analysis to the spectral domain with lowest likelihood for acoustic attenuation (Rappaport et al., *under review*).

References

- Aide, T. M., C. Corrada-Bravo, M. Campos-Cerqueira, C. Milan, G. Vega, and R. Alvarez. 2013. Real-time bioacoustics monitoring and automated species identification. *PeerJ* 1:e103.
- Aide, T. M., A. Hernández-Serna, M. Campos-Cerqueira, O. Acevedo-Charry, and J. L. Deichmann. 2017. Species Richness (of Insects) Drives the Use of Acoustic Space in the Tropics. *Remote Sensing* 9 (11):1096.
- Aragão, L. E. O. C., L. O. Anderson, M. G. Fonseca, T. M. Rosan, L. B. Vedovato, F. H. Wagner, C. V. J. Silva, C. H. L. S. Junior, E. Arai, A. P. Aguiar, J. Barlow, E. Berenguer, M. N. Deeter, L. G. Domingues, L. Gatti, M. Gloor, Y. Malhi, J. A. Marengo, J. B. Miller, O. L. Phillips, and S. Saatchi. 2018. 21st Century drought-related fires counteract the decline of Amazon deforestation carbon emissions. *Nature Communications* 9 (1):536.
- Arroyo-Rodríguez, V., F. P. L. Melo, M. Martínez-Ramos, F. Bongers, R. L. Chazdon, J. A. Meave, N. Norden, B. A. Santos, I. R. Leal, and M. Tabarelli. 2017. Multiple successional pathways in human-modified tropical landscapes: new insights from forest succession, forest fragmentation and landscape ecology research. *Biological Reviews* 92 (1):326–340.
- Barlow, J., G. D. Lennox, J. Ferreira, E. Berenguer, A. C. Lees, R. Mac Nally, J. R. Thomson, S. F. de Barros Ferraz, J. Louzada, and V. H. F. Oliveira. 2016. Anthropogenic disturbance in tropical forests can double biodiversity loss from deforestation. *Nature* 535 (7610):144–147.
- Berenguer, E., J. Ferreira, T. A. Gardner, L. E. O. C. Aragão, P. B. De Camargo, C. E. Cerri, M. Durigan, R. C. D. Oliveira, I. C. G. Vieira, and J. Barlow. 2014. A large-scale

- field assessment of carbon stocks in human-modified tropical forests. *Global change biology*. <http://onlinelibrary.wiley.com/doi/10.1111/gcb.12627/full> (last accessed 22 August 2014).
- Brando, P. M., L. Paolucci, C. C. Ummenhofer, E. M. Ordway, H. Hartmann, M. E. Cattau, L. Rattis, V. Medjibe, M. T. Coe, and J. Balch. 2019. Droughts, Wildfires, and Forest Carbon Cycling: A Pantropical Synthesis. *Annual Review of Earth and Planetary Sciences* 47 (1):555–581.
- Burivalova, Z., T. M. Lee, X. Giam, Ç. H. Şekerciöğlü, D. S. Wilcove, and L. P. Koh. 2015. Avian responses to selective logging shaped by species traits and logging practices. *Proceedings of the Royal Society of London B: Biological Sciences* 282 (1808):20150164.
- Burivalova, Z., Purnomo, B. Wahyudi, T. M. Boucher, P. Ellis, A. Truskinger, M. Towsey, P. Roe, D. Marthinus, B. Griscom, and E. T. Game. 2019. Using soundscapes to investigate homogenization of tropical forest diversity in selectively logged forests. *Journal of Applied Ecology* 0 (0). <https://besjournals.onlinelibrary.wiley.com/doi/abs/10.1111/1365-2664.13481> (last accessed 30 October 2019).
- Burivalova, Z., M. Towsey, T. Boucher, A. Truskinger, C. Apelis, P. Roe, and E. T. Game. 2018. Using soundscapes to detect variable degrees of human influence on tropical forests in Papua New Guinea. *Conservation Biology* 32 (1):205–215.
- de Camargo, U., T. Roslin, and O. Ovaskainen. 2019. Spatio-temporal scaling of biodiversity in acoustic tropical bird communities. *Ecography*.
- Chakraborty, S., and S. W. K. Wong. 2017. BAMBI: An R package for Fitting Bivariate Angular Mixture Models. *arXiv:1708.07804 [stat]*. <http://arxiv.org/abs/1708.07804> (last accessed 14 May 2019).
- Duffy, P. B., P. Brando, G. P. Asner, and C. B. Field. 2015. Projections of future meteorological drought and wet periods in the Amazon. *Proceedings of the National Academy of Sciences* 112 (43):13172–13177.
- Dumyahn, S. L., and B. C. Pijanowski. 2011. Soundscape conservation. *Landscape Ecology* 26 (9):1327–1344.
- Edwards, D. P., J. B. Socolar, S. C. Mills, Z. Burivalova, L. P. Koh, and D. S. Wilcove. 2019. Conservation of Tropical Forests in the Anthropocene. *Current Biology* 29 (19):R1008–R1020.

- Eldridge, A., M. Casey, P. Moscoso, and M. Peck. 2016. A new method for ecoacoustics? Toward the extraction and evaluation of ecologically-meaningful soundscape components using sparse coding methods. *PeerJ* 4:e2108.
- Eldridge, A., P. Guyot, P. Moscoso, A. Johnston, Y. Eyre-walker, and M. Peck. 2018. Sounding out ecoacoustic metrics: avian species richness is predicted by acoustic indices in temperate but not tropical habitats. *Ecological Indicators*.
- Ferreira, J., G. D. Lennox, T. A. Gardner, J. R. Thomson, E. Berenguer, A. C. Lees, R. Mac Nally, L. E. Aragão, S. F. Ferraz, and J. Louzada. 2018. Carbon-focused conservation may fail to protect the most biodiverse tropical forests. *Nature Climate Change* 8 (8):744.
- Gardner, T. A., J. Barlow, R. Chazdon, R. M. Ewers, C. A. Harvey, C. A. Peres, and N. S. Sodhi. 2009. Prospects for tropical forest biodiversity in a human-modified world. *Ecology Letters* 12 (6):561–582.
- Gibb, R., E. Browning, P. Glover-Kapfer, and K. E. Jones. 2018. Emerging opportunities and challenges for passive acoustics in ecological assessment and monitoring. *Methods in Ecology and Evolution*.
- Hargita, Y., S. Günter, and M. Köthke. 2016. Brazil submitted the first REDD+ reference level to the UNFCCC—Implications regarding climate effectiveness and cost-efficiency. *Land Use Policy* 55:340–347.
- Hillebrand, H., B. Blasius, E. T. Borer, J. M. Chase, J. A. Downing, B. K. Eriksson, C. T. Filstrup, W. S. Harpole, D. Hodapp, S. Larsen, A. M. Lewandowska, E. W. Seabloom, D. B. Van de Waal, and A. B. Ryabov. 2018. Biodiversity change is uncoupled from species richness trends: Consequences for conservation and monitoring ed. M. Cadotte. *Journal of Applied Ecology* 55 (1):169–184.
- Krause, B. 1987. Bioacoustics, habitat ambience in ecological balance. *Whole Earth Review* 57:14–18.
- Le Page, Y., D. Morton, C. Hartin, B. Bond-Lamberty, J. M. C. Pereira, G. Hurtt, and G. Asrar. 2017. Synergy between land use and climate change increases future fire risk in Amazon forests. *Earth System Dynamics (Online)* 8 (PNNL-SA-119758).
- Longo, M., M. M. Keller, M. N. dos-Santos, V. Leitold, E. R. Pinagé, A. Baccini, S. Saatchi, E. M. Nogueira, M. Batistella, and D. C. Morton. 2016. Aboveground biomass variability across intact and degraded forests in the Brazilian Amazon. *Global Biogeochemical Cycles* :2016GB005465.

- Meyer, C., H. Kreft, R. Guralnick, and W. Jetz. 2015. Global priorities for an effective information basis of biodiversity distributions. *Nature Communications* 6:8221.
- Meyer, V., S. S. Saatchi, J. Chave, J. Dalling, S. Bohlman, G. A. Fricker, C. Robinson, and M. Neumann. 2013. Detecting tropical forest biomass dynamics from repeated airborne Lidar measurements. *Biogeosciences Discuss.* 10 (2):1957–1992.
- Mittermeier, R. A., G. A. b. Da Fonseca, A. B. Rylands, and K. Brandon. 2005. A Brief History of Biodiversity Conservation in Brazil. *Conservation Biology* 19 (3):601–607.
- Morton, D. C., Y. L. Page, R. DeFries, G. J. Collatz, and G. C. Hurtt. 2013. Understorey fire frequency and the fate of burned forests in southern Amazonia. *Philosophical Transactions of the Royal Society B: Biological Sciences* 368 (1619):20120163.
- Muller, C. B., I. C. T. Adriaanse, R. Belshaw, and H. C. J. Godfray. 1999. The structure of an aphid–parasitoid community. *Journal of Animal Ecology* 68 (2):346–370.
- Nepstad, D., S. Schwartzman, B. Bamberger, M. Santilli, D. Ray, P. Schlesinger, P. Lefebvre, A. Alencar, E. Prinz, G. Fiske, and A. Rolla. 2006. Inhibition of Amazon Deforestation and Fire by Parks and Indigenous Lands. *Conservation Biology* 20 (1):65–73.
- Pekin, B. K., J. Jung, L. J. Villanueva-Rivera, B. C. Pijanowski, and J. A. Ahumada. 2012. Modeling acoustic diversity using soundscape recordings and LIDAR-derived metrics of vertical forest structure in a neotropical rainforest. *Landscape ecology* 27 (10):1513–1522.
- Planqué, R., and H. Slabbekoorn. 2008. Spectral Overlap in Songs and Temporal Avoidance in a Peruvian Bird Assemblage. *Ethology* 114 (3):262–271.
- Rabin, L. A., and C. M. Greene. 2002. Changes to acoustic communication systems in human-altered environments. *Journal of Comparative Psychology* 116 (2):137–141.
- Rappaport, D. I., D. C. Morton, M. Longo, M. Keller, R. Dubayah, and M. N. dos-Santos. 2018. Quantifying long-term changes in carbon stocks and forest structure from Amazon forest degradation. *Environmental Research Letters* 13 (6):065013.
- Rappaport, D. I., L. R. Tambosi, and J. P. Metzger. 2015. A landscape triage approach: Combining spatial and temporal dynamics to prioritize restoration and conservation. *Journal of Applied Ecology* 52 (3):590–601.
- Royle, J. A. 2018. Modelling sound attenuation in heterogeneous environments for improved bioacoustic sampling of wildlife populations ed. R. Freckleton. *Methods in Ecology and Evolution* 9 (9):1939–1947.

- Saatchi, S. S., N. L. Harris, S. Brown, M. Lefsky, E. T. A. Mitchard, W. Salas, B. R. Zutta, W. Buermann, S. L. Lewis, S. Hagen, S. Petrova, L. White, M. Silman, and A. Morel. 2011. Benchmark map of forest carbon stocks in tropical regions across three continents. *Proceedings of the National Academy of Sciences* 108 (24):9899–9904.
- Schmidt, A. K., H. Römer, and K. Riede. 2012. Spectral niche segregation and community organization in a tropical cricket assemblage. *Behavioral Ecology* 24 (2):470–480.
- Schwartzman, S., A. V. Boas, K. Y. Ono, M. G. Fonseca, J. Doblas, B. Zimmerman, P. Junqueira, A. Jerozolimski, M. Salazar, R. P. Junqueira, and others. 2013. The natural and social history of the indigenous lands and protected areas corridor of the Xingu River basin. *Philosophical Transactions of the Royal Society B: Biological Sciences* 368 (1619):20120164.
- Su, J. C., D. M. Debinski, M. E. Jakubauskas, and K. Kindscher. 2004. Beyond Species Richness: Community Similarity as a Measure of Cross-Taxon Congruence for Coarse-Filter Conservation. *Conservation Biology* 18 (1):167–173.
- Sueur, J. 2002. Cicada acoustic communication: potential sound partitioning in a multispecies community from Mexico (Hemiptera: Cicadomorpha: Cicadidae). *Biological Journal of the Linnean Society* 75 (3):379–394.
- Sueur, J., A. Farina, A. Gasc, N. Pieretti, and S. Pavoine. 2014. Acoustic indices for biodiversity assessment and landscape investigation. *Acta Acustica united with Acustica* 100 (4):772–781.
- Tobias, J. A., R. Planqué, D. L. Cram, and N. Seddon. 2014. Species interactions and the structure of complex communication networks. *Proceedings of the National Academy of Sciences of the United States of America* 111 (3):1020–1025.
- Van der Werf, G. R., D. C. Morton, R. S. DeFries, J. G. Olivier, P. S. Kasibhatla, R. B. Jackson, G. J. Collatz, and J. T. Randerson. 2009. CO₂ emissions from forest loss. *Nature Geoscience* 2 (11):737–738.
- Watts, D. J., and S. H. Strogatz. 1998. Collective dynamics of ‘small-world’ networks. *Nature* 393 (6684):440–442.

4.5 Supplemental Materials

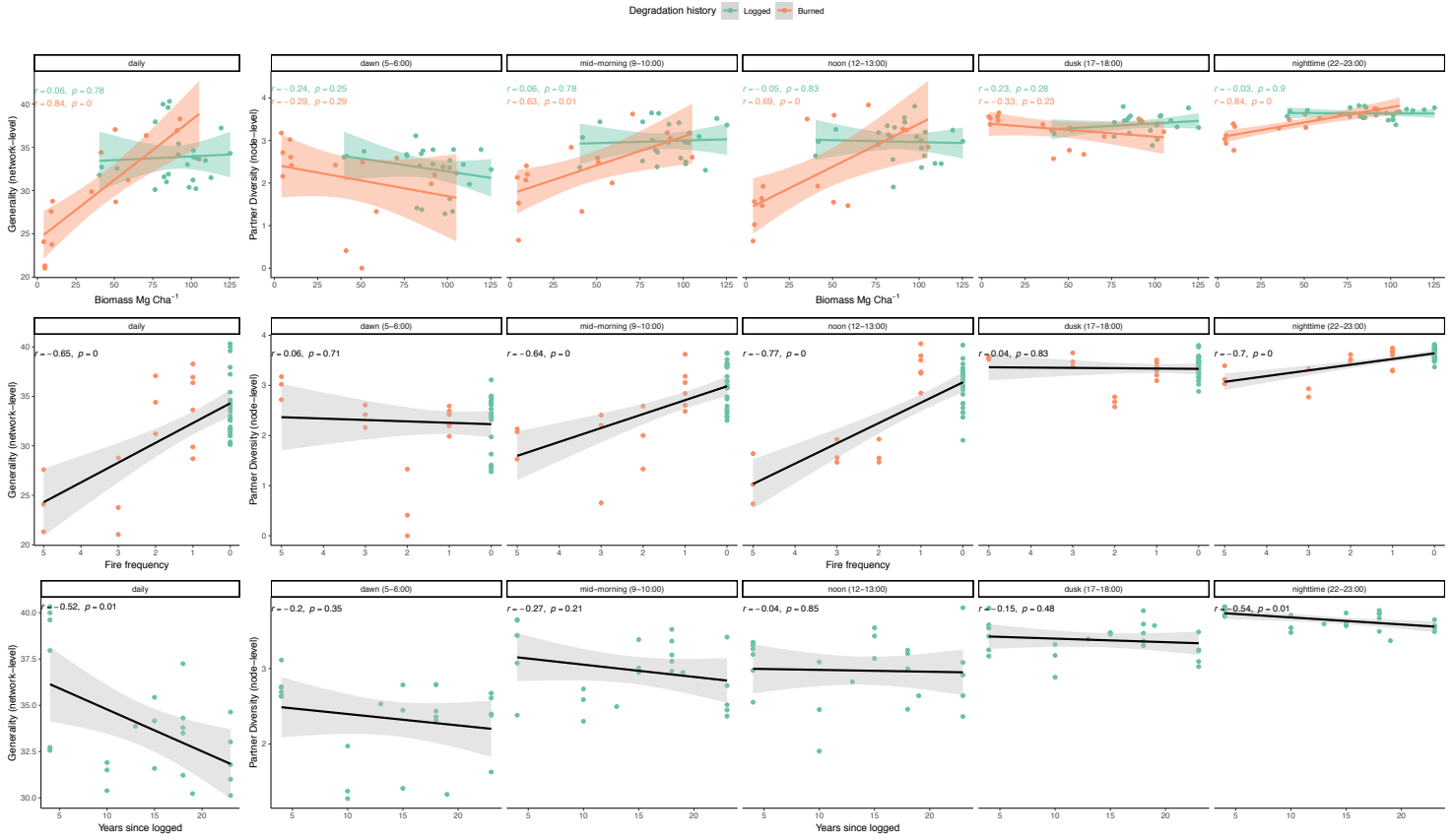


Figure S 4-1. Companion figure to Fig. 4-2, which shows consistent results with ASO-based analyses. Partner diversity of hours is shown for key time intervals, along with the system-level network analog, generality, which shows the mean number of sounds per hour calculated at the daily time step.

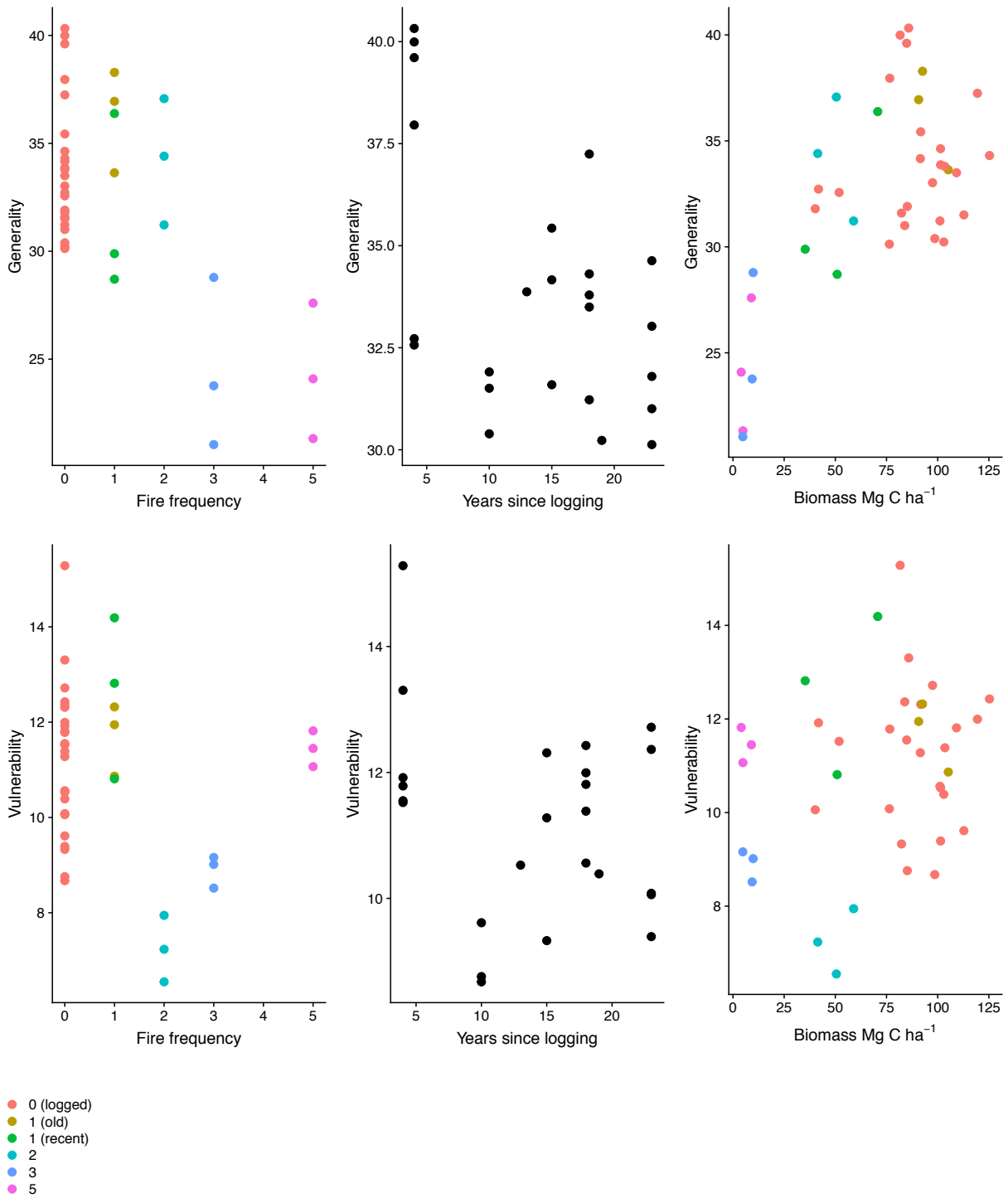


Figure S 4-2. The mean number of links per frequency (generality) and per hour (vulnerability).

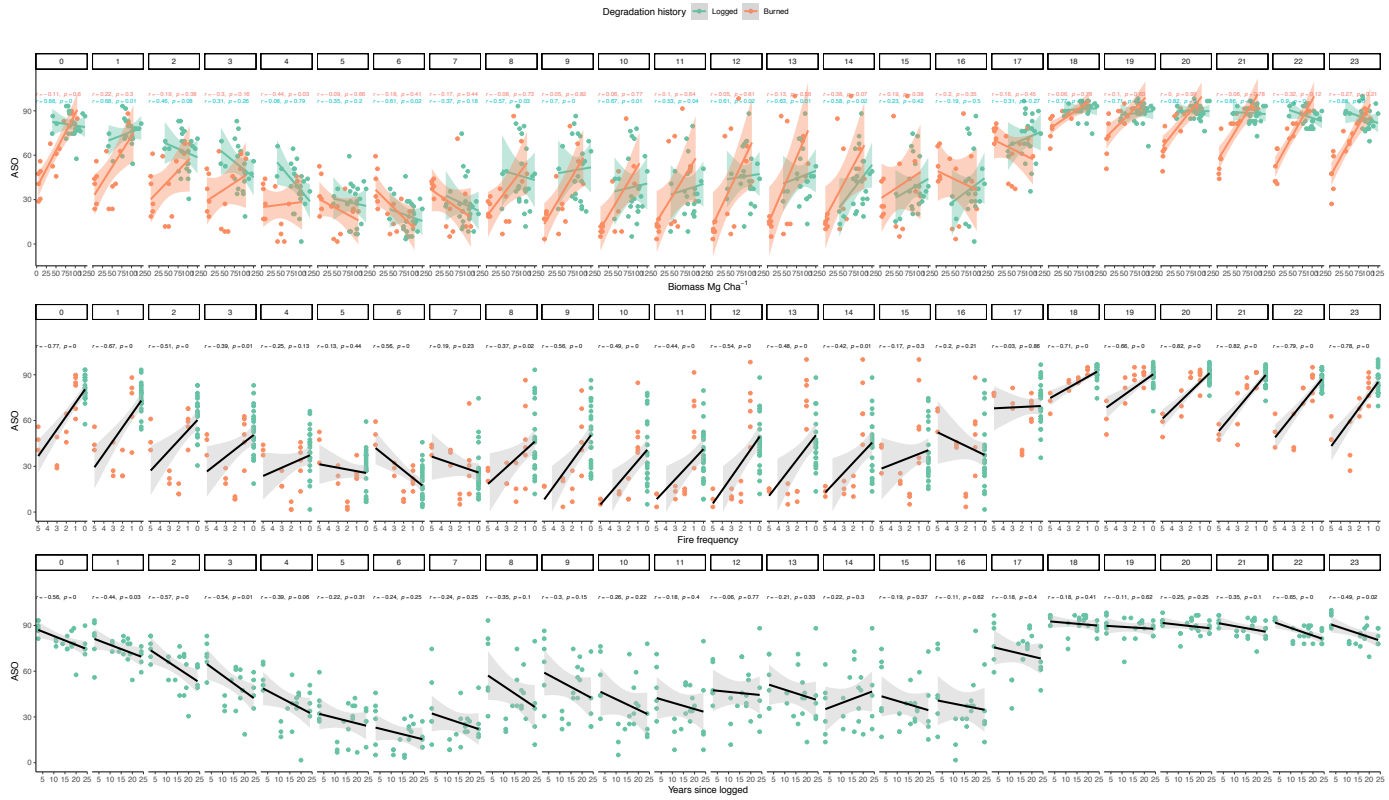


Figure S 4-3. ASO-degradation relationships aggregated hourly for the 24-hour cycle.

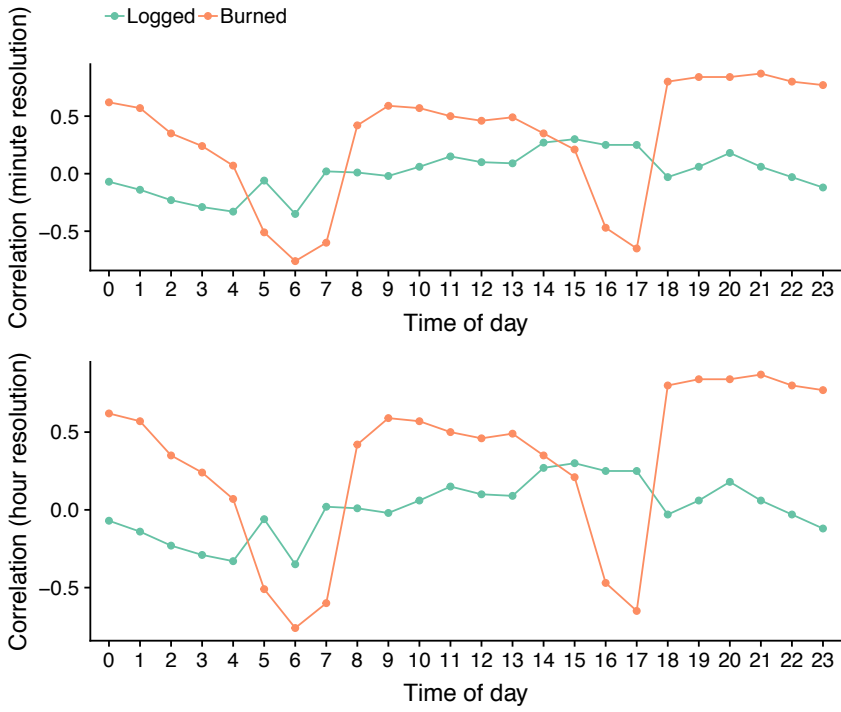
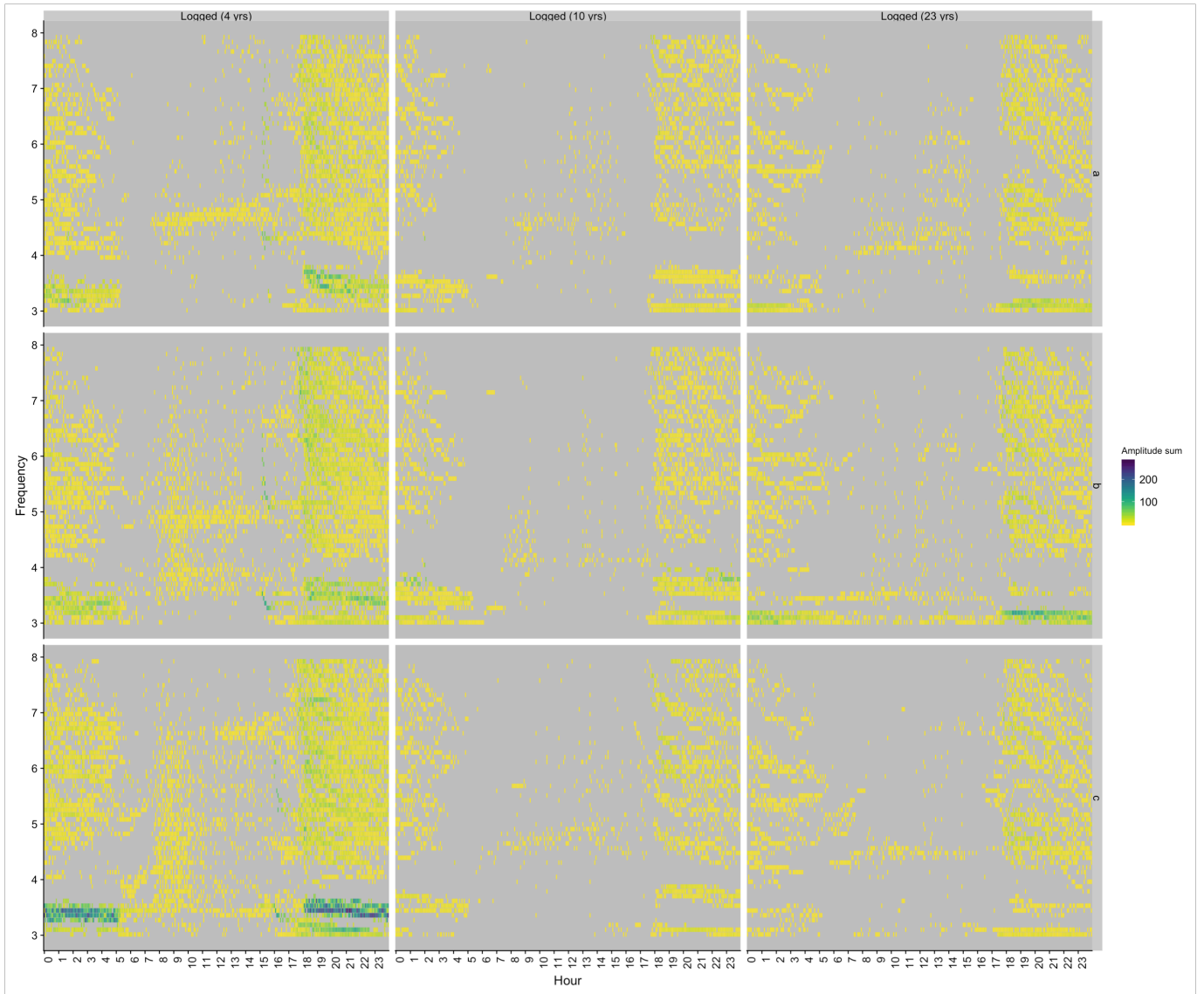


Figure S 4-4. Comparison of correlations show comparable ASO-degradation relationships irrespective of scale of aggregation (hourly vs. minute).



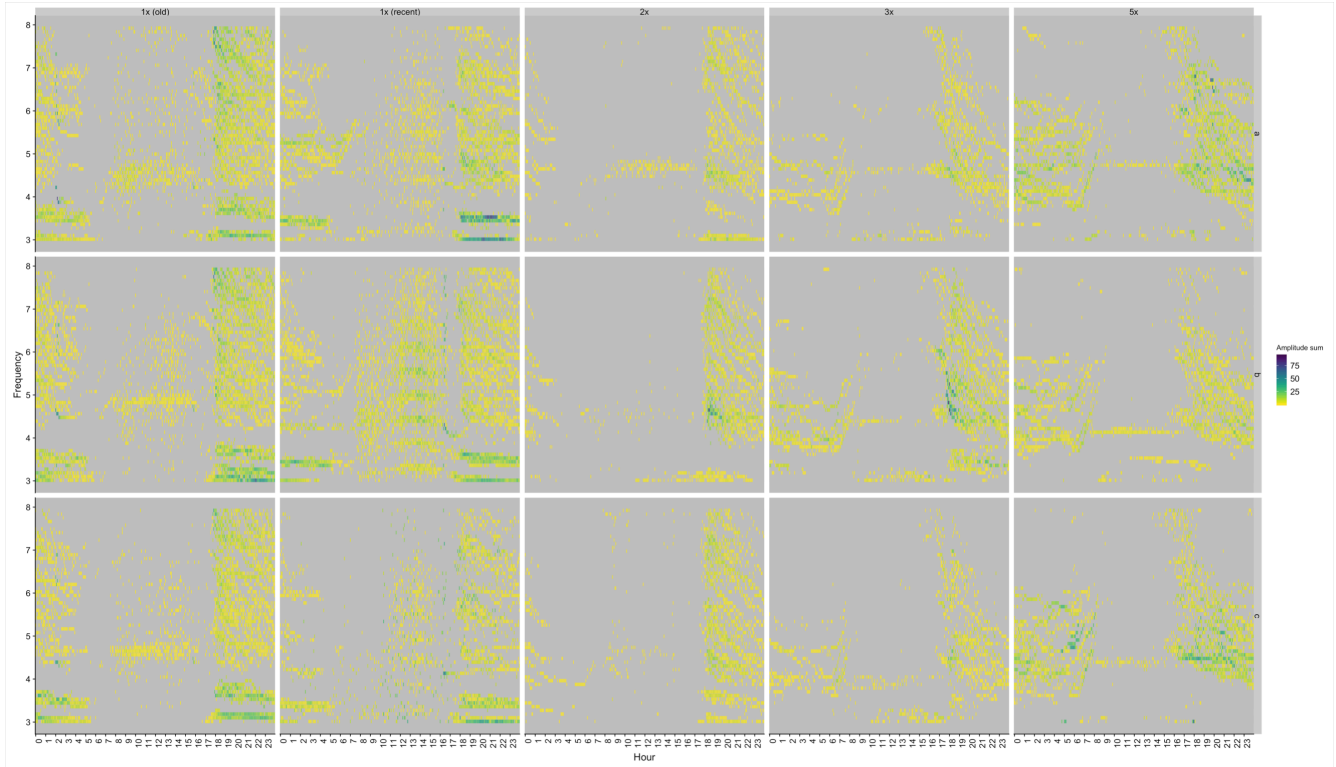


Figure S 4-5. Raw soundscape matrices aggregated at the minute level for an example range of logged (top) and burned (bottom) forests stratified by degradation strata (columns) and site replicate (row). For each time-frequency cell, the sum of the amplitude of detected activity peaks is calculated across the entire survey period.

5 Research Synthesis and Future Directions

Abstract

In this final chapter, I synthesize the combined set of results from my dissertation research (Chapters 2-4) and its broader significance for the carbon cycling and conservation communities. I discuss future avenues to improve and build upon this research to support enhanced monitoring capabilities of ecosystem degradation in the carbon-rich, biodiverse tropics. The novel synergies from lidar and ecoacoustics confirm the long-term legacy of forest degradation on both forest structure and animal communities in frontier Amazon forests. Looking forward, monitoring approaches that provide repeat measurements may further refine our understanding of the breakpoints that drive the loss and regeneration of carbon and biodiversity in degraded Amazon forests.

5.1 Research synthesis, significance, and next steps

Widespread Amazon fire activity in 2019 highlighted the incredible vulnerability of Amazon forests to further degradation, making this dissertation as timely now as when it began. The synergy of land-use pressures and climate change constitutes a chronic threat to Amazon forests (Le Page et al. 2017). Economic conditions drive fire activity, and climate conditions govern the risk of land-use fires escaping into neighboring forest areas. Frontier forests along the leading edge of agricultural development in southern Amazonia—where fire ignitions are

concentrated and seasonality is most pronounced—may help us predict trajectories of tropical forests in a hotter, drier, economically uncertain future. Routine ecosystem monitoring is needed to constrain our understanding of threshold conditions from human degradation that threaten to drive Amazon forests into alternative steady state systems (Brando et al. 2019).

In this dissertation, I present three complementary lines of evidence to better understand the nature of frontier landscapes. Chapters 2-4 present an innovative, multi-sensor perspective on the time-varying changes in the structure of forests and acoustic communities based on high-density airborne lidar, 11000 hours of acoustic surveys, and annual time series of Landsat data to characterize the forest degradation process over time. Together, these studies provide a unique look at the distinct ecosystem effects of fire versus logging (Chapters 2, 4), degradation persistence and the correspondence between biomass, habitat and biodiversity recovery following degradation (Chapters 2-4), and finally, the interactions between sound and structure that reflect community composition and influence detection (Chapter 3).

5.1.1 The ecosystem legacy of forest degradation

The combined set of results is based on a comprehensive survey of burned and logged forests in terms of the structural diversity present across frontier Amazonia. First, I wanted to know how much of this structural diversity among degraded forests relative to intact forests was driven by historical differences in forest degradation (Chapter 2). Second, I evaluated whether forest structure can be used to predict the diversity of acoustic community assemblages, and simultaneously, failure to detect

animal-generated signals (i.e. attenuation) (Chapter 3). Last, I used sound to supersede my understanding from structure alone in order to probe differences among community assemblages as a function of forest degradation (Chapter 4). Together, these findings may help us plan for likely changes from fire activity, and evaluate possible pathways for mitigating degradation impact.

Fire, in comparison to logging, poses the greatest risk to forest carbon stocks and biodiversity along the Amazon arc of deforestation. The frequency of Amazon forest fires is the single most important factor governing the spatial heterogeneity and recovery of carbon stocks, canopy structure, and acoustic diversity after human degradation. Recurrent fire turns Amazon forests into simplified, carbon-poor ecosystems. Forests burned multiple times may lose as much as 90% of their carbon stocks, and 95% of their original canopy tree clusters (Chapter 2). Chapter 2 estimates that the carbon mitigation potential of avoiding just one additional fire in a previously burned forest is equivalent to retaining a third of intact forest carbon stocks. Furthermore, detection of acoustic signals is heavily skewed by fire, as evidenced by Chapter 3, which predicted strongest relationships between detection likelihood, biomass and the standard deviation of shrub returns, a proxy for low fractional tree cover after recurrent fire. Furthermore, animal communication networks become quieter, less connected, and more homogenous after multiple burns (Chapter 4). By all accounts, fire damages become increasingly worse with each successive fire event (from 1-5 fires), but I identified a critical ecosystem breakpoint after the second fire. The set of taxonomically inclusive acoustic measurements used in Chapter 4 suggests major community reassembly after a once-burned forest becomes exposed to an

additional burn. Combined, these results highlight large possible benefits to protecting Amazon forests from recurrent fire activity in the face of worsening Amazon drought and human ignitions.

The immediate effects of a single burn appear somewhat comparable to the effects of logging from a carbon perspective, but they clearly differ in magnitude from a habitat and biodiversity perspective. Within the first year of regrowth, once-burned and logged forests lose an average of 54% and 45% of aboveground carbon stocks, respectively (Chapter 2). Habitat differences are more pronounced; more than twice as many residual large canopy tree clusters are retained immediately after selective logging than fire. These habitat differences strongly influence the composition of the acoustic guild (Chapters 3-4). Once-burned and logged forests are comparably noisy, but the acoustic communities are active in different time and frequency ranges, suggesting different community assemblages (Chapter 4).

Accounting for the time-integrated effects of degradation is necessary to estimate the net ecosystem benefits from avoided degradation. By modeling the loss and recovery of Amazon forest carbon stocks for specific Amazon forest degradation pathways along 1- to 15-year time horizons, this dissertation provides the first comprehensive assessment of carbon emissions factors from fire and logging. The slow recovery of degraded carbon stocks over time suggests that omitting degradation from national carbon accounting frameworks, as has been done to date (see Hargita, Günter, and Köthke 2016), risks underestimating carbon emissions, and compromises mitigation outcomes. Furthermore, by tracking the loss and recovery of complex canopy structure, this dissertation shows that lidar may also provide quantitative

estimates of ecosystem co-benefits, an important but poorly established component of REDD+ MRV.

The three sets of results show that the time-dependent effects of degradation on biomass do not necessarily coincide with the recovery patterns of canopy structure and biodiversity. Chapter 2 suggests that carbon stocks may recover faster than biodiversity during the first two decades after degradation, based on the slower recovery of emergent trees and other habitat characteristics critical for biodiversity. Chapter 3 models soundscapes with information about biomass, while Chapter 4 highlights the need to confront acoustic data with additional information about degradation history. The flexibility afforded by the hierarchical model introduced in Chapter 3 allowed us to separate apart the detection and ecological processes that give rise to differences in soundscape samples. Interestingly, biomass was not selected as a predictor of acoustic space occupancy, but was selected for detection. Chapter 4 offers one reason for why this might be by showing that degradation mediates the relationship between acoustic space in-filling and forest in-filling (i.e. biomass), as biomass was not a reliable predictor of biodiversity following logging, only fire. This dissertation offers compelling evidence that soundscapes may provide a much-needed alternative to biomass as a metric of forest community impact that can be measured over time.

Lastly, differences in initial fire severity leave a clear and lasting imprint on both habitat structure and acoustic community structure (Chapters 2, 4). High-severity fires that burn during the day leave a larger and longer lasting imprint on ecosystem structure when compared to slower burning nighttime fires. This has important

implications for fire management, including the allocation of fire brigades to minimize fire damages. Carbon losses may vary by as much as 15% depending on when fire damages are incurred, and such differences from initial severity are preserved through time (Chapter 2). Acoustic measurements also reflect localized differences in animal community responses to initial burn severity, even within a single stand (Chapter 4).

Assuming worsening drought conditions, this research portends potential catastrophic consequences in the absence of improved fire management. It uses multiple lines of evidence to identify critical ecosystem thresholds associated with fire, and possible low-hanging fruit in terms of mitigation pathways that would yield large returns for both carbon storage and biodiversity. It shows that full accounting of the cumulative effect of human degradation requires a multi-sensor perspective that controls for degradation type, recurrence, severity, and recovery.

5.1.2 Making the most of acoustic data for biodiversity monitoring

Remote audio recordings hold great promise for routine monitoring of tropical forest biodiversity. The innovative analytical techniques used in this dissertation revealed fine-scale differences associated with human activity, representing new, cost-effective pathways for estimating biodiversity variation over traditionally unavailable scales. Furthermore, this dissertation reveals novel synergies between ecoacoustic and lidar data. Chapter 3 draws upon such synergies to capture aspects of the physical interactions between sound and structure to model acoustic community structure and acoustic attenuation. Chapter 4 combines these datasets within an ecological

framework to identify acoustic markers of biotic communities along the structural spectrum of degraded forests.

During the course of this dissertation, I discovered three distinct and promising pathways for disciplinary crossover, which all merit further investigation:

First, this dissertation indicates that hierarchical models provide a path forward for handling observation bias in soundscape studies. It introduces a novel soundscape analysis framework based on occupancy modeling, an approach traditionally developed to account for bias in species-level surveys, applied here to multi-dimensional soundscapes for the first time (Chapter 3). It shows that presence-absence modeling may help address several key limitations of present-day soundscape analysis methods by providing more rigorous accounting of observation bias, including frequency-dependent sound attenuation. The resulting model from this research has broad applicability to diverse circumstances to account for imperfect detection of sound-producing animals. Results from the case study application of the model confirmed that the likelihood for detection failure varies as a function of vegetation structure and signal frequency, and it demonstrates a new promising application of airborne lidar for modeling these interactions. Additionally, this research advances methods for predicting variation in 2D acoustic community structure based on 3D forest structure. The analytic framework introduced in this study models variation in community composition without species ID by abstracting the acoustic fingerprint of a site into predictable ‘pseudo-taxa’ using habitat metrics from lidar. Furthermore, this framework supports inferences into taxa-specific responses to environmental variability, including chronically under-sampled and

poorly identifiable taxonomic groups (e.g. insects). Lastly, application of the occupancy model reveals helpful insight for the ecoacoustic community, supported by physics, on the spectral ranges of ‘pseudo-taxa’ that are likely to be most robust to attenuation in the absence of formal statistical correction in degraded tropical forests (3-8 kHz), and it provides a flexible framework for evaluating detection probability in other ecosystem contexts with distinct habitat constraints on sound transmission.

Chapter 3 provides a clear confirmation of detection bias in tropical forests based on structure, but it is clear that the occupancy modeling solution that it proposes for addressing observation bias cannot be applied at scale without improved methods for screening abiotic noise from wind and rain. To meet model assumptions in Chapter 3, I had to discard all detected instances of rainfall, which equated to over 50% of all recordings—a huge loss of hard-fought data. These issues with rain may be comparable to the constraints imposed on optical sensors from variation in cloud coverage. Still, they need to be addressed, either through improved instrumentation or automated screening of rainfall. Furthermore, isolating the biotic fraction of the soundscape is critical for making accurate biological attributions to soundscape differences. I did not find any justifiable methods to automate rain detection, so I developed my own machine learning-based model to be able to screen through the thousands of hours of recordings for the presence of rain spectra using algorithms originally developed to detect species-level spectra (Aide et al. 2013). In Chapter 3, I used conservative criteria to search for rainfall to ensure 0% false negatives at the known cost of generating a higher rate of false positives (7%). A post-hoc

investigation of the machine learning rain model confirmed curious temporal incoherence in detected rainfall from surveys sampled within 300 m of one another. Later on, through attempting to model the 2D soundscapes surfaces using mixture modeling, we discovered this mismatch was linked to spectral confusion with certain insect stridulations. Using the occupancy model from Chapter 3 to drive the analyses in Chapter 4 would have omitted valuable biologic content. Given these technological challenges in filtering out rain-contaminated recordings, we opted not to use the modeled results in Chapter 4 so we could utilize all recordings for our ecological analysis and keep the insect component of the soundscape intact. Instead, Chapter 4 incorporates the learning about the role of structure in sound attenuation by targeting the frequency bands with the lowest predicted likelihood of detection bias from interference with structure (3-8 kHz). As a general recommendation, future sampling campaigns should consider co-deploying a rainfall monitoring system to better account for acoustic contamination from rain, in order to conform to the statistical assumptions for modeling observation bias with occupancy models.

Additionally, this dissertation made two other cross-disciplinary methodological contributions by translating concepts from surface modeling and network theory to characterize the 3D structure of the “acoustic fingerprint.” Since I came to ecoacoustics at the start of this dissertation from a lidar-based perspective, what seemed most intuitive to me was to search for ways to exploit the space-filling properties of sound in a similar way that lidar captures the space-filling properties of light to retrieve volumetric measurements. I pursued these two additional approaches to capture different aspects of the 3D richness of the soundscape (or perhaps “sound

cloud” is more germane in this context) to extend beyond frequency-agnostic measures of occupancy and pinpoint the specific acoustic pseudo-taxa that drive differences in overall ASO. Both approaches warrant additional investigation, although the first is more complicated and parameterized, and probably less tractable than the second.

The first approach aimed to compare hotspots of acoustic activity in time-frequency space by modeling the 2D soundscape surface with a bivariate mixture modeling approach originally developed for angular wind data (Chakraborty and Wong 2017, Figs. 5-1, 5-2). Before subsequently shifting my focus to networks, I pursued this approach to try and find a set of synthetic metrics that could allow me to quantitatively compare 2D soundscapes across my sampled diversity of degraded forests, while preserving information about time- and frequency-dependence. Comparing the locations and spread of acoustic activity modes derived from the modeled soundscape surfaces along degradation recovery pathways revealed some intriguing early results that conformed to certain aspects of our understanding of degradation history (Fig. 5-1). Based on the performance of the model fits from the preliminary results, this approach warrants further investigation in future research. However, it still needs additional testing and validation for ecological analysis and was therefore too complicated to be justified within the immediate context of this dissertation. In particular, parameters governing how to standardize for the optimal number of components, which we determined with approximate Bayesian methods and an automatic incremental fitting procedure (Chakraborty and Wong 2017), would need to be carefully refined to provide robust, repeatable information about acoustic

community composition. In certain instances, activity modes that appeared distinct from visual inspection (e.g. from temporally distinct choruses) were at times modeled with the same component mixture, and vice versa—which relates to the persistent issue of ‘lumping and splitting’ common to classification and clustering problems in ecology. Still, one reason why acoustic activity modes might be informative and worth exploring is that tracking modes, “activity hotspots,” makes us more sensitive to large adjacent clusters that occupy large swaths of acoustic space (i.e. cicadas, multi-taxa insect choruses), which network clustering results from Chapter 4 point to as a useful indicator of forest degradation from fire. Lastly, I pursued this approach after developing a more complete appreciation for the limitations around rain contamination so I am also intrigued by the possible value of modeling soundscape surfaces to smooth over spurious abiotic elements, like wind and rain.

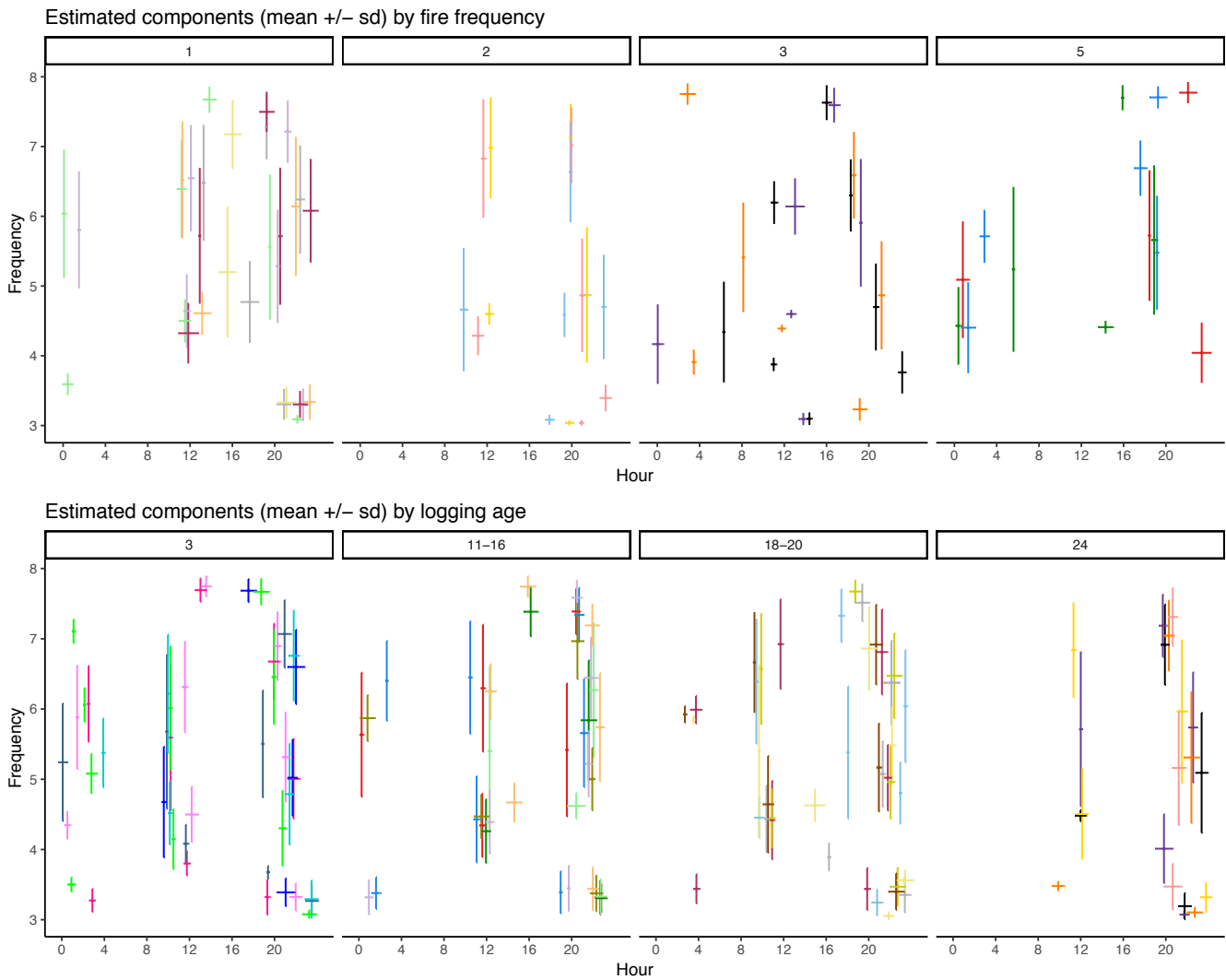


Figure 5-1. Modeled peaks of acoustic activity from mixture model analysis (mean +/- sd) of burned (top) and logged (bottom) sites (distinct color per site) show the appearance and disappearance of pseudo-taxa, conforming to our understanding of degradation history.

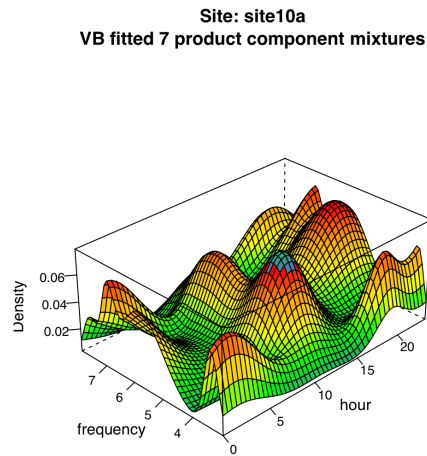
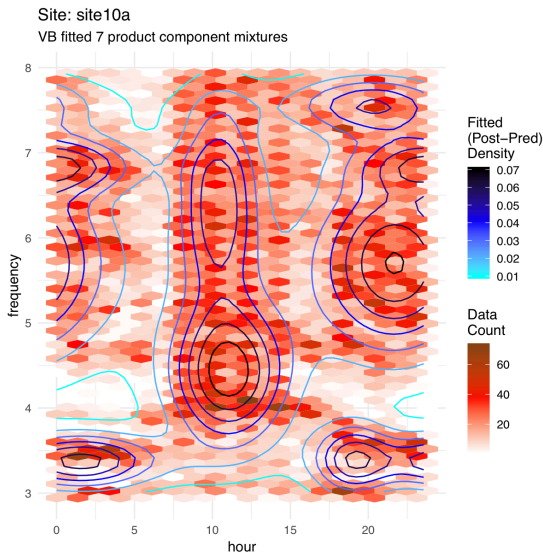
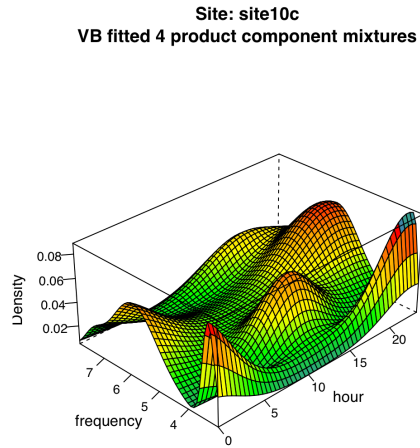
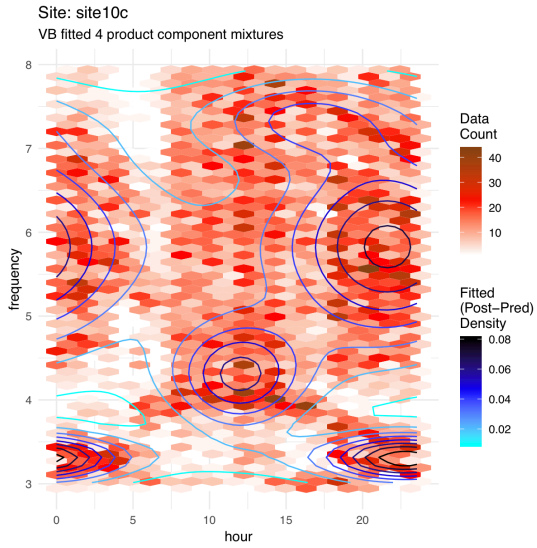


Figure 5-2. These two examples of soundscape predictions from the mixture model for two spatially proximate replicates within the same logging class (15 yr) indicate that the modes of the predicted soundscape surface do not consistently conform with our visual inspection, which suggests further testing needs to be done to standardize optimal selection of component mixtures, which curiously varied between 4 and 7 in the examples shown above.

Ecological network theory offered a more tractable framework for analyzing the 2D soundscapes to characterize variation in the acoustic guild while preserving time- and frequency-dependence to understand the component elements of presence and absence that explain differences in ASO. Ecological network theory was originally developed to understand predator-prey relationships, but this dissertation demonstrates its utility for characterizing the topology of acoustic communication networks. Networks offered a more synthetic understanding of the coordinated behavior of sound signals that may reflect differences in biotic assembly after forest degradation. There are hundreds of local- and global-level network metrics that may be applied to soundscape analysis. With further investigation, it is possible that additional network metrics could be applied to acoustic data to further elucidate the potential of networks to track compositional change through objective acoustic records of biodiversity responses through time.

The different analysis approaches in this dissertation offer varying levels of biologic interpretability. I found that the amount of acoustic space used by animal communities is a helpful predictor of residual biomass after fire (ASO). Going an additional step beyond that, network-based analyses allowed me to probe the driving factors that give rise to differences in ASO (e.g. interactions among adjacent pseudo-taxa, “cliques”). This enables greater biological interpretation of the soundscape than what was possible with ASO alone, but it does not allow us to identify or inventory sound producers for biological attribution. In future research, it may be possible to access species-level information from the existing recordings. This would necessitate

the use of library recordings or expert interpretation, likely in conjunction with additional field campaigns.

Continued investigations that link ecoacoustic and traditional field observations may provide further support for avoided degradation if evidence of changing soundscapes reflect local extirpations of specific avian, amphibian, or insect species. One goal of this dissertation was to use as much of the acoustic data as possible. To this end, I developed modeling frameworks and analytic techniques that covered the full soundscape and evaluated community composition through the lens of pseudo-taxa, rather than species. These analyses yielded important new insights from the perspective of the ‘acoustic guild’. For example, the network-based perspective from Chapter 4 showed that different spectra differentiate once-burned forests from recurrently burned forests based on the diversity of sound hours in which they occur, but this finding may be even more useful from an ecological standpoint if we can ascribe the variation in sounds at specific frequencies to the loss of particular taxa.

The chronosequence of soundscapes that I collected could help generate further insights into the legacy effects of forest degradation in conjunction with additional data. For example, multi-temporal observations from repeat visits and inter-seasonal surveys could be used to build upon my limited chronosequence of logged forests (sampled after 4-23 years of regeneration) to further constrain our understanding of the necessary time-scales for recovery, which this dissertation indicates biomass may not be an effective proxy for (Chapter 4). Additional information is needed to elucidate the non-linearity that we identified between ASO

and logging age, and whether the consistent shift between 4 and 10 years after logging (across both ASO and network measures), is evidence of time-lagged recovery, or whether our understanding is being confounded by idiosyncrasies among replicates, which are limited in number and contain possible sources of unaccounted variation (e.g. logging severity, lianas/bamboo invasions, etc.). For example, one of the biggest curiosities that stood out for me during my several months of field work examining these forests from the inside was why liana and bamboo invasions were found in some logged forests but not others, something that was not readily apparent to me based on differences from logging age and structure alone. Further investigation should confirm whether there are co-evolving feedbacks between floristic composition and acoustic composition that could help us further understand successional processes after degradation (e.g. liana invasion/arrested succession) and anticipate bottlenecks driven by local extirpations of seed dispersers and pollinators. Lastly, I planned my field season to correspond with the end of the dry season to be able to specifically target breeding birds. Revisiting my field sites during the rainy season would help us confirm whether ANH is better supported with increased sensitivity to anurans.

The lack of an intact reference soundscape is a clear limitation of this investigation, but a constraint that is unfortunately common across many tropical frontier regions, where intact refugia are scarce. Furthermore, given the practical constraints to working across this complex landscape, I could not account for differences in matrix configuration, forest fragment size, or connectivity, which are all important drivers of biodiversity variation across both space and time, as I have

investigated previously (e.g. Rappaport et al. 2015), and most likely introduced some confounding elements into my space-for-time survey design that I could not account for.

Lastly, this dissertation points to potential indicators that may be useful for rapidly assessing the degradation status of burned forests, but additional data is needed to evaluate robustness across different regions, seasons, etc. Given the obvious synergies between conservation and forest management, it would be interesting to deploy ecoacoustic devices in logging concessions with known levels of harvesting intensity, to inform “best practices” guidelines, or to establish permanent acoustic sensor networks in field studies with permanent floristic inventory plots to ensure longitudinal continuity.

5.2 Scaling up my understanding of forest degradation in future work

5.2.1 To inform management

I envision several research opportunities to build upon this work in order to extend our understanding of the cumulative effects of degradation across broader scales. Originally, when I started thinking about the possibility of a fourth chapter at the start of this dissertation, I imagined linking the discrete lidar and acoustic observations with continuous satellite information to extend our understanding of the differences between logged and burned forests to the regional scale. Since then, I have learned a lot about the complexity and heterogeneity of frontier forests. Chapter 4 shows strong relationships that link fire history (timing, severity, and frequency) with soundscape structure. However, the story around logging is much more

nebulous; I could not find a justifiable predictable relationship to explain the full heterogeneity of frontier forest soundscapes with degradation history alone. Based on this learning, what would now be more immediately interesting to me would be to focus instead on scaling up our understanding of the cumulative effects of Amazon fire, the most obvious marker of change, to the landscape scale. Specifically, I think it would be interesting from both a science and conservation/management perspective to conduct a scaling study in the adjacent landscape, the Xingu Indigenous Park, which is the last remnant of large intact forest refugia in this region, a critically important landscape in this region with undeniable conservation value. In Chapter 2, I sampled intact forests from the Xingu using lidar to measure the relative magnitude of structural changes following fire; however, I was not able to acquire the necessary sampling permissions to physically access the park during my field campaign to sample acoustic data from the ground. It would be interesting to make predictions over this landscape for a number of reasons. For one, this landscape has an extensive history of repeated burning, and it appears to have been much less affected by logging. An improved understanding of how this remaining stronghold of contiguous Amazon forest has been affected by repeated fire disturbance could help us better plan for and respond to likely changes in fire risk. Given what I know now about the importance of fire frequency in shaping habitat structure and habitat use, I have more reason to believe that the long history of fire and indigenous land management practices that has been traced back to prehistoric times in the Xingu (Schwartzman et al. 2013) has probably given rise to a diversity of habitats with likely shifts in species composition and carbon storage that have not been fully accounted for by park

management. This type of scoping study would have clear management and conservation relevance, and could confront existing narratives that tout indigenous reserves as intact and unaltered, which are based on about active fire detections, not the actual understory extent of fire damages (Nepstad et al. 2006).

5.2.2 To inform policy

Furthermore, the findings from this research, which confirm the long-term impact of forest degradation on both carbon and biodiversity, and confirm important differences between logging and fire, can also be extended to help inform policy. For example, the first study (Chapter 2) has direct policy relevance in terms of supporting international efforts to reduce greenhouse gas emissions from forest degradation (e.g. REDD+) by targeting key data gaps that have hampered full accounting of degradation from fire and logging in carbon monitoring systems. The most obvious next step would be to combine the time-varying emissions factors from Chapter 2 with activity data on degradation extent to help confirm the relative contributions of fire and logging to net regional carbon emissions in the Amazon.

Lastly, there is an immediate need to better understand the spatial correspondences between carbon and biodiversity values at broader regional scales to prevent the unintended loss of biodiversity from carbon-based conservation. Climate change policies that aim to protect forest carbon through avoided degradation and deforestation (e.g. REDD+) may also have co-benefits for biodiversity so long as biodiversity safeguards are established. Predictive maps of biomass and biodiversity values would be useful to help navigate climate-conservation trade-offs. For example,

I could envision a scaling study that builds off this work to compare likely centers of high biomass and acoustic occupancy.

5.3 Conclusion

The Anthropocene is expected to shrink and simplify Earth's remaining tropical forests, which are critical for stabilizing climate and supporting life (Edwards et al. 2019). To enable better land stewardship, we need improved remote sensing and analysis approaches for monitoring ecosystem services across space and time. This dissertation provides key contributions that enhance the utility of lidar and ecoacoustics to help reduce uncertainties around the carbon mitigation and conservation benefits of avoided forest degradation from logging and fire.

References

- Aide, T. Mitchell, Carlos Corrada-Bravo, Marconi Campos-Cerqueira, Carlos Milan, Giovany Vega, and Rafael Alvarez. 2013. “Real-Time Bioacoustics Monitoring and Automated Species Identification.” *PeerJ* 1 (July): e103.
- Brando, Paulo M., Lucas Paolucci, Caroline C. Ummenhofer, Elsa M. Ordway, Henrik Hartmann, Megan E. Cattau, Ludmila Rattis, Vincent Medjibe, Michael T. Coe, and Jennifer Balch. 2019. “Droughts, Wildfires, and Forest Carbon Cycling: A Pantropical Synthesis.” *Annual Review of Earth and Planetary Sciences* 47 (1): 555–81.
- Chakraborty, Saptarshi, and Samuel W. K. Wong. 2017. “BAMBI: An R Package for Fitting Bivariate Angular Mixture Models.” *ArXiv:1708.07804 [Stat]*, August.
- Edwards, David P., Jacob B. Socolar, Simon C. Mills, Zuzana Burivalova, Lian Pin Koh, and David S. Wilcove. 2019. “Conservation of Tropical Forests in the Anthropocene.” *Current Biology* 29 (19): R1008–20.
- Hargita, Yvonne, Sven Günter, and Margret Köthke. 2016. “Brazil Submitted the First REDD+ Reference Level to the UNFCCC—Implications Regarding Climate Effectiveness and Cost-Efficiency.” *Land Use Policy* 55 (September): 340–47.
- Le Page, Yannick, Douglas Morton, Corinne Hartin, Ben Bond-Lamberty, José Miguel Cardoso Pereira, George Hurtt, and Ghassem Asrar. 2017. “Synergy between Land Use and Climate Change Increases Future Fire Risk in Amazon Forests.” *Earth System Dynamics (Online)* 8 (PNNL-SA-119758).
- Nepstad, D., S. Schwartzman, B. Bamberger, M. Santilli, D. Ray, P. Schlesinger, P. Lefebvre, et al. 2006. “Inhibition of Amazon Deforestation and Fire by Parks and Indigenous Lands: Inhibition of Amazon Deforestation and Fire.” *Conservation Biology* 20 (1): 65–73.
- Rappaport, Danielle I., Leandro R. Tambosi, and Jean P. Metzger. 2015. “A Landscape Triage Approach: Combining Spatial and Temporal Dynamics to Prioritize Restoration and Conservation.” *Journal of Applied Ecology* 52 (3): 590–601.
- Schwartzman, Stephan, André Villas Boas, Katia Yukari Ono, Marisa Gesteira Fonseca, Juan Doblás, Barbara Zimmerman, Paulo Junqueira, et al. 2013. “The Natural and Social History of the Indigenous Lands and Protected Areas Corridor of the Xingu River Basin.” *Phil. Trans. R. Soc. B* 368 (1619): 20120164.